

BERNOULLI-LoRA: A THEORETICAL FRAMEWORK FOR RANDOMIZED LOW-RANK ADAPTATION

005 **Anonymous authors**

006 Paper under double-blind review

ABSTRACT

011 Parameter-efficient fine-tuning (PEFT) has emerged as a crucial approach for adapting
 012 large foundational models to specific tasks, particularly as model sizes continue
 013 to grow exponentially. Among PEFT methods, **Low-Rank Adaptation (LoRA)** (Hu
 014 et al., 2022) stands out for its effectiveness and simplicity, expressing adaptations as
 015 a product of two low-rank matrices. While extensive empirical studies demonstrate
 016 LoRA’s practical utility, theoretical understanding of such methods remains limited.
 017 Recent work on **RAC-LoRA** (Malinovsky et al., 2024) took initial steps toward
 018 rigorous analysis. In this work, we introduce **Bernoulli-LoRA**, a novel theoretical
 019 framework that unifies and extends existing **LoRA** approaches. Our method intro-
 020 duces a probabilistic Bernoulli mechanism for selecting which matrix to update.
 021 This approach encompasses and generalizes various existing update strategies while
 022 maintaining theoretical tractability. Under standard assumptions from non-convex
 023 optimization literature, we analyze several variants of our framework: **Bernoulli-
 024 LoRA-GD**, **Bernoulli-LoRA-SGD**, **Bernoulli-LoRA-PAGE**, and **Bernoulli-LoRA-MVR**,
 025 **Bernoulli-LoRA-QGD**, **Bernoulli-LoRA-MARINA**, **Bernoulli-LoRA-EF21**, establishing
 026 convergence guarantees for each variant. Additionally, we extend our analysis
 027 to convex non-smooth functions, providing convergence rates for both constant
 028 and adaptive (Polyak-type) stepsizes. Through extensive experiments on various
 029 tasks, we validate our theoretical findings and demonstrate the practical efficacy of
 030 our approach. This work is a step toward developing theoretically grounded yet
 031 practically effective PEFT methods.

1 INTRODUCTION

035 Fine-tuning adapts pre-trained models to new datasets, a central task in modern deep learning,
 036 particularly NLP (Peters et al., 2018; Devlin et al., 2019). However, full fine-tuning is computationally
 037 expensive for large models. Parameter-Efficient Fine-Tuning (PEFT) (He et al., 2021) addresses
 038 this by updating only a fraction of parameters (Richtárik & Takáč, 2016; Demidovich et al., 2023a),
 039 matching full fine-tuning performance with significantly lower costs (Radford et al., 2019; Brown
 040 et al., 2020; Han et al., 2024).

041 Leveraging the low intrinsic dimensionality of pre-trained models (Li et al., 2018; Aghajanyan et al.,
 042 2020), **Low-Rank Adaptation (LoRA)** (Hu et al., 2022) optimizes updates in a reduced subspace. It
 043 replaces large matrix updates with the product of two trainable low-rank matrices:

$$W = W^0 + \frac{\alpha}{r} BA,$$

044 where $W^0 \in \mathbb{R}^{m \times n}$ is fixed, and $B \in \mathbb{R}^{m \times r}$, $A \in \mathbb{R}^{r \times n}$ are trainable ($r \ll \min\{m, n\}$). While
 045 typically initialized with Gaussian A and zero B , other strategies exist (Zhu et al., 2024; Hayou et al.,
 046 2024; Meng et al., 2024; Wang et al., 2025). Beyond improving efficiency (Cherniuk et al., 2023;
 047 Mao et al., 2025), **LoRA** mitigates catastrophic forgetting and enhances output diversity (Biderman
 048 et al., 2024).

049 To approach full fine-tuning performance, Xia et al. (2024) introduced **Chain of LoRA (COLA)**. This
 050 framework iteratively builds higher-rank updates from a sequence of low-rank modules at no extra
 051 computational cost. By merging updates into fixed parameters, it yields:

$$W = W^0 + \frac{\alpha}{r} \sum_{t=0}^{T-1} B^t A^t.$$

054 Unlike standard LoRA, COLA uses sequential decompositions to efficiently approximate high-rank
 055 adaptations.

056 Recent theoretical works analyze LoRA from complementary angles. Jang et al. (2024) prove that
 057 sufficiently high-rank LoRA eliminates spurious local minima in the NTK regime. Kim et al. (2025)
 058 show that training typically converges to a low-rank global minimum or diverges toward high-rank
 059 solutions. In continuous-time settings, Xu et al. (2025) highlight the pivotal role of initialization in
 060 matrix factorization gradient flows, while Dayi & Chen (2025) position low-rank fine-tuning between
 061 lazy training and feature learning.

063 2 MOTIVATION

064 Theoretical advances above highlight what happens in specific regimes, but they leave open whether
 065 practical, discrete-time LoRA updates converge under realistic training noise and communication
 066 constraints. This gap motivates our framework: we seek general convergence guarantees for random-
 067 ized low-rank adaptation with stochastic gradients, variance reduction, and federated communication
 068 savings. At the same time, despite their practical success, Low-Rank Adaptation (LoRA) and its
 069 variants like Chain of LoRA (COLA) still lack a unified and practically relevant convergence theory.
 070 LoRA’s re-parameterization makes smooth loss functions non-smooth, creating significant theoretical
 071 hurdles (Sun et al., 2024). Second, existing COLA analysis ignores its core low-rank updates by fo-
 072 cusing on full-rank optimization, thus failing to explain its efficiency (Xia et al., 2024). Consequently,
 073 most LoRA-based methods are heuristics without convergence guarantees, making them sensitive to
 074 hyperparameters (Khodak et al., 2021; Kuang et al., 2024). Malinovsky et al. (2024) even showed
 075 COLA can diverge and introduced RAC-LoRA, the first framework to establish convergence rates
 076 for LoRA-style updates. However, the RAC-LoRA framework is limited. It lacks optimal variance-
 077 reduced techniques for non-convex problems and fails to address advanced Federated Learning (FL)
 078 scenarios incorporating communication compression and error feedback (Alistarh et al., 2018; Wen
 079 et al., 2017; Horváth et al., 2022; Panferov et al., 2024). The need for distributed optimization like
 080 FL is driven by the challenge of training massive models (Brown et al., 2020; Kolesnikov et al., 2020;
 081 Goyal et al., 2017; You et al., 2019; Le Scão et al., 2023). Our work aims to bridge this gap by
 082 extending a theoretically sound LoRA framework to these vital, practical optimization settings. In
 083 the next section, we formalize the optimization problems we study.

085 3 PROBLEM STATEMENT

086 Supervised learning is an optimization problem that minimizes a loss function. We focus on this
 087 challenge in fine-tuning, using a general, model-agnostic formulation:

$$\min_{\Delta W \in \mathbb{R}^{m \times n}} f(W^0 + \Delta W). \quad (1)$$

088 Here, W^0 represents the pre-trained parameters, ΔW is the trainable adaptation, and f is the
 089 empirical loss. Since $m \times n$ is very large, ΔW requires a simple, trainable structure.

090 Throughout the paper, we treat W^0 as a fixed pre-trained model and view f as the fine-tuning loss
 091 that already encodes the effect of the pre-training and fine-tuning data distributions (including any
 092 mismatch between them). All of our convergence guarantees are therefore conditional on this given
 093 W^0 and the associated fine-tuning objective f . We do not model the representation-learning dynamics
 094 of the pre-training phase, nor do we analyze generalization; our focus is purely on the optimization
 095 behavior of low-rank LoRA-style updates when minimizing the fine-tuning loss.

096 For our stochastic methods, we consider these objective structures:

- 101 • **Finite-Sum Setting:** The objective is an average over N data samples, used in methods like
 102 Bernoulli-LoRA-PAGE:

$$103 \quad f(W^0 + \Delta W) = \frac{1}{N} \sum_{i=1}^N f_i(W^0 + \Delta W). \quad (2)$$

- 106 • **Expectation Setting:** The objective is an expectation over a data distribution \mathcal{D} , for methods
 107 like Bernoulli-LoRA-MVR:

$$108 \quad f(W^0 + \Delta W) = \mathbb{E}_{\xi \sim \mathcal{D}} [f_\xi(W^0 + \Delta W)]. \quad (3)$$

108 We also address the **distributed optimization setting** for our proposed Federated Learning (FL)
 109 algorithms (e.g., [Fed-Bernoulli-LoRA-QGD](#)). Here, the goal is to minimize a global objective averaged
 110 over M clients:

$$111 \quad 112 \quad 113 \quad 114 \quad 115 \quad 116 \quad 117 \quad 118 \quad 119 \quad 120 \quad 121 \quad 122 \quad 123 \quad 124 \quad 125 \quad 126 \quad 127 \quad 128 \quad 129 \quad 130 \quad 131 \quad 132 \quad 133 \quad 134 \quad 135 \quad 136 \quad 137 \quad 138 \quad 139 \quad 140 \quad 141 \quad 142 \quad 143 \quad 144 \quad 145 \quad 146 \quad 147 \quad 148 \quad 149 \quad 150 \quad 151 \quad 152 \quad 153 \quad 154 \quad 155 \quad 156 \quad 157 \quad 158 \quad 159 \quad 160 \quad 161$$

$$f(W^0 + \Delta W) = \frac{1}{M} \sum_{l=1}^M f_l(W^0 + \Delta W), \quad (4)$$

where f_l is the local loss for client l . The goal is to find ΔW that minimizes this global objective.

In practical applications, LoRA is often applied to many matrices across multiple layers (e.g., query, key, value, and feed-forward projections). Our analysis covers this case as well: one can view all LoRA-modified matrices as being stacked or arranged in block-diagonal form inside a single W^0 and ΔW . Because we work with the Frobenius norm and inner product, our assumptions and convergence results extend verbatim to this concatenated/block-diagonal representation, following the same abstraction used in [Hu et al. \(2022\)](#); [Sun et al. \(2024\)](#); [Malinovsky et al. \(2024\)](#); [Xia et al. \(2024\)](#); [Zhu et al. \(2024\)](#).

4 CONTRIBUTIONS

[LoRA](#)-based methods are sensitive to hyperparameters ([Khodak et al., 2021](#); [Kuang et al., 2024](#)) and require a stronger theoretical foundation. While [Malinovsky et al. \(2024\)](#) provided an initial framework with [RAC-LoRA](#), we aim to further advance the theory and versatility of low-rank adaptation.

Low-rank PEFT updates two matrices, A and B , either individually or alternating deterministically ([Malinovsky et al., 2024](#); [Xia et al., 2024](#); [Zhu et al., 2024](#)). Our main contribution, [Bernoulli-LoRA](#), is a generic framework with a probabilistic update: at each step, a Bernoulli trial selects either A or B for optimization while the other is fixed. This randomized selection unifies and generalizes existing update strategies. Similar to [COLA](#) ([Xia et al., 2024](#)), our framework applies a sequence of these probabilistic low-rank updates.

Our analysis uses standard non-convex optimization assumptions, like L -smoothness. We instantiate [Bernoulli-LoRA](#) with several algorithms, from foundational gradient methods to advanced stochastic, variance-reduced, and federated learning variants. We establish rigorous convergence guarantees for each method. Our key contributions include:

- ◆ **Foundational Algorithmic Variants:** We establish the framework’s properties with two fundamental schemes to understand the interplay between randomized selection and standard descent.
 - [Bernoulli-LoRA-GD](#) (Algorithm 2) uses full gradients, providing a foundational analysis of convergence in an idealized setting.
 - [Bernoulli-LoRA-SGD](#) (Algorithm 4) uses practical stochastic gradients, offering insights into the interplay of stochasticity and randomized adaptation for large-scale tasks.
- ◆ **Advanced Variance Reduction for Non-Convex Optimization:** To counter variance from stochastic gradients, we develop VR-enhanced variants, providing the first theoretical analysis of LoRA-type methods with advanced VR schemes in L -smooth non-convex settings.
 - [Bernoulli-LoRA-PAGE](#) (Algorithm 6) adapts the optimal and simple [PAGE](#) ([Li et al., 2021](#)) for the finite-sum setting (2).
 - [Bernoulli-LoRA-MVR](#) (Algorithm 5) uses [Momentum Variance Reduction](#) inspired by [STORM](#) ([Cutkosky & Orabona, 2019](#)) for the expectation setting, proving its effectiveness in our framework.
- ◆ **Communication-Efficient Federated Learning Extensions:** We extend [Bernoulli-LoRA](#) to FL, addressing communication overhead. We provide the first comprehensive analysis of LoRA-type methods integrated with established communication-saving techniques like quantization, gradient difference compression, and error feedback.
 - [Fed-Bernoulli-LoRA-QGD](#) (Algorithm 7) incorporates [QSGD](#)-style quantization ([Alistarh et al., 2017](#); [Wen et al., 2017](#); [Horváth et al., 2022](#); [Panferov et al., 2024](#)) to compress gradients and reduce communication bandwidth.
 - [Fed-Bernoulli-LoRA-MARINA](#) (Algorithm 8) adapts the [MARINA](#) strategy ([Gorbunov et al., 2021](#)) to efficiently compress gradient differences.

162 – **Fed-Bernoulli-LoRA-EF21** (Algorithm 9) integrates the **EF21** error feedback mechanism (Richtárik et al., 2021) to stabilize training with contractive compressors.

164 ◆ **Analysis for Non-Smooth Convex Functions:** We broaden our framework’s applicability by
165 providing the first theoretical analysis of LoRA-type methods for non-smooth convex optimization.
166 We present a version of **Bernoulli-LoRA-GD** (Algorithm 3) and establish its convergence rates with
167 different stepsize policies.

169 5 BERNOUlli-LoRA FRAMEWORK

172 In this section, we introduce the **Bernoulli-LoRA** framework, a novel and generic approach for low-
173 rank adaptation. The core idea is to perform a sequence of low-rank updates, where at each step, a
174 probabilistic choice determines which of the two factor matrices (A or B) is trained. This randomized
175 mechanism, formalized in Algorithm 1, not only provides a flexible and unifying theoretical construct
176 for existing LoRA-style methods but also allows for a rigorous convergence analysis.

177 At each iteration, one of the two low-rank matrices is sampled from a fixed distribution and remains
178 frozen, while the other is trained to minimize the objective. This strategy prevents optimization
179 from being confined to a fixed subspace, reducing the risk of converging to a suboptimal point. We
180 formalize these two configurations as Left and Right sketch updates.

181 **Definition 1** (Left and Right Sketch Updates). *We define two complementary update rules based on
182 which factor matrix is sampled from a fixed distribution and which is adjustable. The **Left Sketch**
183 and **Right Sketch** updates are given, respectively, by:*

$$184 \Delta W = \frac{\alpha}{r} B_S \hat{A}, \quad \text{with } B_S \sim \mathcal{D}_B \text{ fixed and } \hat{A} \in \mathbb{R}^{r \times n} \text{ adjustable,} \quad (5)$$

$$186 \Delta W = \frac{\alpha}{r} \hat{B} A_S, \quad \text{with } A_S \sim \mathcal{D}_A \text{ fixed and } \hat{B} \in \mathbb{R}^{m \times r} \text{ adjustable,} \quad (6)$$

187 where \mathcal{D}_B and \mathcal{D}_A are fixed distributions over $\mathbb{R}^{m \times r}$ and $\mathbb{R}^{r \times n}$ matrices.

190 Algorithm 1 Bernoulli-LoRA Framework

191 1: **Parameters:** pre-trained model $W^0 \in \mathbb{R}^{m \times n}$, rank $r \ll \min\{m, n\}$, scaling factor $\alpha > 0$, chain
192 length T , sketch distributions \mathcal{D}_S^B and \mathcal{D}_S^A , Bernoulli probability p .
193 2: **for** $t = 0, 1, \dots, T - 1$ **do**
194 3: Sample $c^t \sim \text{Be}(p)$ Bernoulli random variable
195 4: **if** $c^t = 1$ **then**
196 5: Sample $B_S^t \sim \mathcal{D}_S^B$ (Left sketch)
197 6: Using a chosen optimizer, approximately solve $\hat{A}^t \approx \arg \min_A f(W^t + \frac{\alpha}{r} B_S^t A)$.
198 7: $W^{t+1} = W^t + \frac{\alpha}{r} B_S^t \hat{A}^t$.
199 8: **else**
200 9: Sample $A_S^t \sim \mathcal{D}_S^A$ (Right sketch)
201 10: Using a chosen optimizer, approximately solve $\hat{B}^t \approx \arg \min_B f(W^t + \frac{\alpha}{r} B A_S^t)$.
202 11: $W^{t+1} = W^t + \frac{\alpha}{r} \hat{B}^t A_S^t$.
203 12: **end if**
204 13: **end for**

206 5.1 REFORMULATION AS A PROJECTED GRADIENT STEP

208 Building upon the work of Malinovsky et al. (2024) on their **RAC-LoRA** framework, the update steps
209 in Algorithm 1 can be reformulated as projected gradient steps. The subproblems in lines 6 and 10
210 are typically solved approximately, for instance, by taking a single step of a suitable optimizer like
211 Gradient Descent (**GD**) or its variants. More discussion can be found in Appendix E.

212 While **RAC-LoRA** employs a deterministic choice for which matrix to update, our **Bernoulli-LoRA**
213 framework generalizes this concept by introducing a probabilistic selection at each step. This allows
214 us to express the update for any of our proposed methods in a single, unified form:

$$215 W^{t+1} = W^t - \gamma \hat{G}^t, \quad (7)$$

Setting	Method & Base Gradient Estimator G^t	NC convergence rate	PL convergence rate
(1)	Bernoulli-LoRA-GD (Alg. 2) $G^t = \nabla f(W^t)$	Thm. 1: $\frac{\Delta^0}{\gamma \lambda_{\min} T}$	Thm. 9: $(1 - \gamma \mu \lambda_{\min})^T \Delta^0$
(1)	Bernoulli-LoRA-SGD (Alg. 4) $G^t = g(W^t)$	Thm. 2: $\frac{\Delta^0}{\gamma \lambda_{\min} T} + \frac{\gamma L C_1 \lambda_{\max}}{\lambda_{\min}}$	Thm. 12: $(1 - \gamma \mu \lambda_{\min})^T \Delta^0 + \frac{\gamma L C_1 \lambda_{\max}}{\mu \lambda_{\min}}$
(1)+(3)	Bernoulli-LoRA-MVR (Alg. 5) $G^t = \nabla f_{\xi^t}(W^t) + (1-b)(G^{t-1} - \nabla f_{\xi^t}(W^{t-1}))$	Thm. 3: $\frac{\Phi_1}{\gamma \lambda_{\min} T} + \frac{b \sigma^2 \lambda_{\max}}{(2-b) \lambda_{\min}}$ (1)	Thm. 14: $(1 - \gamma \mu \lambda_{\min})^T \Phi_1 + \frac{b \sigma^2 \lambda_{\max}}{(2-b) \mu \lambda_{\min}}$
(1)+(2)	Bernoulli-LoRA-PAGE (Alg. 6) $G^t = \begin{cases} \nabla f(W^t), & \text{w.p. } q \\ G^{t-1} + \nabla f_{i_t}(W^t) - \nabla f_{i_t}(W^{t-1}), & \text{w.p. } 1-q \end{cases}$	Thm. 4: $\frac{\Phi_2}{\gamma \lambda_{\min} T}$ (2)	Thm. 16: $(1 - \gamma \mu \lambda_{\min})^T \Phi_2$ (2)
(1)+(4)	Fed-Bernoulli-LoRA-QGD (Alg. 7) $G^t = \frac{1}{M} \sum_{l=1}^M \mathcal{Q}_l^t(\nabla f_l(W^t))$	Thm. 5: $\frac{\Delta^0}{\gamma \lambda_{\min} T} + \frac{\gamma L \omega \Delta^* \lambda_{\max}}{M \lambda_{\min}}$	Thm. 18: $(1 - \gamma \mu \lambda_{\min})^T \Delta^0 + \frac{\gamma L^2 \omega \lambda_{\max}}{M \mu \lambda_{\min}}$
(1)+(4)	Fed-Bernoulli-LoRA-MARINA (Alg. 8) $G_l^t = \begin{cases} \nabla f_l(W^t), & \text{w.p. } q \\ G_l^{t-1} + \mathcal{Q}_l^t(\nabla f_l(W^t) - \nabla f_l(W^{t-1})), & \text{w.p. } 1-q \end{cases}$ $G^t = \frac{1}{M} \sum_{l=1}^M G_l^t$	Thm. 6: $\frac{\Phi_2}{\gamma \lambda_{\min} T}$ (2)	Thm. 20: $(1 - \gamma \mu \lambda_{\min})^T \Phi_2$ (2)
(1)+(4)	Fed-Bernoulli-LoRA-EF21 (Alg. 9) $G_l^t = G_l^{t-1} + \mathcal{C}_l^t(\nabla f_l(W^t) - G_l^{t-1})$ $G^t = \frac{1}{M} \sum_{l=1}^M G_l^t$	Thm. 7: $\frac{\Phi_3}{\gamma \lambda_{\min} T}$ (3)	Thm. 22: $(1 - \gamma \mu \lambda_{\min})^T \Phi_3$ (3)

$$\begin{aligned}
 (1) \Phi_1 &:= \Delta^0 + \frac{\gamma}{b(2-b)} \mathcal{G}^0; \\
 (2) \Phi_2 &:= \Delta^0 + \frac{\gamma}{q} \mathcal{G}^0; \\
 (3) \Phi_3 &:= \Delta^0 + \frac{\gamma}{1-\sqrt{1-\beta}} \hat{\mathcal{G}}^0.
 \end{aligned}$$

Table 1: Unified summary of the proposed methods, their base gradient estimators, and convergence rates for smooth non-convex (“NC”) and PL settings. All methods follow the general update rule $W^{t+1} = W^t - \gamma \hat{G}^t$, where the projected estimator \hat{G}^t is defined in (8). The table specifies the definition of the base gradient estimator G^t for each method. Absolute constant factors are omitted. Notation: $\Delta^0 := f(W^0) - f^*$; $\mathcal{G}^0 := \|G^0 - \nabla f(W^0)\|_F^2$; $\hat{\mathcal{G}}^0 := \frac{1}{M} \sum_{l=1}^M \|G_l^0 - \nabla f_l(W^0)\|_F^2$; T is the chain length; ω is the compression parameter; $\Delta^* := f^* - \frac{1}{M} \sum_{l=1}^M f_l^*$; C_1 is a constant from Asm. 4; q is the probability of a full gradient computation; β is the contractive compression parameter; b is the momentum parameter; $\lambda_{\min} = \lambda_{\min}^p := p \lambda_{\min}^{H_B} + (1-p) \lambda_{\min}^{H_A}$, and $\lambda_{\max} = \lambda_{\max}^p := p \lambda_{\max}^{H_B} + (1-p) \lambda_{\max}^{H_A}$.

where \hat{G}^t is the *projected gradient estimator*. It is formed by taking a *base gradient estimator* G^t (e.g., a full gradient, a stochastic gradient, or a variance-reduced one) and projecting it based on the outcome of a Bernoulli trial:

$$\hat{G}^t = \begin{cases} H_B^t G^t, & \text{with probability } p \\ G^t H_A^t, & \text{with probability } 1-p \end{cases}. \quad (8)$$

The specific choice of the base estimator G^t defines the particular algorithm within the Bernoulli-LoRA family. We summarize our proposed methods and their convergence guarantees in Table 1 and describe them next.

6 CONVERGENCE RESULTS

The optimization dynamics of our framework depend on the spectral properties of the expected projection matrix (Section 5.1). To derive non-asymptotic guarantees, we rely on standard modeling abstractions used in the analysis of first-order methods (e.g., Lipschitz smoothness, PL condition). Our results are conditional on these assumptions, consistent with classical analyses of GD, SGD, and FL (Bottou et al., 2018; Bubeck, 2015; Nesterov, 2018; Khaled & Richtárik, 2023).

270 **Assumption 1.** (Positive Expected Projection) Consider the projection matrices associated with the
 271 Left and Right Sketch updates:

272 $H_B := B_S(B_S^\top B_S)^\dagger B_S^\top$ and $H_A := A_S^\top(A_S A_S^\top)^\dagger A_S$,
 273 where \dagger denotes the Moore-Penrose pseudoinverse. We assume that for the sampling distributions
 274 \mathcal{D}_S^B and \mathcal{D}_S^A , the smallest eigenvalues of the expected projection matrices are strictly positive:

$$275 \lambda_{\min}^{H_B} = \lambda_{\min}(\mathbb{E}[H_B]) > 0 \quad \text{and} \quad \lambda_{\min}^{H_A} = \lambda_{\min}(\mathbb{E}[H_A]) > 0.$$

276 **Remark 1** (On the practicality of Assumption 1). At first sight Assumption 1 may look restrictive:
 277 every single projector has eigenvalues in $\{0, 1\}$, so $\lambda_{\min}(H_B) = \lambda_{\min}(H_A) = 0$ whenever $r < m$ or
 278 $r < n$. Crucially, we never require individual projectors to be positive definite, only their expectation
 279 over the sketch distribution. Intuitively, each step updates along a low-dimensional subspace, but the
 280 random subspaces collectively “cover” all directions over time. In fact, the assumption is mild: as
 281 shown in Section D, it is satisfied with $\mathbb{E}[H_B] = \frac{r}{m} I_m$, $\mathbb{E}[H_A] = \frac{r}{n} I_n$ for standard choices such
 282 as Gaussian, i.i.d. uniform, Kaiming-uniform, and SVD-based orthonormal sketches widely used in
 283 practice (Xia et al., 2024; Mao et al., 2025; Zhu et al., 2024; Hayou et al., 2024; Li et al., 2025;
 284 Kopiczko et al., 2023).

285 **Assumption 2.** (Lower Bounded Function) The objective function f has a finite infimum $f^* \in \mathbb{R}$.

286 Following classical literature (Nemirovski et al., 2009; Beck, 2017; Duchi, 2018; Lan, 2020; Drusvy-
 287 atskiy, 2020; Nesterov, 2018), we seek an ε -suboptimal solution for convex (or PL) objectives,
 288 satisfying

$$289 \mathbb{E} \left[f(\hat{W}) - f(W^*) \right] \leq \varepsilon, \quad (9)$$

290 where W^* minimizes f . For smooth non-convex problems, we aim for an ε -stationary point \hat{W} such
 291 that

$$293 \mathbb{E} \left[\left\| \nabla f(\hat{W}) \right\|_F^2 \right] \leq \varepsilon^2. \quad (10)$$

294 We quantify algorithmic efficiency via iteration complexity. To establish convergence rates, we use
 295 the standard assumption of gradient Lipschitz continuity (Bubeck, 2015; Nesterov, 2018; Beck, 2017;
 296 Demidovich et al., 2023b; Khaled & Richtárik, 2023; Bottou et al., 2018; Sun, 2020).

297 **Assumption 3.** (Lipschitz Smooth Gradient) A function f is differentiable, and there exists a constant
 298 $L > 0$ such that

$$300 \|\nabla f(W) - \nabla f(V)\|_F \leq L \|W - V\|_F,$$

301 for all $W, V \in \mathbb{R}^{m \times n}$.

302 To unify our analysis, we define a probability-weighted eigenvalue $\lambda_{\min(\max)}^p := p\lambda_{\min(\max)}^{H_B} + (1 -$
 303 $p)\lambda_{\min(\max)}^{H_A}$. Let \widetilde{W}^T be an iterate drawn randomly from the sequence $\{W^0, W^1, \dots, W^{T-1}\}$, with
 304 the specific sampling distribution depending on the method.

305 We begin by presenting the convergence result for the foundational Bernoulli-LoRA-GD method.

306 **Theorem 1** (Smooth Non-Convex Setting). Let Assumptions 1, 2, and 3 hold, and let the stepsize
 307 satisfy $0 < \gamma \leq \frac{1}{L}$. Then the iterates of Bernoulli-LoRA-GD (Algorithm 2), with matrices \hat{A}^t and \hat{B}^t
 308 computed according to Lemma 10, satisfy

$$311 \mathbb{E} \left[\left\| \nabla f(\widetilde{W}^T) \right\|_F^2 \right] \leq \frac{2\Delta^0}{\gamma\lambda_{\min}^p T},$$

313 where $\Delta^0 := f(W^0) - f^*$.

314 While insightful, full-gradient methods are often impractical for large-scale problems. We therefore
 315 extend our analysis to the stochastic setting, where the gradient is replaced by an unbiased estimator
 316 $g(W)$. For this, we use the general *expected smoothness* assumption.

317 **Assumption 4** (Expected Smoothness (Khaled & Richtárik, 2023)). The stochastic gradient estimator
 318 $g(W)$ satisfies

$$320 \mathbb{E} \left[\|g(W)\|_F^2 \right] \leq 2A_1(f(W) - f^*) + B_1 \cdot \|\nabla f(W)\|_F^2 + C_1,$$

321 for some constants $A_1, B_1, C_1 \geq 0$ and all $W \in \mathbb{R}^{m \times n}$.

322 The following theorem establishes the convergence for Bernoulli-LoRA-SGD. Its proof is in Ap-
 323 pendix H.2.

324 **Theorem 2.** *Let Assumptions 2, 3, and 4 hold, and let the stepsize satisfy*

$$325 \quad 0 < \gamma \leq \min \left\{ \frac{1}{\sqrt{LA_1\lambda_{\max}^p T}}, \frac{1}{LB_1} \left(\frac{\lambda_{\max}^p}{\lambda_{\min}^p} \right)^{-1} \right\}.$$

326 *Then the iterates generated by Bernoulli-LoRA-SGD (Algorithm 4) satisfy*

$$327 \quad \mathbb{E} \left[\left\| \nabla f(\widetilde{W}^T) \right\|_F^2 \right] \leq \frac{6\Delta^0}{\gamma\lambda_{\min}^p T} + \gamma LC_1 \cdot \frac{\lambda_{\max}^p}{\lambda_{\min}^p},$$

328 *where $\Delta^0 := f(W^0) - f^*$.*

329 To analyze our variance-reduced methods, we consider a specific bounded variance assumption.

330 **Assumption 5 (Bounded Variance (Nemirovski et al., 2009)).** *There exists a constant $\sigma > 0$ such*
 331 *that, for all $W \in \mathbb{R}^{m \times n}$,*

$$332 \quad \mathbb{E} [\nabla f_\xi(W)] = \nabla f(W), \quad \mathbb{E} [\|\nabla f_\xi(W) - \nabla f(W)\|_F^2] \leq \sigma^2.$$

333 The next result establishes convergence for Bernoulli-LoRA-MVR.

334 **Theorem 3.** *Let Assumptions 1, 2, 3, and 5 hold, and let the stepsize satisfy $0 < \gamma \leq$*
 335 $\frac{1}{L \left(1 + \sqrt{\frac{2\lambda_{\max}^p(1-b)^2}{b}} \right)}$. *Then the iterates of Bernoulli-LoRA-MVR (Algorithm 5) satisfy*

$$336 \quad \mathbb{E} \left[\left\| \nabla f(\widetilde{W}^T) \right\|_F^2 \right] \leq \frac{2\Delta^0}{\gamma\lambda_{\min}^p T} + \left(\frac{\mathcal{G}^0}{bT} + \frac{2b\sigma^2}{2-b} \right) \cdot \frac{\lambda_{\max}^p}{\lambda_{\min}^p},$$

337 *where $\Delta^0 := f(W^0) - f^*$ and $\mathcal{G}^0 := \|G^0 - \nabla f(W^0)\|_F^2$.*

338 For the finite-sum setting, we analyze Bernoulli-LoRA-PAGE, with its convergence detailed in the
 339 following theorem and proven in Appendix H.4.

340 **Theorem 4.** *Let Assumptions 1, 2, and 3 hold, and let the stepsize satisfy $0 < \gamma \leq \frac{1}{L \left(1 + \sqrt{\frac{1-q}{q} \lambda_{\max}^p} \right)}$.*

341 *Then the iterates of Bernoulli-LoRA-PAGE (Algorithm 6) satisfy*

$$342 \quad \mathbb{E} \left[\left\| \nabla f(\widetilde{W}^T) \right\|_F^2 \right] \leq \frac{2\Delta^0}{\gamma\lambda_{\min}^p T} + \frac{\mathcal{G}^0}{qT} \cdot \frac{\lambda_{\max}^p}{\lambda_{\min}^p},$$

343 *where $\Delta^0 := f(W^0) - f^*$ and $\mathcal{G}^0 := \|G^0 - \nabla f(W^0)\|_F^2$.*

344 We now shift to our Federated Learning variants. The following theorem provides convergence
 345 guarantees for Fed-Bernoulli-LoRA-QGD, with the proof available in Appendix I.1.

346 **Theorem 5.** *Let Assumptions 1, 2, 3, and 11 hold, and let the stepsize satisfy*

347 $0 < \gamma \leq \min \left\{ \frac{1}{L\sqrt{\frac{\omega}{M}}\lambda_{\max}^p T}, \frac{1}{L} \left(\frac{\lambda_{\max}^p}{\lambda_{\min}^p} \right)^{-1} \right\}$. *Then the iterates of Fed-Bernoulli-LoRA-QGD (Algorithm 7) satisfy*

$$348 \quad \mathbb{E} \left[\left\| \nabla f(\widetilde{W}^T) \right\|_F^2 \right] \leq \frac{6\Delta^0}{\gamma\lambda_{\min}^p T} + \frac{2\gamma L\omega\Delta^*}{M} \cdot \frac{\lambda_{\max}^p}{\lambda_{\min}^p},$$

349 *where $\Delta^0 := f(W^0) - f^*$.*

350 Next, we present the convergence result for Fed-Bernoulli-LoRA-MARINA. The proof can be found in
 351 Appendix I.2.

352 **Theorem 6.** *Let Assumptions 1, 2, and 3 hold, and let the stepsize satisfy $0 < \gamma \leq$*
 353 $\frac{1}{L \left(1 + \sqrt{\lambda_{\max}^p \frac{1-q}{q} \cdot \frac{\omega}{M}} \right)}$. *Then the iterates of Fed-Bernoulli-LoRA-MARINA (Algorithm 8) satisfy*

$$354 \quad \mathbb{E} \left[\left\| \nabla f(\widetilde{W}^T) \right\|_F^2 \right] \leq \frac{2\Delta^0}{\gamma\lambda_{\min}^p T} + \frac{\mathcal{G}^0}{qT} \cdot \frac{\lambda_{\max}^p}{\lambda_{\min}^p},$$

355 *where $\Delta^0 := f(W^0) - f^*$ and $\mathcal{G}^0 := \|G^0 - \nabla f(W^0)\|_F^2$.*

356 The convergence of Fed-Bernoulli-LoRA-EF21 is established below, with a detailed proof in
 357 Appendix I.3.

378 **Theorem 7.** Let Assumptions 1, 2, and 3 hold, and let the stepsize satisfy $0 < \gamma \leq \frac{1}{L \left(1 + \frac{\sqrt{\lambda_{\max}^p(1-\beta)}}{1-\sqrt{1-\beta}} \right)}$.
 379
 380 Then the iterates of Fed-Bernoulli-LoRA-EF21 (Algorithm 9) satisfy

$$381 \mathbb{E} \left[\left\| \nabla f(\widetilde{W}^T) \right\|_F^2 \right] \leq \frac{2\Delta^0}{\gamma\lambda_{\min}^p T} + \frac{2\hat{\mathcal{G}}^0}{\beta T} \cdot \frac{\lambda_{\max}^p}{\lambda_{\min}^p},$$

382 where $\Delta^0 := f(W^0) - f^*$ and $\hat{\mathcal{G}}^0 := \frac{1}{M} \sum_{l=1}^M \left\| G_l^0 - \nabla f_l(W^0) \right\|_F^2$.
 383
 384

385 To obtain stronger, linear convergence rates, we introduce the Polyak–Łojasiewicz condition, a
 386 common generalization of strong convexity.
 387

388 **Assumption 6** (Polyak–Łojasiewicz condition (Polyak, 1963; Łojasiewicz, 1963)). There exists
 389 $\mu > 0$ such that

$$390 \frac{1}{2} \left\| \nabla f(W) \right\|_F^2 \geq \mu (f(W) - f^*).$$

391 The next theorem states the convergence of Bernoulli-LoRA-SGD under this condition. It is proven in
 392 Appendix H.2.

393 **Theorem 8.** Let Assumptions 2, 3, 4, and 6 hold, and let the stepsize satisfy

394 $0 < \gamma \leq \min \left\{ \frac{\mu\lambda_{\min}^p}{2LA_1\lambda_{\max}^p}, \frac{2}{\mu\lambda_{\min}^p}, \frac{1}{LB_1} \left(\frac{\lambda_{\max}^p}{\lambda_{\min}^p} \right)^{-1} \right\}$. Then the iterates of Bernoulli-LoRA-SGD
 395 (Algorithm 4) satisfy

$$396 \mathbb{E} [f(W^T) - f^*] \leq \left(1 - \frac{\gamma\mu\lambda_{\min}^p}{2} \right)^T \Delta^0 + \frac{\gamma LC_1}{\mu} \cdot \frac{\lambda_{\max}^p}{\lambda_{\min}^p},$$

397 where $\Delta^0 := f(W^0) - f^*$.
 398

401 All other PL-condition results are relegated to the Appendix.

404 7 EXPERIMENTS

407 To validate our theoretical findings, we conducted numerical experiments across multiple machine
 408 learning tasks.
 409

411 7.1 LINEAR REGRESSION WITH NON-CONVEX REGULARIZATION.

412 We begin with a controlled linear regression problem with non-convex regularization, split into
 413 pre-training and fine-tuning phases. We use (\cdot) for pre-training quantities and $(\hat{\cdot})$ for fine-tuning.

414 During the **pre-training phase**, we solve $\min_{x \in \mathbb{R}^n} \left\{ \tilde{f}(x) := \frac{1}{2\tilde{m}} \left\| \tilde{D}x - \tilde{b} \right\|_2^2 + \tilde{\lambda} \sum_{j=1}^d \frac{x_j^2}{1+x_j^2} \right\}$,

415 where $\tilde{D} \in \mathbb{R}^{\tilde{m} \times n}$, $\tilde{b} \in \mathbb{R}^{\tilde{m}}$, $\tilde{m} = 9 \times 10^4$, and $n = 4096$. We set $\tilde{\lambda} = \left\| \tilde{D} \right\|_2 \approx 18.2$, giving

416 $\tilde{L} \approx 54.7$. We optimize until $\left\| \nabla f(\tilde{x}^*) \right\|^2 \leq 10^{-8}$ to obtain \tilde{x}^* . For the **fine-tuning phase**, we

417 use \tilde{x}^* as the initialization and then solve $\min_{x \in \mathbb{R}^n} \left\{ \hat{f}(x) := \frac{1}{2\hat{m}} \left\| \hat{D}x - \hat{b} \right\|_2^2 + \hat{\lambda} \sum_{j=1}^d \frac{x_j^2}{1+x_j^2} \right\}$,

418 where $\hat{D} \in \mathbb{R}^{\hat{m} \times n}$, $\hat{b} \in \mathbb{R}^{\hat{m}}$, and $\hat{m} = 10^4$. We keep $n = 4096$ and set $\hat{\lambda} = \left\| \hat{D} \right\|_2 \approx 4101.7$,
 419 yielding $\hat{L} \approx 12305.3$. This second phase uses a dataset with notably different characteristics to
 420 mirror realistic domain shifts.
 421

422 **Stochastic setting.** We consider the stochastic setting, comparing RAC-LoRA-SGD, Bernoulli-LoRA-
 423 SGD, and Bernoulli-LoRA-PAGE. In all experiments, we use a batch size of 100, which corresponds
 424 to 1% of the data.
 425

426 Figure 1 shows that Bernoulli-LoRA-PAGE successfully reduces variance and converges to the target
 427 tolerance, whereas all SGD variants stall at a certain accuracy. This underscores the practical
 428 advantage of Bernoulli-LoRA-PAGE over the baseline RAC-LoRA-SGD in the stochastic setting from
 429 an optimization standpoint.
 430

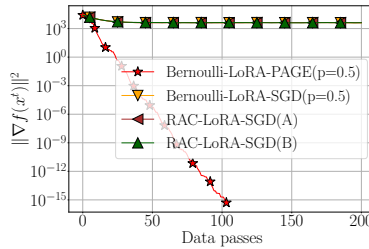


Figure 1: Comparison of **RAC-LoRA-SGD**, **Bernoulli-LoRA-SGD** and **Bernoulli-LoRA-PAGE** on linear regression fine-tuning. Curves with $p = 0.01, 0.2, \dots$ indicate **Bernoulli-LoRA** sampling parameters. **RAC-LoRA-SGD(A)** trains B after resampling A , while **RAC-LoRA-SGD(B)** does the reverse. All methods use $\gamma = c/L$ with c tuned individually.

7.2 MLP ON MNIST

In this section, we evaluate **Bernoulli-LoRA** against established baselines in parameter-efficient fine-tuning, following the setup of [Malinovsky et al. \(2024\)](#).

Methodology. We first pre-train a three-layer MLP on MNIST digits 0–4 ([LeCun et al., 1998](#)), then adapt it with various **LoRA**-type methods to classify digits 5–9. Only unseen classes are used for evaluation. All adaptations use rank $r = 1$ and train for 50 epochs with **AdamW** ([Loshchilov, 2017](#)) ($\beta_1 = 0.9$, $\beta_2 = 0.999$, $\epsilon = 10^{-8}$), a fixed learning rate of 2×10^{-4} , and batch size 128. Each method is run 20 times using different seeds, and Table 2 reports the median accuracy (with standard deviation). For **Bernoulli-LoRA**, we show the best median accuracy among all tested settings.

Method	\mathcal{D}_A	\mathcal{D}_B	Acc. (test)	Train Params
FPFT	-	-	99.5	54,700
LoRA	Gaussian	Zero	85.69 ± 1.60	1K
LoRA	Zero	Gaussian	89.82 ± 0.90	1K
COLA	Gaussian	Zero	93.32 ± 0.50	1K
COLA	Zero	Gaussian	96.55 ± 0.20	1K
AsymmLoRA	Gaussian	Zero	64.04 ± 6.90	133
AsymmLoRA	Zero	Gaussian	74.52 ± 7.20	912
RAC-LoRA	Gaussian	Zero	93.02 ± 0.50	133
RAC-LoRA	Zero	Gaussian	96.49 ± 0.20	912
Bernoulli-LoRA ²	Zero ¹	Gaussian	96.46 ± 0.17	≈ 904

¹ Although **Bernoulli-LoRA** prescribes probabilistic selection from the first iteration, a deterministic assignment of fixed and trainable matrices at initialization yielded better performance.

² Achieved with $p = 0.99$, giving an expected trainable parameter count $p \cdot 912 + (1 - p) \cdot 133 \approx 904$. Here, 912 and 133 are the parameter counts for matrices A and B , respectively.

Table 2: Performance on MNIST classification using an MLP with rank r and scaling $\alpha = 1$. For **AsymmLoRA** and **RAC-LoRA**, only the zero-initialized matrix is trained.

Discussion. From Table 2, standard **LoRA** attains roughly 86% of full-parameter fine-tuning (FPFT) accuracy, indicating room for improvements via chaining. **COLA** improves upon vanilla **LoRA**, though both lack formal convergence guarantees. **AsymmLoRA** approximates **LoRA** in practice ([Sun et al., 2024](#)) but similarly lacks convergence analysis, whereas **RAC-LoRA** and **Bernoulli-LoRA** both boost accuracy and have theoretical backing. Notably, **Bernoulli-LoRA** matches **RAC-LoRA** in generalization and also guarantees convergence. An additional benefit is that **RAC-LoRA** and **Bernoulli-LoRA** each train only one matrix per **LoRA** block, whereas **COLA** needs two. In **RAC-LoRA**, either A or B is trained deterministically; in **Bernoulli-LoRA**, the choice is probabilistic, yielding an expected $pmr + (1 - p)rn$ trainable parameters. This advantage is especially valuable in resource-constrained settings such as Federated Learning.

Detailed configurations, hardware specs, and dataset descriptions are provided in Appendix J.

486 REFERENCES
487

488 Armen Aghajanyan, Luke Zettlemoyer, and Sonal Gupta. Intrinsic dimensionality explains the
489 effectiveness of language model fine-tuning. *arXiv preprint arXiv:2012.13255*, 2020.

490 Dan Alistarh, Demjan Grubic, Jerry Li, Ryota Tomioka, and Milan Vojnovic. QSGD: Communication-
491 efficient SGD via gradient quantization and encoding. *Advances in Neural Information Processing
492 Systems*, 30, 2017.

493 Dan Alistarh, Torsten Hoefer, Mikael Johansson, Nikola Konstantinov, Sarit Khirirat, and Cédric
494 Renggli. The convergence of sparsified gradient methods. *Advances in Neural Information
495 Processing Systems*, 31, 2018.

496 Amir Beck. *First-order methods in optimization*. SIAM, 2017.

497 Dan Biderman, Jacob Portes, Jose Javier Gonzalez Ortiz, Mansheej Paul, Philip Greengard, Connor
498 Jennings, Daniel King, Sam Havens, Vitaliy Chiley, Jonathan Frankle, et al. LoRa learns less and
499 forgets less. *arXiv preprint arXiv:2405.09673*, 2024.

500 Léon Bottou, Frank E Curtis, and Jorge Nocedal. Optimization methods for large-scale machine
501 learning. *SIAM review*, 60(2):223–311, 2018.

502 Tom Brown, Benjamin Mann, Nick Ryder, Melanie Subbiah, Jared D Kaplan, Prafulla Dhariwal,
503 Arvind Neelakantan, Pranav Shyam, Girish Sastry, Amanda Askell, et al. Language models are
504 few-shot learners. *Advances in Neural Information Processing Systems*, 33:1877–1901, 2020.

505 Sébastien Bubeck. Convex optimization: Algorithms and complexity. *Foundations and Trends® in
506 Machine Learning*, 8(3-4):231–357, 2015.

507 Daria Cherniuk, Aleksandr Mikhalev, and Ivan Oseledets. Run lora run: Faster and lighter lora
508 implementations. *arXiv preprint arXiv:2312.03415*, 2023.

509 Ashok Cutkosky and Francesco Orabona. Momentum-based variance reduction in non-convex SGD.
510 *Advances in Neural Information Processing Systems*, 32, 2019.

511 Arif Kerem Dayi and Sitan Chen. Low-rank fine-tuning lies between lazy training and feature learning.
512 In Nika Haghtalab and Ankur Moitra (eds.), *Proceedings of Thirty Eighth Conference on Learning
513 Theory*, volume 291 of *Proceedings of Machine Learning Research*, pp. 1415–1471. PMLR, 30
514 Jun–04 Jul 2025. URL <https://proceedings.mlr.press/v291/dayi25a.html>.

515 Yury Demidovich, Grigory Malinovsky, Egor Shulgin, and Peter Richtárik. MAST: Model-agnostic
516 sparsified training. *arXiv preprint arXiv:2311.16086*, 2023a.

517 Yury Demidovich, Grigory Malinovsky, Igor Sokolov, and Peter Richtárik. A guide through the zoo
518 of biased SGD. *Advances in Neural Information Processing Systems*, 36:23158–23171, 2023b.

519 Yury Demidovich, Grigory Malinovsky, and Peter Richtárik. Streamlining in the riemannian realm: Ef-
520 ficient riemannian optimization with loopless variance reduction. *arXiv preprint arXiv:2403.06677*,
521 2024a.

522 Yury Demidovich, Petr Ostroukhov, Grigory Malinovsky, Samuel Horváth, Martin Takáč, Peter
523 Richtárik, and Eduard Gorbunov. Methods with local steps and random reshuffling for generally
524 smooth non-convex federated optimization. *arXiv preprint arXiv:2412.02781*, 2024b.

525 Jacob Devlin, Ming-Wei Chang, Kenton Lee, and Kristina Toutanova. BERT: pre-training of
526 deep bidirectional transformers for language understanding. In Jill Burstein, Christy Doran, and
527 Thamar Solorio (eds.), *Proceedings of the 2019 Conference of the North American Chapter of
528 the Association for Computational Linguistics: Human Language Technologies, NAACL-HLT
529 2019, Minneapolis, MN, USA, June 2-7, 2019, Volume 1 (Long and Short Papers)*, pp. 4171–
530 4186. Association for Computational Linguistics, 2019. doi: 10.18653/V1/N19-[]1423. URL
531 [https://doi.org/10.18653/v1/n19-\[\]1423](https://doi.org/10.18653/v1/n19-[]1423).

532 Dmitriy Drusvyatskiy. Convex analysis and nonsmooth optimization. *University Lecture*, 2020.

540 John C Duchi. Introductory lectures on stochastic optimization. *The mathematics of data*, 25:99–186,
 541 2018.

542

543 Cong Fang, Chris Junchi Li, Zhouchen Lin, and Tong Zhang. SPIDER: near-optimal non-convex
 544 optimization via stochastic path-integrated differential estimator. *Advances in Neural Information
 545 Processing Systems*, 31, 2018.

546 Ilyas Fatkhullin, Igor Sokolov, Eduard Gorbunov, Zhize Li, and Peter Richtárik. EF21 with
 547 bells & whistles: Practical algorithmic extensions of modern error feedback. *arXiv preprint
 548 arXiv:2110.03294*, 2021.

549

550 Eduard Gorbunov, Konstantin P Burlachenko, Zhize Li, and Peter Richtárik. MARINA: Faster non-
 551 convex distributed learning with compression. In *International Conference on Machine Learning*,
 552 pp. 3788–3798. PMLR, 2021.

553

554 Robert Mansel Gower, Nicolas Loizou, Xun Qian, Alibek Sailanbayev, Egor Shulgin, and Peter
 555 Richtárik. SGD: General analysis and improved rates. In *International conference on machine
 556 learning*, pp. 5200–5209. PMLR, 2019.

557

558 Priya Goyal, Piotr Dollár, Ross Girshick, Pieter Noordhuis, Lukasz Wesolowski, Aapo Kyrola,
 559 Andrew Tulloch, Yangqing Jia, and Kaiming He. Accurate, large minibatch SGD: Training
 560 ImageNet in 1 hour. *arXiv preprint arXiv:1706.02677*, 2017.

561

562 Zeyu Han, Chao Gao, Jinyang Liu, Jeff Zhang, and Sai Qian Zhang. Parameter-efficient fine-tuning
 563 for large models: A comprehensive survey. *arXiv preprint arXiv:2403.14608*, 2024.

564

565 Soufiane Hayou, Nikhil Ghosh, and Bin Yu. The impact of initialization on LoRA finetuning
 566 dynamics. *Advances in Neural Information Processing Systems*, 37:117015–117040, 2024.

567

568 Junxian He, Chunting Zhou, Xuezhe Ma, Taylor Berg-Kirkpatrick, and Graham Neubig. Towards a
 569 unified view of parameter-efficient transfer learning. *arXiv preprint arXiv:2110.04366*, 2021.

570

571 Samuel Horváth, Chen-Yu Ho, Ludovit Horvath, Atal Narayan Sahu, Marco Canini, and Peter
 572 Richtárik. Natural compression for distributed deep learning. In *Mathematical and Scientific
 573 Machine Learning*, pp. 129–141. PMLR, 2022.

574

575 Edward J Hu, Yelong Shen, Phillip Wallis, Zeyuan Allen-Zhu, Yuanzhi Li, Shean Wang, Lu Wang,
 576 Weizhu Chen, et al. LoRA: Low-rank adaptation of large language models. *ICLR*, 1(2):3, 2022.

577

578 Sashank J Reddi, Ahmed Hefny, Suvrit Sra, Barnabas Poczos, and Alexander J Smola. On variance
 579 reduction in stochastic gradient descent and its asynchronous variants. *Advances in Neural
 580 Information Processing Systems*, 28, 2015.

581

582 Uijeong Jang, Jason D. Lee, and Ernest K. Ryu. LoRA training in the NTK regime has no spurious
 583 local minima. *arXiv preprint arXiv:2402.11867*, 2024.

584

585 Peter Kairouz, H. B. McMahan, Brendan Avent, Aurélien Bellet, Mehdi Bennis, Arjun Nitin
 586 Bhagoji, Keith Bonawitz, Zachary B. Charles, Graham Cormode, Rachel Cummings, Rafael
 587 G. L. D’Oliveira, Salim Y. El Rouayheb, David Evans, Josh Gardner, Zachary Garrett, Adrià
 588 Gascón, Badih Ghazi, Phillip B. Gibbons, Marco Gruteser, Zaïd Harchaoui, Chaoyang He, Lie He,
 589 Zhouyuan Huo, Ben Hutchinson, Justin Hsu, Martin Jaggi, Tara Javidi, Gauri Joshi, Mikhail Kho-
 590 dak, Jakub Konečný, Aleksandra Korolova, Farinaz Koushanfar, Oluwasanmi Koyejo, Tancrède
 591 Lepoint, Yang Liu, Prateek Mittal, Mehryar Mohri, Richard Nock, Ayfer Özgür, R. Pagh, Mariana
 592 Raykova, Hang Qi, Daniel Ramage, Ramesh Raskar, Dawn Xiaodong Song, Weikang Song, Sebas-
 593 tian U. Stich, Ziteng Sun, Ananda Theertha Suresh, Florian Tramèr, Praneeth Vepakomma, Jianyu
 594 Wang, Li Xiong, Zheng Xu, Qiang Yang, Felix X. Yu, Han Yu, and Sen Zhao. Advances and open
 595 problems in federated learning. *Found. Trends Mach. Learn.*, 14:1–210, 2019.

596

597 Avetik Karagulyan, Egor Shulgin, Abdurakhmon Sadiev, and Peter Richtárik. SPAM: Stochastic
 598 proximal point method with momentum variance reduction for non-convex cross-device federated
 599 learning. *arXiv preprint arXiv:2405.20127*, 2024.

594 Ahmed Khaled and Peter Richtárik. Better theory for SGD in the nonconvex world. *Transactions*
 595 *on Machine Learning Research*, 2023. ISSN 2835-8856. URL [https://openreview.net/](https://openreview.net/forum?id=AU4qHN2Vks)
 596 [forum?id=AU4qHN2Vks](https://openreview.net/forum?id=AU4qHN2Vks). Survey Certification.

597

598 Ahmed Khaled, Othmane Sebbouh, Nicolas Loizou, Robert M Gower, and Peter Richtárik. Unified
 599 analysis of stochastic gradient methods for composite convex and smooth optimization. *Journal of*
 600 *Optimization Theory and Applications*, 199(2):499–540, 2023.

601 Sarit Khirirat, Abdurakhmon Sadiev, Artem Riabinin, Eduard Gorbunov, and Peter Richtárik.
 602 Error feedback under (L_0, L_1) -smoothness: Normalization and momentum. *arXiv preprint*
 603 *arXiv:2410.16871*, 2024.

604

605 Mikhail Khodak, Renbo Tu, Tian Li, Liam Li, Maria-Florina F Balcan, Virginia Smith, and Ameet
 606 Talwalkar. Federated hyperparameter tuning: Challenges, baselines, and connections to weight-
 607 sharing. *Advances in Neural Information Processing Systems*, 34:19184–19197, 2021.

608 Junsu Kim, Jaeyeon Kim, and Ernest K. Ryu. LoRA training provably converges to a low-rank global
 609 minimum or it fails loudly (but it probably won’t fail). *arXiv preprint arXiv:2502.09376*, 2025.

610

611 Alexander Kolesnikov, Lucas Beyer, Xiaohua Zhai, Joan Puigcerver, Jessica Yung, Sylvain Gelly, and
 612 Neil Houlsby. Big transfer (bit): General visual representation learning. In *Computer Vision–ECCV*
 613 *2020: 16th European Conference, Glasgow, UK, August 23–28, 2020, Proceedings, Part V 16*, pp.
 614 491–507. Springer, 2020.

615 Jakub Konečný, H Brendan McMahan, Felix X Yu, Peter Richtárik, Ananda Theertha Suresh, and
 616 Dave Bacon. Federated learning: Strategies for improving communication efficiency. *arXiv*
 617 *preprint arXiv:1610.05492*, 2016.

618 Dawid J Kopiczko, Tijmen Blankevoort, and Yuki M Asano. Vera: Vector-based random matrix
 619 adaptation. *arXiv preprint arXiv:2310.11454*, 2023.

620

621 Weirui Kuang, Bingchen Qian, Zitao Li, Daoyuan Chen, Dawei Gao, Xuchen Pan, Yuexiang Xie,
 622 Yaliang Li, Bolin Ding, and Jingren Zhou. FederatedScope-LLM: A comprehensive package for
 623 fine-tuning large language models in federated learning. In *Proceedings of the 30th ACM SIGKDD*
 624 *Conference on Knowledge Discovery and Data Mining*, pp. 5260–5271, 2024.

625 Guanghui Lan. *First-order and stochastic optimization methods for machine learning*, volume 1.
 626 Springer, 2020.

627

628 Teven Le Scao, Angela Fan, Christopher Akiki, Ellie Pavlick, Suzana Ilić, Daniel Hesslow, Roman
 629 Castagné, Alexandra Sasha Luccioni, François Yvon, Matthias Gallé, et al. Bloom: A 176b-
 630 parameter open-access multilingual language model. 2023.

631 Yann LeCun, Léon Bottou, Yoshua Bengio, and Patrick Haffner. Gradient-based learning applied to
 632 document recognition. *Proceedings of the IEEE*, 86(11):2278–2324, 1998.

633

634 Chuan Li. Demystifying gpt-3 language model: A technical overview, 2020. URL [https://lambdalabs.com/blog/demystifying-\[\]gpt-\[\]3](https://lambdalabs.com/blog/demystifying-[]gpt-[]3).

635

636 Chunyuan Li, Heerad Farkhoor, Rosanne Liu, and Jason Yosinski. Measuring the intrinsic dimension
 637 of objective landscapes. *arXiv preprint arXiv:1804.08838*, 2018.

638

639 Shiwei Li, Xiandi Luo, Xing Tang, Haozhao Wang, Hao Chen, Weihong Luo, Yuhua Li, Xiuqiang
 640 He, and Ruixuan Li. Beyond zero initialization: Investigating the impact of non-zero initialization
 641 on lora fine-tuning dynamics. *arXiv preprint arXiv:2505.23194*, 2025.

642

643 Zhize Li, Hongyan Bao, Xiangliang Zhang, and Peter Richtárik. PAGE: A simple and optimal
 644 probabilistic gradient estimator for nonconvex optimization. In *International conference on*
 645 *machine learning*, pp. 6286–6295. PMLR, 2021.

646 Stanislaw Lojasiewicz. A topological property of real analytic subsets. *Coll. du CNRS, Les équations*
 647 *aux dérivées partielles*, 117(87-89):2, 1963.

I Loshchilov. Decoupled weight decay regularization. *arXiv preprint arXiv:1711.05101*, 2017.

648 Grigory Malinovsky, Kai Yi, and Peter Richtárik. Variance reduced ProxSkip: Algorithm, theory
 649 and application to federated learning. *Advances in Neural Information Processing Systems*, 35:
 650 15176–15189, 2022.

651

652 Grigory Malinovsky, Umberto Michieli, Hasan Abed Al Kader Hammoud, Taha Ceritli, Hayder
 653 Elesedy, Mete Ozay, and Peter Richtárik. Randomized asymmetric chain of LoRA: The first
 654 meaningful theoretical framework for low-rank adaptation. *arXiv preprint arXiv:2410.08305*,
 655 2024.

656 Yuren Mao, Yuhang Ge, Yijiang Fan, Wenyi Xu, Yu Mi, Zhonghao Hu, and Yunjun Gao. A
 657 survey on lora of large language models. *Frontiers of Computer Science*, 19(7):197605, 2025.
 658 doi: 10.1007/s11704-024-04063-9. URL https://journal.hep.com.cn/fcs/EN/abstract/article_47717.shtml.

659

660 H. B. McMahan, Eider Moore, Daniel Ramage, Seth Hampson, and Blaise Agüera y Arcas.
 661 Communication-efficient learning of deep networks from decentralized data. In *International
 662 Conference on Artificial Intelligence and Statistics*, 2016.

663

664 Fanxu Meng, Zhaohui Wang, and Muhan Zhang. PiSSA: Principal singular values and singular
 665 vectors adaptation of large language models. *Advances in Neural Information Processing Systems*,
 666 37:121038–121072, 2024.

667 Arkadi Nemirovski, Anatoli Juditsky, Guanghui Lan, and Alexander Shapiro. Robust stochastic
 668 approximation approach to stochastic programming. *SIAM Journal on optimization*, 19(4):1574–
 669 1609, 2009.

670

671 Yurii Nesterov. *Introductory lectures on convex optimization: A basic course*, volume 87. Springer
 672 Science & Business Media, 2013.

673

674 Yurii Nesterov. *Lectures on convex optimization*, volume 137. Springer, 2018.

675

676 Andrei Panferov, Yury Demidovich, Ahmad Rammal, and Peter Richtárik. Correlated quantization
 677 for faster nonconvex distributed optimization. *arXiv preprint arXiv:2401.05518*, 2024.

678

679 Matthew E. Peters, Mark Neumann, Mohit Iyyer, Matt Gardner, Christopher Clark, Kenton Lee, and
 680 Luke Zettlemoyer. Deep contextualized word representations. In Marilyn A. Walker, Heng Ji,
 681 and Amanda Stent (eds.), *Proceedings of the 2018 Conference of the North American Chapter
 682 of the Association for Computational Linguistics: Human Language Technologies, NAACL-HLT
 683 2018, New Orleans, Louisiana, USA, June 1-6, 2018, Volume 1 (Long Papers)*, pp. 2227–2237.
 684 Association for Computational Linguistics, 2018. doi: 10.18653/V1/N18-1202. URL <https://doi.org/10.18653/v1/n18-1202>.

685

686 Nhan H Pham, Lam M Nguyen, Dzung T Phan, and Quoc Tran-Dinh. ProxSARAH: An efficient
 687 algorithmic framework for stochastic composite nonconvex optimization. *Journal of Machine
 688 Learning Research*, 21(110):1–48, 2020.

689

690 Boris Polyak. Gradient methods for the minimisation of functionals. *Ussr Computational Mathematics
 691 and Mathematical Physics*, 3:864–878, 1963.

692

693 Alec Radford, Jeffrey Wu, Rewon Child, David Luan, Dario Amodei, Ilya Sutskever, et al. Language
 694 models are unsupervised multitask learners. *OpenAI blog*, 1(8):9, 2019.

695

696 Peter Richtárik and Martin Takáč. Parallel coordinate descent methods for big data optimization.
 697 *Mathematical Programming*, 156:433–484, 2016.

698

699 Peter Richtárik, Igor Sokolov, and Ilyas Fatkhullin. EF21: A new, simpler, theoretically better,
 700 and practically faster error feedback. *Advances in Neural Information Processing Systems*, 34:
 701 4384–4396, 2021.

702

703 Peter Richtárik, Igor Sokolov, Elnur Gasanov, Ilyas Fatkhullin, Zhize Li, and Eduard Gorbunov. 3PC:
 704 Three point compressors for communication-efficient distributed training and a better theory for
 705 lazy aggregation. In *International Conference on Machine Learning*, pp. 18596–18648. PMLR,
 706 2022.

702 Peter Richtárik, Abdurakhmon Sadiev, and Yury Demidovich. A unified theory of stochastic proximal
 703 point methods without smoothness. *arXiv preprint arXiv:2405.15941*, 2024.

704

705 Herbert Robbins and Sutton Monro. A stochastic approximation method. *The annals of mathematical
 706 statistics*, pp. 400–407, 1951.

707

708 Abdurakhmon Sadiev, Grigory Malinovsky, Eduard Gorbunov, Igor Sokolov, Ahmed Khaled,
 709 Konstantin Pavlovich Burlachenko, and Peter Richtárik. Don’t compress gradients in random
 710 reshuffling: Compress gradient differences. In *The Thirty-eighth Annual Conference on Neu-
 711 ral Information Processing Systems*, 2024. URL <https://openreview.net/forum?id=CzPtBzgfae>.

712

713 Frank Seide, Hao Fu, Jasha Droppo, Gang Li, and Dong Yu. 1-bit stochastic gradient descent and its
 714 application to data-parallel distributed training of speech DNNs. In *Fifteenth Annual Conference
 715 of the International Speech Communication Association*, 2014.

716

717 Fanhua Shang, Kaiwen Zhou, Hongying Liu, James Cheng, Ivor W Tsang, Lijun Zhang, Dacheng Tao,
 718 and Licheng Jiao. Vr-sgd: A simple stochastic variance reduction method for machine learning.
IEEE Transactions on Knowledge and Data Engineering, 32(1):188–202, 2018.

719

720 Igor Sokolov and Peter Richtárik. MARINA-P: Superior performance in non-smooth federated
 721 optimization with adaptive stepsizes. *arXiv preprint arXiv:2412.17082*, 2024.

722

723 Sebastian U Stich, Jean-Baptiste Cordonnier, and Martin Jaggi. Sparsified SGD with memory.
Advances in Neural Information Processing Systems, 31, 2018.

724

725 Ruo-Yu Sun. Optimization for deep learning: An overview. *Journal of the Operations Research
 Society of China*, 8(2):249–294, 2020.

726

727 Youbang Sun, Zitao Li, Yaliang Li, and Bolin Ding. Improving LoRA in privacy-preserving federated
 728 learning. *arXiv preprint arXiv:2403.12313*, 2024.

729

730 Alexander Tyurin and Peter Richtárik. DASHA: Distributed nonconvex optimization with com-
 731 munication compression and optimal oracle complexity. In *The Eleventh International Confer-
 732 ence on Learning Representations*, 2023. URL <https://openreview.net/forum?id=VALYpcNr7ul>.

733

734 Evgeniya Vorontsova, Roland Hildebrand, Alexander Gasnikov, and Fedor Stonyakin. Convex
 735 optimization. *arXiv preprint arXiv:2106.01946*, 2021.

736

737 Hanqing Wang, Yixia Li, Shuo Wang, Guanhua Chen, and Yun Chen. MiLoRA: Harnessing minor
 738 singular components for parameter-efficient LLM finetuning. pp. 4823–4836, 2025.

739

740 Wei Wen, Cong Xu, Feng Yan, Chunpeng Wu, Yandan Wang, Yiran Chen, and Hai Li. TernGrad:
 741 Ternary gradients to reduce communication in distributed deep learning. *Advances in Neural
 742 Information Processing Systems*, 30, 2017.

743

744 Wenhan Xia, Chengwei Qin, and Elad Hazan. Chain of LoRA: efficient fine-tuning of language
 745 models via residual learning. *arXiv preprint arXiv:2401.04151*, 2024.

746

747 Ziqing Xu, Hancheng Min, Salma Tarmoun, Enrique Mallada, Lachlan Ewen MacDonald, Jinqi Luo,
 748 and Rene Vidal. Understanding the learning dynamics of LoRA: A gradient flow perspective on
 749 low-rank adaptation in matrix factorization. In *Proceedings of the 28th International Conference
 750 on Artificial Intelligence and Statistics*. PMLR, 2025.

751

752 Kai Yi, Timur Kharisov, Igor Sokolov, and Peter Richtárik. Cohort squeeze: Beyond a single commu-
 753 nication round per cohort in cross-device federated learning. *arXiv preprint arXiv:2406.01115*,
 2024.

754

755 Yang You, Jing Li, Sashank Reddi, Jonathan Hseu, Sanjiv Kumar, Srinadh Bhojanapalli, Xiaodan
 756 Song, James Demmel, Kurt Keutzer, and Cho-Jui Hsieh. Large batch optimization for deep
 757 learning: Training BERT in 76 minutes. *arXiv preprint arXiv:1904.00962*, 2019.

758

Jiacheng Zhu, Kristjan Greenewald, Kimia Nadjahi, Haitz Saez De Ocariz Borde, Rickard Brüel
 759 Gabrielsson, Leshem Choshen, Marzyeh Ghassemi, Mikhail Yurochkin, and Justin Solomon.
 760 Asymmetry in low-rank adapters of foundation models. *arXiv preprint arXiv:2402.16842*, 2024.

756	A APPENDIX	
757		
758	CONTENTS	
759		
760		
761	1 Introduction	1
762		
763	2 Motivation	2
764		
765	3 Problem Statement	2
766		
767	4 Contributions	3
768		
769		
770	5 Bernoulli-LoRA Framework	4
771	5.1 Reformulation as a Projected Gradient Step	4
772		
773	6 Convergence Results	5
774		
775		
776	7 Experiments	8
777	7.1 Linear Regression with Non-convex Regularization	8
778		
779	7.2 MLP on MNIST	9
780		
781	A Appendix	15
782		
783	B Basic Facts and Useful Inequalities	17
784		
785	C Notation	18
786		
787		
788	D Discussion on Positive Expected Projection (Assumption 1)	19
789	D.1 Rotational and signed-permutation symmetries	19
790		
791	D.2 Gaussian initialization	21
792		
793	D.3 i.i.d. uniform initialization on $[-a, a]$	22
794		
795	D.4 Kaiming-uniform initialization	24
796		
797	D.5 Random Orthonormal Sketches via SVD	25
798		
799	E Reformulation as a Projected Gradient Step	29
800		
801	F Core Algorithmic Variants	30
802		
803	G Extensions for Federated Learning	30
804	H Proofs for Core Algorithmic Variants	32
805	H.1 Analysis of Bernoulli-LoRA-GD	32
806		
807	H.1.1 Convergence for Smooth Non-Convex Functions	33
808		
809	H.1.2 Convergence under Polyak-Łojasiewicz Condition	36
	H.1.3 Convergence for Non-Smooth Convex Functions	36

810	H.2 Analysis of Bernoulli-LoRA-SGD	42
811	H.2.1 Convergence for Smooth Non-Convex Functions	42
812	H.2.2 Convergence under Polyak-Łojasiewicz Condition	44
813	H.3 Analysis of Bernoulli-LoRA-MVR	46
814	H.3.1 Convergence for Smooth Non-Convex Functions	48
815	H.3.2 Convergence under Polyak-Łojasiewicz Condition	49
816	H.4 Analysis of Bernoulli-LoRA-PAGE	50
817	H.4.1 Convergence for Smooth Non-Convex Functions	51
818	H.4.2 Convergence under Polyak-Łojasiewicz Condition	52
819		
820	I Proofs for Federated Learning Extensions	53
821	I.1 Analysis of Fed-Bernoulli-LoRA-QGD	53
822	I.1.1 Convergence for Smooth Non-Convex Functions	55
823	I.1.2 Convergence under Polyak-Łojasiewicz Condition	55
824	I.2 Analysis of Fed-Bernoulli-LoRA-MARINA	56
825	I.2.1 Convergence for Smooth Non-Convex Functions	57
826	I.2.2 Convergence under Polyak-Łojasiewicz Condition	58
827	I.3 Analysis of Fed-Bernoulli-LoRA-EF21	59
828	I.3.1 Convergence for Smooth Non-Convex Functions	60
829	I.3.2 Convergence under Polyak-Łojasiewicz Condition	61
830		
831	J Experiments: Missing Details	62
832	J.1 Linear Regression with Non-convex Regularization	62
833		
834		
835		
836		
837		
838		
839		
840		
841		
842		
843		
844		
845		
846		
847		
848		
849		
850		
851		
852		
853		
854		
855		
856		
857		
858		
859		
860		
861		
862		
863		

864 **B BASIC FACTS AND USEFUL INEQUALITIES**
865866 **Tower property.** For any random variables X and Y , we have
867

$$\mathbb{E}[\mathbb{E}[X | Y]] = \mathbb{E}[X]. \quad (11)$$

868
869 **Cauchy-Bunyakovsky-Schwarz inequality.** For any random variables X and Y , we have
870

$$|\mathbb{E}[XY]| \leq \sqrt{\mathbb{E}[X^2]\mathbb{E}[Y^2]}. \quad (12)$$

871
872 **Variance decomposition.** For any random vector $X \in \mathbb{R}^d$ and any non-random $c \in \mathbb{R}^d$, we have
873

$$\mathbb{E}[\|X - c\|_2^2] = \mathbb{E}[\|X - \mathbb{E}[X]\|_2^2] + \|\mathbb{E}[X] - c\|_2^2. \quad (13)$$

874
875 **Jensen's inequality.** For any random vector $X \in \mathbb{R}^d$ and any convex function $g : \mathbb{R}^d \mapsto \mathbb{R}$, we
876 have
877

$$g(\mathbb{E}[X]) \leq \mathbb{E}[g(X)]. \quad (14)$$

878
879
880
881
882
883
884
885
886
887
888
889
890
891
892
893
894
895
896
897
898
899
900
901
902
903
904
905
906
907
908
909
910
911
912
913
914
915
916
917

918 C NOTATION
919

920 For matrices $W \in \mathbb{R}^{m \times n}$, where m and n denote the input and output dimensions respectively,
921 we employ the Frobenius norm $\|\cdot\|_{\text{F}}$, defined as $\|W\|_{\text{F}} = \sqrt{\text{Tr}(W^{\top}W)}$, where $\text{Tr}(\cdot)$ denotes the
922 matrix trace. The inner product between two matrices A and B is denoted by $\langle A, B \rangle = \text{Tr}(A^{\top}B)$.
923 In our low-rank adaptation framework, $B \in \mathbb{R}^{m \times r}$ and $A \in \mathbb{R}^{r \times n}$ represent the factors of rank
924 $r \ll \min\{m, n\}$. We use $\mathcal{O}(\cdot)$ to hide absolute constants. We denote $\Delta^0 := f(W^0) - f^*$,
925 $\mathcal{G}^0 := \|G^0 - \nabla f(W^0)\|_{\text{F}}^2$ and $\hat{\mathcal{G}}^0 := \frac{1}{M} \sum_{l=1}^M \|G_l^0 - \nabla f_l(W^0)\|_{\text{F}}^2$. For differentiable functions
926 f , the gradient $\nabla f(W) \in \mathbb{R}^{m \times n}$ is computed with respect to the trace inner product, while for
927 non-smooth functions, the subgradient $\partial f(W) \in \mathbb{R}^{m \times n}$ is similarly defined. The superscript \dagger
928 denotes the Moore-Penrose pseudoinverse.
929

930
931
932
933
934
935
936
937
938
939
940
941
942
943
944
945
946
947
948
949
950
951
952
953
954
955
956
957
958
959
960
961
962
963
964
965
966
967
968
969
970
971

972 **D DISCUSSION ON POSITIVE EXPECTED PROJECTION (ASSUMPTION 1)**
973

974 Recall that in our Bernoulli-LoRA framework, at each iteration we update only one of the low-rank
975 factors (A or B) while the other is treated as a fixed “sketch” sampled from a prescribed distribution.
976 The resulting updates can be written as projected gradient steps with respect to the full parameter
977 matrix W :

978
$$W^{t+1} = W^t - \gamma \hat{G}^t,$$

979

980 where the projected estimator \hat{G}^t has the form

981
$$\hat{G}^t = \begin{cases} H_B^t G^t, & \text{(left sketch),} \\ G^t H_A^t, & \text{(right sketch),} \end{cases}$$

982

983 and H_B^t and H_A^t are projection matrices defined by the current sketch. In particular, for a left sketch
984 we use

985
$$H_B := B (B^\top B)^\dagger B^\top \in \mathbb{R}^{m \times m}, \quad (15)$$

986

987 with $B \in \mathbb{R}^{m \times r}$, and for a right sketch we use

988
$$H_A := A^\top (A A^\top)^\dagger A \in \mathbb{R}^{n \times n}, \quad (16)$$

989

990 with $A \in \mathbb{R}^{r \times n}$. Here \dagger denotes the Moore–Penrose pseudoinverse. Both H_B and H_A are orthogonal
991 projectors onto the column spaces of B and A^\top , respectively:

992
$$H_B^2 = H_B, \quad H_B^\top = H_B, \quad \text{Tr}(H_B) = \text{rank}(H_B) \leq r,$$

993

994
$$H_A^2 = H_A, \quad H_A^\top = H_A, \quad \text{Tr}(H_A) = \text{rank}(H_A) \leq r.$$

995

996 Our convergence guarantees are derived under Assumption 1, which requires the smallest eigenvalues
997 of the *expected* projection matrices to be strictly positive:

998
$$\lambda_{\min}(\mathbb{E}[H_B]) > 0, \quad \lambda_{\min}(\mathbb{E}[H_A]) > 0.$$

999

1000 At first glance this may appear restrictive: any single projector has eigenvalues in $\{0,1\}$, so
1001 $\lambda_{\min}(H_B) = 0$ and $\lambda_{\min}(H_A) = 0$ whenever $r < m$ or $r < n$. However, the key point is
1002 that we never require *individual* projectors to be positive definite. Instead, we only require that the
1003 *average* projection (over the random sketches) be positive definite. Intuitively, this means that while
1004 each update acts in a low-dimensional subspace, the sequence of random subspaces collectively
1005 “covers” all directions over time.

1006 In this section we show that Assumption 1 is satisfied for several widely used sketch distributions,
1007 including Gaussian, i.i.d. uniform, Kaiming-uniform and random orthonormal initializations. Our
1008 strategy is to exploit symmetry: for many random matrix ensembles the expected projection commutes
1009 with a large group of orthogonal transformations, which forces it to be a scalar multiple of the identity.
1010 The scalar is then determined by the rank/trace constraint.

1007 **D.1 ROTATIONAL AND SIGNED-PERMUTATION SYMMETRIES**
1008

1009 We begin with a classical result: if a matrix commutes with every orthogonal matrix, it must be a
1010 scalar multiple of the identity.

1011 **Lemma 1** (Rotational invariance implies scalar matrix). *Let $M \in \mathbb{R}^{n \times n}$ be a matrix satisfying*

1012
$$M = Q M Q^\top \quad \text{for all orthonormal matrices } Q \in \mathbb{R}^{n \times n}. \quad (17)$$

1013

1014 *Then $M = \alpha I_n$ for some scalar $\alpha \in \mathbb{R}$.*

1015 *Proof.* Condition (17) is equivalent to $QM = MQ$ for all orthogonal Q , i.e., M commutes with
1016 every orthogonal transformation. In particular, M commutes with all rotations.

1017 Since M is a real symmetric matrix (indeed, $M = Q M Q^\top$ for all orthogonal Q implies $M^\top = M$),
1018 it admits an orthonormal eigenbasis. Let v be an eigenvector of M with eigenvalue λ , and normalize
1019 v to unit length:

1020
$$u_1 := \frac{v}{\|v\|}.$$

1021

1022 Then $Mu_1 = \lambda u_1$.

1023 Take any other unit vector u on the sphere S^{n-1} . There exists an orthogonal matrix $Q \in \mathbb{R}^{n \times n}$ such
1024 that $u = Qu_1$ (geometrically, Q is a rotation sending u_1 to u). Using $QM = MQ$,

1025
$$Mu = M(Qu_1) = QMu_1 = Q(\lambda u_1) = \lambda(Qu_1) = \lambda u.$$

1026 Thus *every* unit vector u is an eigenvector of M with the same eigenvalue λ .
 1027

1028 Now let $x \in \mathbb{R}^n$ be arbitrary and non-zero, and write $x = \|x\| u_x$ with $u_x := x / \|x\|$ a unit vector.
 1029 Then

$$1030 \quad Mx = M(\|x\| u_x) = \|x\| Mu_x = \|x\| (\lambda u_x) = \lambda x.$$

1031 So every vector x is an eigenvector with eigenvalue λ , which implies $M = \lambda I_n$. Setting $\alpha = \lambda$
 1032 completes the proof. \square

1033 For many random initializations we do not have full rotational invariance, but we *do* have invariance
 1034 under row permutations and independent sign flips. The corresponding group is the set of all signed
 1035 permutation matrices

$$1037 \quad G_n := \{Q \in \mathbb{R}^{n \times n} : Q = PD, P \text{ permutation, } D = \text{diag}(\pm 1, \dots, \pm 1)\}.$$

1038 The following lemma shows that invariance under G_n is already enough to force a scalar matrix.

1039 **Lemma 2** (Signed-permutation invariance implies scalar matrix). *Let $M \in \mathbb{R}^{n \times n}$ satisfy*

$$1040 \quad QMQ^\top = M \quad \text{for all } Q \in G_n. \quad (18)$$

1041 Then $M = \alpha I_n$ for some $\alpha \in \mathbb{R}$.

1042 *Proof.* We write $M = (m_{ij})$ to mean that m_{ij} is the entry of M in row i and column j .

1043 **Step 1: sign-flip invariance forces M to be diagonal.** First consider only those $Q \in G_n$ that are
 1044 pure sign-flip matrices, i.e.,

$$1047 \quad Q = D = \text{diag}(q_{11}, \dots, q_{nn}), \quad q_{ii} \in \{\pm 1\}.$$

1048 These are orthogonal and belong to G_n (with $P = I_n$). For such Q , the (i,j) -entry of QMQ^\top is

$$1049 \quad (QMQ^\top)_{ij} = \sum_{k,\ell} q_{ik} m_{k\ell} q_{j\ell} = q_{ii} m_{ij} q_{jj},$$

1051 because Q is diagonal. By (18),

$$1052 \quad q_{ii} q_{jj} m_{ij} = m_{ij} \quad \text{for all } i, j \text{ and all } (q_{11}, \dots, q_{nn}) \in \{\pm 1\}^n. \quad (19)$$

1053 Fix any $i \neq j$. We are free to choose q_{ii} and q_{jj} independently. Let $q_{ii} = 1$, $q_{jj} = -1$ and $q_{kk} = 1$
 1054 for all $k \notin \{i, j\}$. Then (19) yields

$$1055 \quad (-1) m_{ij} = m_{ij} \implies m_{ij} = 0.$$

1056 Since $i \neq j$ was arbitrary, all off-diagonal entries vanish, and M must be diagonal:

$$1057 \quad M = \text{diag}(m_{11}, \dots, m_{nn}).$$

1059 **Step 2: permutation invariance forces all diagonal entries to coincide.** Next consider permutation
 1060 matrices $P \in G_n$, i.e., matrices with exactly one entry equal to 1 in each row and column (and
 1061 all other entries 0). Each P is orthogonal and belongs to G_n (with $D = I_n$), so by (18),

$$1062 \quad PMP^\top = M. \quad (20)$$

1063 Let π be the permutation of $\{1, \dots, n\}$ represented by P , so that $Pe_j = e_{\pi(j)}$ for the standard basis
 1064 vectors. One checks that

$$1065 \quad (PMP^\top)_{ii} = m_{\pi(i)\pi(i)},$$

1066 so (20) implies

$$1067 \quad m_{ii} = m_{\pi(i)\pi(i)} \quad \text{for all } i \text{ and all permutations } \pi.$$

1068 This is only possible if all diagonal entries are equal to a common value $\alpha \in \mathbb{R}$:

$$1069 \quad m_{11} = \dots = m_{nn} = \alpha.$$

1070 Therefore $M = \alpha I_n$.

1072 **Step 3: consistency with general signed permutations.** In the argument above we only used two
 1073 special subgroups of G_n : pure sign flips ($P = I_n$) and pure permutations ($D = I_n$). Since both are
 1074 contained in G_n , the assumption (18) applies to them. Once we have shown that $M = \alpha I_n$, it is
 1075 immediate that $QMQ^\top = M$ holds for all $Q = PD \in G_n$:

$$1076 \quad QMQ^\top = (PD)(\alpha I_n)(D^\top P^\top) = \alpha P D D^\top P^\top = \alpha I_n = M.$$

1077 This completes the proof. \square

1078 We will use Lemma 1 in the Gaussian case (where full rotational invariance holds) and Lemma 2 in
 1079 the uniform and Kaiming cases (where we have signed-permutation invariance).

1080 D.2 GAUSSIAN INITIALIZATION
1081

1082 Gaussian sketches are a standard choice in LoRA-style methods; see, for example, [Xia et al. \(2024\)](#);
1083 [Mao et al. \(2025\)](#). The next lemma shows that for Gaussian initialization, the expected projection
1084 matrices are isotropic and their eigenvalues are exactly r/m and r/n .

1085 **Lemma 3** (Expected projections for Gaussian sketches). *Let $r \leq \min\{m,n\}$ and consider two
1086 random matrices:*

1088 $\blacklozenge B \in \mathbb{R}^{m \times r}$ with entries i.i.d. $\mathcal{N}(0,1)$,
1089
1090 $\blacklozenge A \in \mathbb{R}^{r \times n}$ with entries i.i.d. $\mathcal{N}(0,1)$.

1092 Define H_B and H_A as in (15) and (16). Then

$$1093 \mathbb{E}[H_B] = \frac{r}{m} I_m, \quad \mathbb{E}[H_A] = \frac{r}{n} I_n,$$

1094 which implies

$$1095 \lambda_{\min}(\mathbb{E}[H_B]) = \frac{r}{m}, \quad \lambda_{\min}(\mathbb{E}[H_A]) = \frac{r}{n}.$$

1098 *Proof.* We first prove the statement for H_B , then explain the analogous argument for H_A .

1101 **Step 1: $\mathbb{E}[H_B]$ is a scalar multiple of the identity.** Let $B \in \mathbb{R}^{m \times r}$ with i.i.d. $\mathcal{N}(0,1)$ entries, and
1102 let $Q \in \mathbb{R}^{m \times m}$ be an arbitrary orthogonal matrix. By rotational invariance of the standard Gaussian
1103 distribution,

$$1104 QB \stackrel{d}{=} B.$$

1105 Consider the projector built from QB :

$$\begin{aligned} 1106 H_{QB} &:= (QB)((QB)^\top QB)^\dagger (QB)^\top \\ 1107 &= QB(B^\top Q^\top QB)^\dagger B^\top Q^\top \\ 1108 &= QB(B^\top B)^\dagger B^\top Q^\top \\ 1109 &= Q(B(B^\top B)^\dagger B^\top) Q^\top \\ 1110 &= QH_B Q^\top. \end{aligned}$$

1113 Since QB and B are identically distributed, H_{QB} and H_B have the same distribution and hence the
1114 same expectation:

$$1115 \mathbb{E}[H_{QB}] = \mathbb{E}[H_B].$$

1116 Using $H_{QB} = QH_B Q^\top$ and linearity of expectation,

$$1117 \mathbb{E}[H_B] = \mathbb{E}[H_{QB}] = \mathbb{E}[QH_B Q^\top] = Q\mathbb{E}[H_B]Q^\top \quad \text{for all orthogonal } Q \in \mathbb{R}^{m \times m}.$$

1118 By Lemma 1, a matrix commuting with all orthogonal matrices must be a scalar multiple of the
1119 identity. Hence there exists $\alpha \in \mathbb{R}$ such that

$$1120 \mathbb{E}[H_B] = \alpha I_m.$$

1122 **Step 2: determine α via the rank/trace.** For any realization of B with full column rank (which
1123 holds almost surely, since B has i.i.d. continuous entries and $r \leq m$), the matrix H_B is the orthogonal
1124 projector onto the r -dimensional column space of B . Thus

$$1125 \text{rank}(H_B) = r, \quad \text{Tr}(H_B) = r.$$

1126 Taking expectations and using linearity of the trace,

$$1127 \text{Tr}(\mathbb{E}[H_B]) = \mathbb{E}[\text{Tr}(H_B)] = r.$$

1128 Since $\mathbb{E}[H_B] = \alpha I_m$, we also have

$$1129 \text{Tr}(\mathbb{E}[H_B]) = \text{Tr}(\alpha I_m) = \alpha m.$$

1130 Equating the two expressions yields $\alpha m = r$ and hence

$$1131 \mathbb{E}[H_B] = \frac{r}{m} I_m.$$

1133 Because $\mathbb{E}[H_B]$ is a scalar multiple of the identity, all of its eigenvalues are equal to r/m , so in
particular $\lambda_{\min}(\mathbb{E}[H_B]) = r/m$.

1134 **Step 3: the case of H_A .** Now let $A \in \mathbb{R}^{r \times n}$ with i.i.d. $\mathcal{N}(0,1)$ entries and define

$$1135 \quad H_A = A^\top (AA^\top)^\dagger A \in \mathbb{R}^{n \times n}.$$

1136 Note that $A^\top \in \mathbb{R}^{n \times r}$ also has i.i.d. $\mathcal{N}(0,1)$ entries. Repeating the same argument as above with A^\top 1137 in place of B (and with ambient dimension n instead of m) gives

$$1139 \quad \mathbb{E}[H_A] = \frac{r}{n} I_n,$$

1140 and all eigenvalues of $\mathbb{E}[H_A]$ are equal to r/n . This completes the proof. \square

1142 **D.3 I.I.D. UNIFORM INITIALIZATION ON $[-a,a]$**

1144 We now consider sketches whose entries are i.i.d. uniform on an interval $[-a,a]$, where $a > 0$. This
1145 initialization strategy is employed, for instance, in **AsymmLoRA** (Zhu et al., 2024). This setting covers
1146 both simple uniform initializations and serves as a stepping stone to Kaiming-uniform initialization.

1147 Our analysis relies on three ingredients:

- 1149 ◆ *equivariance* of H_B under left multiplication by an orthogonal matrix,
- 1150 ◆ *equivariance* of H_A under right multiplication by an orthogonal matrix,
- 1152 ◆ *signed-permutation invariance* of the distribution of the sketch matrix.

1153 **Lemma 4** (Equivariance of H_B and H_A under orthogonal transforms). *Let $B \in \mathbb{R}^{m \times r}$ with
1154 $\text{rank}(B) = r$ and $A \in \mathbb{R}^{r \times n}$ with $\text{rank}(A) = r$.*

1156 (i) *For any orthogonal matrix $Q \in \mathbb{R}^{m \times m}$, define*

$$1157 \quad H_{QB} := (QB) ((QB)^\top QB)^\dagger (QB)^\top.$$

1158 *Then*

$$1159 \quad H_{QB} = Q H_B Q^\top, \tag{21}$$

1160 *where H_B is defined in (15).*

1162 (ii) *For any orthogonal matrix $R \in \mathbb{R}^{n \times n}$, define*

$$1163 \quad H_{AR} := (AR)^\top ((AR)(AR)^\top)^\dagger (AR).$$

1164 *Then*

$$1165 \quad H_{AR} = R^\top H_A R, \tag{22}$$

1166 *where H_A is defined in (16).*

1168 *Proof.* We prove the two parts separately.

1170 **(i) Equivariance of H_B under left orthogonal transforms.** Recall that $Q \in \mathbb{R}^{m \times m}$ is orthogonal,
1171 so $Q^\top Q = QQ^\top = I_m$. We compute

$$1173 \quad (QB)^\top QB = B^\top Q^\top QB = B^\top B.$$

1174 Hence the inner Gram matrix is unchanged and

$$1175 \quad ((QB)^\top QB)^\dagger = (B^\top B)^\dagger.$$

1176 Substituting into the definition of H_{QB} , we obtain

$$\begin{aligned} 1177 \quad H_{QB} &= QB (B^\top B)^\dagger B^\top Q^\top \\ 1178 &= Q \left(B (B^\top B)^\dagger B^\top \right) Q^\top \\ 1179 &= Q H_B Q^\top, \end{aligned}$$

1181 which proves (21).

1183 **(ii) Equivariance of H_A under right orthogonal transforms.** Now let $R \in \mathbb{R}^{n \times n}$ be orthogonal,
1184 so $R^\top R = RR^\top = I_n$. We first compute the Gram matrix for AR :

$$1185 \quad (AR)(AR)^\top = ARR^\top A^\top = AA^\top.$$

1186 Thus

$$1187 \quad ((AR)(AR)^\top)^\dagger = (AA^\top)^\dagger.$$

1188 Using the definition of H_{AR} , we have
 1189
 1190

$$\begin{aligned} H_{AR} &= (AR)^\top ((AR)(AR)^\top)^\dagger (AR) \\ &= R^\top A^\top (AA^\top)^\dagger AR \\ &= R^\top (A^\top (AA^\top)^\dagger A) R \\ &= R^\top H_{AR}, \end{aligned}$$

1195 which establishes (22). This completes the proof. \square
 1196

1197 **Lemma 5** (Signed-permutation invariance of i.i.d. uniform sketches for B and A). *Let $a > 0$ and
 1198 consider:*

1199 (i) *A random matrix $B_S \in \mathbb{R}^{m \times r}$ with i.i.d. entries $(B_S)_{ij} \sim \text{Unif}([-a, a])$.*
 1200

1201 (ii) *A random matrix $A_S \in \mathbb{R}^{r \times n}$ with i.i.d. entries $(A_S)_{ij} \sim \text{Unif}([-a, a])$.*
 1202

1203 *Let G_m and G_n denote the groups of $m \times m$ and $n \times n$ signed permutation matrices, respectively:*

$$G_m := \{Q \in \mathbb{R}^{m \times m} : Q = PD, P \text{ permutation}, D = \text{diag}(\pm 1, \dots, \pm 1)\},$$

$$G_n := \{R \in \mathbb{R}^{n \times n} : R = P'D', P' \text{ permutation}, D' = \text{diag}(\pm 1, \dots, \pm 1)\}.$$

1204 *Then:*

1205 (i) *For any $Q \in G_m$, the random matrix QB_S has the same distribution as B_S .*
 1206

1207 (ii) *For any $R \in G_n$, the random matrix A_SR has the same distribution as A_S .*

1208 *Proof.* We again treat the two cases separately.
 1209

1210 **(i) Left signed-permutation invariance for B_S .** Write $Q = PD$ with P a permutation matrix
 1211 and $D = \text{diag}(\pm 1, \dots, \pm 1)$. Left-multiplying B_S by P permutes its rows. Since the entries of B_S
 1212 are i.i.d., each row has the same joint distribution, and permuting rows does not change the joint
 1213 distribution of the matrix. Thus PB_S has the same distribution as B_S .

1214 Next, left-multiplication by D flips the sign of some rows. More precisely, if $D = \text{diag}(d_1, \dots, d_m)$
 1215 with $d_i \in \{\pm 1\}$, then the i -th row of DB_S is d_i times the i -th row of B_S . For a single scalar random
 1216 variable $X \sim \text{Unif}([-a, a])$, we have

$$-X \sim \text{Unif}([-a, a]),$$

1217 so flipping signs leaves the marginal distribution of each entry unchanged, and independence across
 1218 entries is preserved (since the sign pattern is deterministic here). Therefore DB_S has the same
 1219 distribution as B_S .

1220 Combining the two transformations, we see that

$$QB_S = P(DB_S)$$

1221 is obtained from B_S by a sequence of operations (row permutations and sign flips) that each leave
 1222 the joint distribution invariant. Hence QB_S has the same distribution as B_S for any $Q \in G_m$.
 1223

1224 **(ii) Right signed-permutation invariance for A_S .** The argument for A_S is analogous, but now
 1225 signed permutations act on the *columns* rather than the rows. Let $R \in G_n$ and write $R = P'D'$ with
 1226 P' a permutation matrix and $D' = \text{diag}(\pm 1, \dots, \pm 1)$.

1227 Right-multiplying A_S by P' permutes its columns. Since the entries of A_S are i.i.d., each column
 1228 has the same joint distribution, and permuting columns preserves the joint distribution of the matrix.
 1229 Thus A_SP' has the same distribution as A_S .

1230 Right-multiplying by D' flips the sign of some columns: if $D' = \text{diag}(d'_1, \dots, d'_n)$ with $d'_j \in \{\pm 1\}$,
 1231 then the j -th column of A_SD' is d'_j times the j -th column of A_S . As above, each sign flip preserves
 1232 the marginal $\text{Unif}([-a, a])$ distribution of every entry, and independence across entries is preserved,
 1233 so A_SD' has the same distribution as A_S .

1234 Combining these, we have

$$A_SR = A_S(P'D') = (A_SP')D',$$

1242 which is obtained from A_S by a sequence of column permutations and column-wise sign flips, each
 1243 of which leaves the joint distribution invariant. Therefore $A_S R$ has the same distribution as A_S for
 1244 any $R \in G_n$.

1245 This proves both claims. □

1247 Combining Lemmas 4 and 5, we can derive the expected projections in closed form.

1248 **Lemma 6** (Expected projections for uniform sketches). *Let $r \leq \min\{m, n\}$ and consider two random
 1249 matrices:*

1251 $\blacklozenge B_S \in \mathbb{R}^{m \times r}$ with entries i.i.d. $\text{Unif}([-a, a])$,
 1252 $\blacklozenge A_S \in \mathbb{R}^{r \times n}$ with entries i.i.d. $\text{Unif}([-a, a])$.

1255 Define

$$1256 \quad H_B := B_S (B_S^\top B_S)^\dagger B_S^\top \in \mathbb{R}^{m \times m}, \\ 1257 \quad H_A := A_S^\top (A_S A_S^\top)^\dagger A_S \in \mathbb{R}^{n \times n}.$$

1258 Assume B_S and A_S have full rank r almost surely. Then

$$1259 \quad \mathbb{E}[H_B] = \frac{r}{m} I_m, \quad \mathbb{E}[H_A] = \frac{r}{n} I_n,$$

1260 and hence

$$1261 \quad \lambda_{\min}(\mathbb{E}[H_B]) = \frac{r}{m}, \quad \lambda_{\min}(\mathbb{E}[H_A]) = \frac{r}{n}.$$

1262 *Proof.* We first treat H_B . For any $Q \in G_m$, Lemma 5(i) gives $Q B_S \stackrel{d}{=} B_S$, and Lemma 4(i) gives
 1263 $H_{QB_S} = Q H_B Q^\top$. Since $Q B_S$ and B_S have the same distribution, we obtain

$$1264 \quad \mathbb{E}[H_B] = \mathbb{E}[H_{QB_S}] = \mathbb{E}[Q H_B Q^\top] = Q \mathbb{E}[H_B] Q^\top \quad \text{for all } Q \in G_m.$$

1265 Thus $\mathbb{E}[H_B]$ commutes with every signed permutation matrix $Q \in G_m$. By Lemma 2, there exists
 1266 $\alpha \in \mathbb{R}$ such that

$$1267 \quad \mathbb{E}[H_B] = \alpha I_m.$$

1268 To determine α , note that for any realization with $\text{rank}(B_S) = r$, H_B is an orthogonal projector of
 1269 rank r , so $\text{Tr}(H_B) = r$. Taking expectations and using linearity of the trace,

$$1270 \quad \text{Tr}(\mathbb{E}[H_B]) = \mathbb{E}[\text{Tr}(H_B)] = r.$$

1271 On the other hand,

$$1272 \quad \text{Tr}(\mathbb{E}[H_B]) = \text{Tr}(\alpha I_m) = \alpha m,$$

1273 so $\alpha m = r$ and hence

$$1274 \quad \mathbb{E}[H_B] = \frac{r}{m} I_m.$$

1275 The argument for H_A is analogous, now working in ambient dimension n . Specifically, $A_S^\top \in \mathbb{R}^{n \times r}$
 1276 has i.i.d. $\text{Unif}([-a, a])$ entries. For any $R \in G_n$, Lemma 5(ii) gives $A_S R \stackrel{d}{=} A_S$, and Lemma 4(ii)
 1277 yields $H_{AR} = R^\top H_A R$. Therefore

$$1278 \quad \mathbb{E}[H_A] = \mathbb{E}[H_{AR}] = \mathbb{E}[R^\top H_A R] = R^\top \mathbb{E}[H_A] R \quad \text{for all } R \in G_n.$$

1279 By Lemma 2 applied in $\mathbb{R}^{n \times n}$, we must have $\mathbb{E}[H_A] = \beta I_n$ for some $\beta \in \mathbb{R}$. As before, $\text{rank}(A_S) =$
 1280 r almost surely, so H_A is a rank- r projector and $\text{Tr}(H_A) = r$ almost surely, implying

$$1281 \quad \text{Tr}(\mathbb{E}[H_A]) = \mathbb{E}[\text{Tr}(H_A)] = r.$$

1282 On the other hand, $\text{Tr}(\mathbb{E}[H_A]) = \text{Tr}(\beta I_n) = \beta n$, so $\beta = r/n$ and hence

$$1283 \quad \mathbb{E}[H_A] = \frac{r}{n} I_n.$$

1284 This completes the proof. □

1285 D.4 KAIMING-UNIFORM INITIALIZATION

1286 In this section, we consider the widely used Kaiming-uniform initializer, implemented in PyTorch
 1287 as `nn.init.kaiming_uniform_`. Kaiming-uniform (He) initialization (?) underlies the default
 1288 linear-layer initialization in PyTorch and is therefore inherited by many practical LoRA implemen-
 1289 tations that keep the framework defaults for adapter weights (e.g. [Hayou et al., 2024](#); ?; [Kopczko](#)

1296 et al., 2023). This initializer samples each entry of a weight matrix independently from a symmetric
 1297 uniform distribution on an interval $[-b, b]$, where the bound $b > 0$ depends on the fan-in and the
 1298 activation function. In particular, the entries are i.i.d., continuous, and symmetric about zero.

1299 Let $B_S \in \mathbb{R}^{m \times r}$ and $A_S \in \mathbb{R}^{r \times n}$ be initialized with Kaiming-uniform. Then B_S and A_S satisfy
 1300 exactly the same symmetry properties as in the uniform $[-a, a]$ case:

1302 ◆ The entries are i.i.d. and symmetric around zero, so the distribution is invariant under row
 1303 permutations and sign flips (i.e. under G_m or G_n).
 1304 ◆ With probability one, $\text{rank}(B_S) = r$ and $\text{rank}(A_S) = r$ (since the entries are drawn from a
 1305 continuous distribution).

1307 Therefore the proof of Lemma 6 applies verbatim.

1309 **Lemma 7** (Expected projections for Kaiming-uniform sketches). *Let $r \leq \min\{m, n\}$ and consider
 1310 two random matrices:*

1311 ◆ $B_S \in \mathbb{R}^{m \times r}$ with entries initialized by Kaiming-uniform,
 1312 ◆ $A_S \in \mathbb{R}^{r \times n}$ with entries initialized by Kaiming-uniform.

1315 Define H_B and H_A as in (15) and (16). Then

$$\mathbb{E}[H_B] = \frac{r}{m} I_m, \quad \mathbb{E}[H_A] = \frac{r}{n} I_n,$$

1318 and hence

$$\lambda_{\min}(\mathbb{E}[H_B]) = \frac{r}{m}, \quad \lambda_{\min}(\mathbb{E}[H_A]) = \frac{r}{n}.$$

1321 *Proof.* Because Kaiming-uniform draws each entry independently from a symmetric uniform distribution $[-b, b]$, the distribution of B_S is invariant under any signed permutation of rows: permuting
 1322 rows leaves the joint law unchanged, and multiplying any row by -1 preserves the marginal law of
 1323 each entry (by symmetry). Thus $QB_S \stackrel{d}{=} B_S$ for all $Q \in G_m$, and the same holds for A_S^\top with G_n .
 1325

1326 The rest of the argument is exactly as in Lemma 6: by combining Lemma ?? with signed-permutation
 1327 invariance, we conclude that $\mathbb{E}[H_B] = \alpha I_m$ and $\mathbb{E}[H_A] = \beta I_n$ for some scalars $\alpha, \beta \in \mathbb{R}$. Since H_B
 1328 and H_A are rank- r projectors almost surely, $\text{Tr}(H_B) = r$ and $\text{Tr}(H_A) = r$, and the trace identities
 1329 $\text{Tr}(\mathbb{E}[H_B]) = \alpha m = r$, $\text{Tr}(\mathbb{E}[H_A]) = \beta n = r$
 1330 imply $\alpha = r/m$ and $\beta = r/n$. This yields the stated formulas. \square

1332 In summary, for Gaussian, i.i.d. uniform, and Kaiming-uniform sketch distributions, the expected
 1333 projection matrices are isotropic:

$$\mathbb{E}[H_B] = \frac{r}{m} I_m, \quad \mathbb{E}[H_A] = \frac{r}{n} I_n,$$

1334 and Assumption 1 holds with $\lambda_{\min}^H = \min\{r/m, r/n\} > 0$. This shows that the positive expected
 1335 projection condition is naturally satisfied by a broad class of standard initialization schemes used in
 1336 LoRA and its variants.

1337

1338 D.5 RANDOM ORTHONORMAL SKETCHES VIA SVD

1342 We now consider the initialization where a dense random matrix $W \in \mathbb{R}^{m \times n}$ with i.i.d. entries
 1343 $W_{ij} \sim \text{Unif}([-a, a])$ is first sampled, and then orthonormal sketches are obtained from its singular
 1344 vectors. Specifically, let $W = U \Sigma V^\top$ be an SVD with singular values arranged in strictly decreasing
 1345 order, and set

$$B_S(W) := U_{[:,1:r]} \in \mathbb{R}^{m \times r},$$

$$A_S(W) := V_{[:,1:r]}^\top \in \mathbb{R}^{r \times n}.$$

1346 By construction,

$$B_S(W)^\top B_S(W) = I_r, \quad A_S(W) A_S(W)^\top = I_r.$$

1350 In particular, when we plug $B_S(W)$ and $A_S(W)$ into the general projector definitions
 1351

$$1352 \quad H_B := B_S(W) (B_S(W)^\top B_S(W))^\dagger B_S(W)^\top \in \mathbb{R}^{m \times m},$$

$$1353 \quad H_A := A_S(W)^\top (A_S(W) A_S(W)^\top)^\dagger A_S(W) \in \mathbb{R}^{n \times n},$$

1354 the pseudo-inverse is simply the identity (because $B_S(W)^\top B_S(W) = A_S(W) A_S(W)^\top = I_r$), so
 1355

$$1356 \quad H_B(W) = B_S(W) B_S(W)^\top = U_{[:,1:r]} U_{[:,1:r]}^\top \in \mathbb{R}^{m \times m},$$

$$1357 \quad H_A(W) = A_S(W)^\top A_S(W) = V_{[:,1:r]} V_{[:,1:r]}^\top \in \mathbb{R}^{n \times n}.$$

1358 Both $H_B(W)$ and $H_A(W)$ are orthogonal projectors of rank r , with eigenvalues $\{1\}$ on the chosen
 1359 r -dimensional subspace and $\{0\}$ on its orthogonal complement.

1360 This type of initialization (taking $U_{[:,1:r]}$ or $V_{[:,1:r]}$ from the SVD of a dense random matrix) appears,
 1361 for example, in the experimental studies by [Zhu et al. \(2024\)](#), and is closely related to the orthonormal
 1362 constructions used in [OLoRA](#) (?).

1363 Our first goal is to understand how the sketch projectors $H_B(W)$ and $H_A(W)$ transform when we
 1364 apply signed permutations to the rows or columns of W .
 1365

1366 **Lemma 8** (Equivariance of SVD-based left and right sketches under signed permutations). *Let
 1367 $W \in \mathbb{R}^{m \times n}$ be any matrix with SVD $W = U \Sigma V^\top$, where $\Sigma = \text{diag}(\sigma_1, \dots, \sigma_d)$ with strictly
 1368 decreasing singular values $\sigma_1 > \dots > \sigma_d > 0$ (here $d = \text{rank}(W)$). Define*

$$1369 \quad B_S(W) := U_{[:,1:r]} \in \mathbb{R}^{m \times r}, \quad H_B(W) := B_S(W) B_S(W)^\top,$$

$$1370 \quad A_S(W) := V_{[:,1:r]}^\top \in \mathbb{R}^{r \times n}, \quad H_A(W) := A_S(W)^\top A_S(W).$$

1371 Then:

1372 (i) For any signed permutation $Q \in G_m$, consider an SVD of QW with the singular values ordered
 1373 in the same descending fashion. Up to column-wise sign flips, the left singular vectors of QW are
 1374 QU , and the corresponding left-sketch projector satisfies

$$1375 \quad H_B(QW) = Q H_B(W) Q^\top. \quad (23)$$

1376 (ii) For any signed permutation $R \in G_n$, consider an SVD of WR with the singular values ordered in
 1377 the same descending fashion. Up to column-wise sign flips, the right singular vectors of WR are
 1378 $R^\top V$, and the corresponding right-sketch projector satisfies

$$1379 \quad H_A(WR) = R^\top H_A(W) R. \quad (24)$$

1384 *Proof.* We prove (i) and (ii) separately.

1385 (i) **Left sketches: effect of $Q \in G_m$ acting on rows.** Since $Q \in G_m$ is orthogonal, QW admits
 1386 the factorization

$$1387 \quad QW = (QU) \Sigma V^\top,$$

1388 where QU is also orthogonal. The singular values of QW are the same as those of W , namely
 1389 $\sigma_1, \dots, \sigma_d$, and by assumption they are strictly ordered: $\sigma_1 > \dots > \sigma_d > 0$.

1390 Consider an SVD of QW with singular values written in descending order:

$$1391 \quad QW = U' \Sigma V'^\top,$$

1392 where U' and V' are orthogonal. The uniqueness properties of the SVD when all singular values are
 1393 distinct imply that U' and V' are determined by QU and V up to sign flips of individual singular
 1394 vectors. More precisely, there exists a diagonal orthogonal matrix $R = \text{diag}(\pm 1, \dots, \pm 1) \in \mathbb{R}^{d \times d}$
 1395 such that

$$1396 \quad U' = QUR, \quad V' = VR.$$

1397 (If some singular values were repeated, R could mix singular vectors within blocks corresponding to
 1398 equal singular values; the strict-ordering assumption rules this out.)

1399 Let $R_{1:r}$ denote the leading $r \times r$ diagonal block of R . Then the first r left singular vectors of QW
 1400 can be written as

$$1401 \quad B_S(QW) = U'_{[:,1:r]} = Q U_{[:,1:r]} R_{1:r}.$$

1404 The corresponding projector is

$$\begin{aligned}
 H_B(QW) &= B_S(QW)B_S(QW)^\top \\
 &= (QU_{[:,1:r]}R_{1:r})(QU_{[:,1:r]}R_{1:r})^\top \\
 &= QU_{[:,1:r]}R_{1:r}R_{1:r}^\top U_{[:,1:r]}^\top Q^\top \\
 &= QU_{[:,1:r]}U_{[:,1:r]}^\top Q^\top \\
 &= QH_B(W)Q^\top,
 \end{aligned}$$

1412 since $R_{1:r}R_{1:r}^\top = I_r$. This proves (23).

1414 **(ii) Right sketches: effect of $R \in G_n$ acting on columns.** Now consider WR with $R \in G_n$ 1415 orthogonal. Using the SVD of W , we have

$$WR = U\Sigma V^\top R = U\Sigma (R^\top V)^\top.$$

1418 Since $R^\top V$ is orthogonal, this is an SVD of WR with left singular matrix U and right singular matrix 1419 $\tilde{V} := R^\top V$. The singular values remain $\sigma_1, \dots, \sigma_d$, strictly ordered.

1420 Let

$$WR = \tilde{U}\Sigma\tilde{V}^\top$$

1422 be any SVD of WR with singular values in descending order. By the same uniqueness argument, 1423 there exists a diagonal orthogonal matrix $S = \text{diag}(\pm 1, \dots, \pm 1) \in \mathbb{R}^{d \times d}$ such that

$$\tilde{U} = US, \quad \tilde{V} = \tilde{V}_0 S = (R^\top V)S.$$

1425 Let $V_r = V_{[:,1:r]}$ and $S_{1:r}$ be the leading $r \times r$ block of S . Then the first r right singular vectors of 1426 WR are given by the first r columns of \tilde{V} :

$$\begin{aligned}
 \tilde{V}_{[:,1:r]} &= (R^\top VS)_{[:,1:r]} \\
 &= R^\top V_{[:,1:r]} S_{1:r}.
 \end{aligned}$$

1430 Recalling that $A_S(W) = V_r^\top$, the right-sketch matrix for WR is

$$\begin{aligned}
 A_S(WR) &= \tilde{V}_{[:,1:r]}^\top \\
 &= S_{1:r}^\top V_{[:,1:r]}^\top R \\
 &= S_{1:r} V_r^\top R,
 \end{aligned}$$

1435 where we used that $S_{1:r}$ is diagonal with entries ± 1 , so $S_{1:r}^\top = S_{1:r}$.

1436 The corresponding right-sketch projector is

$$\begin{aligned}
 H_A(WR) &= A_S(WR)^\top A_S(WR) \\
 &= (S_{1:r} V_r^\top R)^\top (S_{1:r} V_r^\top R) \\
 &= R^\top V_r S_{1:r}^\top S_{1:r} V_r^\top R \\
 &= R^\top V_r V_r^\top R \\
 &= R^\top H_A(W)R,
 \end{aligned}$$

1444 since $S_{1:r}^\top S_{1:r} = I_r$. This proves (24) and completes the proof. \square

1446 We now combine this equivariance with the signed-permutation invariance of the i.i.d. uniform matrix 1447 W to obtain closed-form expressions for the expected projectors.

1449 **Lemma 9** (Expected projections for SVD-based uniform orthonormal sketches). *Let $W \in \mathbb{R}^{m \times n}$ 1450 have i.i.d. entries $W_{ij} \sim \text{Unif}([-a, a])$, and let $H_B(W)$ and $H_A(W)$ be defined as above from an 1451 SVD $W = U\Sigma V^\top$ with strictly decreasing singular values. Then*

$$\mathbb{E}[H_B(W)] = \frac{r}{m} I_m, \quad \mathbb{E}[H_A(W)] = \frac{r}{n} I_n,$$

1453 and hence

$$\lambda_{\min}(\mathbb{E}[H_B(W)]) = \frac{r}{m} > 0, \quad \lambda_{\min}(\mathbb{E}[H_A(W)]) = \frac{r}{n} > 0.$$

1454 *Proof.* We treat $H_B(W)$ and $H_A(W)$ in turn.

1458 **Left-sketch projector** $H_B(W)$. The rows of W are i.i.d. vectors in \mathbb{R}^n with continuous, symmetric
 1459 entries. For any signed permutation $Q \in G_m$, left-multiplication by Q permutes and flips the signs
 1460 of rows, so

$$1461 \quad QW \stackrel{d}{=} W \quad \text{for all } Q \in G_m.$$

1462 By Lemma 8(i),

$$1463 \quad H_B(QW) = QH_B(W)Q^\top.$$

1464 Since QW and W are identically distributed, $H_B(QW)$ and $H_B(W)$ are identically distributed, and
 1465 hence

$$1466 \quad \mathbb{E}[H_B(W)] = \mathbb{E}[H_B(QW)] = \mathbb{E}[QH_B(W)Q^\top] = Q\mathbb{E}[H_B(W)]Q^\top \quad \text{for all } Q \in G_m.$$

1467 Thus $\mathbb{E}[H_B(W)]$ commutes with every signed permutation matrix in G_m , and by Lemma 2 there
 1468 exists $\alpha \in \mathbb{R}$ such that

$$1469 \quad \mathbb{E}[H_B(W)] = \alpha I_m.$$

1470 To determine α , recall that $B_S(W)$ has orthonormal columns, so $H_B(W) = B_S(W)B_S(W)^\top$ is a
 1471 rank- r projector with

$$1473 \quad \text{Tr}(H_B(W)) = r$$

1474 for every realization. Taking expectations and using linearity of the trace,

$$1475 \quad \text{Tr}(\mathbb{E}[H_B(W)]) = \mathbb{E}[\text{Tr}(H_B(W))] = r.$$

1476 On the other hand,

$$1477 \quad \text{Tr}(\mathbb{E}[H_B(W)]) = \text{Tr}(\alpha I_m) = \alpha m,$$

1478 so $\alpha m = r$ and hence $\alpha = r/m$. Therefore

$$1479 \quad \mathbb{E}[H_B(W)] = \frac{r}{m} I_m.$$

1480 **Right-sketch projector** $H_A(W)$. The columns of W are also i.i.d. vectors in \mathbb{R}^m with continuous,
 1481 symmetric entries. For any signed permutation $R \in G_n$, right-multiplication by R permutes and flips
 1482 the signs of columns, so

$$1484 \quad WR \stackrel{d}{=} W \quad \text{for all } R \in G_n.$$

1485 By Lemma 8(ii),

$$1486 \quad H_A(WR) = R^\top H_A(W)R.$$

1487 Since WR and W have the same distribution, the random matrices $H_A(WR)$ and $H_A(W)$ are
 1488 identically distributed. Hence

$$1489 \quad \mathbb{E}[H_A(W)] = \mathbb{E}[H_A(WR)] = \mathbb{E}[R^\top H_A(W)R] = R^\top \mathbb{E}[H_A(W)]R \quad \text{for all } R \in G_n.$$

1490 Applying Lemma 2 (now in dimension n) shows that there exists $\beta \in \mathbb{R}$ such that

$$1491 \quad \mathbb{E}[H_A(W)] = \beta I_n.$$

1492 Again, $A_S(W)$ has orthonormal rows, so $H_A(W) = A_S(W)^\top A_S(W)$ is a rank- r projector and

$$1493 \quad \text{Tr}(H_A(W)) = r$$

1494 for every realization. Taking expectations,

$$1495 \quad \text{Tr}(\mathbb{E}[H_A(W)]) = \mathbb{E}[\text{Tr}(H_A(W))] = r.$$

1496 But $\text{Tr}(\mathbb{E}[H_A(W)]) = \text{Tr}(\beta I_n) = \beta n$, hence $\beta n = r$ and therefore $\beta = r/n$. Thus

$$1497 \quad \mathbb{E}[H_A(W)] = \frac{r}{n} I_n.$$

1498 This completes the proof. □

1499 **Remark 2.** Each individual projector $H_B(W)$ (resp. $H_A(W)$) is rank-deficient, with eigenvalues
 1500 $\{1\}$ on an r -dimensional subspace and $\{0\}$ on its orthogonal complement. The lemma above concerns
 1501 the expectation of these projectors over the randomness of W . Because the subspace spanned by the
 1502 leading singular vectors is random and, in distribution, symmetric under signed permutations, the
 1503 expectation $\mathbb{E}[H_B(W)]$ (resp. $\mathbb{E}[H_A(W)]$) becomes a full-rank, isotropic matrix $(r/m)I_m$ (resp.
 1504 $(r/n)I_n$). This is exactly analogous to the classical fact that if u is a random unit vector in \mathbb{R}^d , then
 1505 $\mathbb{E}[uu^\top] = (1/d)I_d$ even though uu^\top has rank 1 for every realization.

1507

1508

1509

1510

1511

1512 E REFORMULATION AS A PROJECTED GRADIENT STEP
1513

1514 Following the approach of [Malinovsky et al. \(2024\)](#), let's consider the update for the trainable matrix
1515 \hat{A}^t in the Left Sketch case. Taking a single [GD](#) step on the subproblem corresponds to minimizing a
1516 quadratic approximation of the objective. This yields the solution for \hat{A}^t :

$$1518 \hat{A}^t = -\eta \left((B_S^t)^\top B_S^t \right)^\dagger (B_S^t)^\top \nabla f(W^t),$$

1519 where η is a learning rate for the subproblem and \dagger denotes the Moore-Penrose pseudoinverse.
1520 Substituting this into the update for W^{t+1} gives:

$$1521 W^{t+1} = W^t + \frac{\alpha}{r} B_S^t \hat{A}^t = W^t - \frac{\alpha\eta}{r} B_S^t \left((B_S^t)^\top B_S^t \right)^\dagger (B_S^t)^\top \nabla f(W^t) \\ 1522 = W^t - \gamma H_B^t \nabla f(W^t),$$

1523 where we define the effective stepsize $\gamma := \frac{\alpha\eta}{r}$ and the projection matrix $H_B^t :=$
1524 $B_S^t \left((B_S^t)^\top B_S^t \right)^\dagger (B_S^t)^\top$. A similar derivation for the Right Sketch case gives the update:

$$1525 W^{t+1} = W^t - \gamma \nabla f(W^t) H_A^t,$$

1526 where $H_A^t := (A_S^t)^\top \left(A_S^t (A_S^t)^\top \right)^\dagger A_S^t$. This reformulation reveals that both Left and Right sketch
1527 updates are equivalent to applying a standard gradient-based update, but projected onto a randomly
1528 chosen low-rank subspace.

1529
1530
1531
1532
1533
1534
1535
1536
1537
1538
1539
1540
1541
1542
1543
1544
1545
1546
1547
1548
1549
1550
1551
1552
1553
1554
1555
1556
1557
1558
1559
1560
1561
1562
1563
1564
1565

1566 **F CORE ALGORITHMIC VARIANTS**
15671568 **Bernoulli-LoRA-GD.** The simplest instantiation of our framework is **Bernoulli-LoRA-GD** (Algorithm 2). This method serves as a foundational building block and a starting point for more elaborate
1569 variants. It uses the full gradient of the objective function as its base estimator, i.e., $G^t = \nabla f(W^t)$.
1570 While impractical for large-scale deep learning, its analysis provides crucial insights into the conver-
1571 gence behavior of the Bernoulli-LoRA mechanism under idealized, deterministic conditions.
15721573
1574 **Bernoulli-LoRA-SGD.** **Stochastic Gradient Descent (SGD)** (Robbins & Monro, 1951) is a highly
1575 effective and widely utilized algorithm for training a variety of machine learning models. The latest
1576 advancements in deep learning training methods are all based on different variations of **SGD** (Sun,
1577 2020). Its advantage over **GD** is that it uses stochastic gradients for updates, rather than relying on
1578 full gradients. Within our framework, we develop **Bernoulli-LoRA-SGD**, where the base estimator G^t
1579 is a general unbiased stochastic gradient of f at W^t .
15801581 **Bernoulli-LoRA-PAGE.** Several optimal algorithms exist for addressing non-convex optimization
1582 problems, such as **SPIDER** (Fang et al., 2018) and **SARAH** (Pham et al., 2020). However, their
1583 optimality is supported by a known lower bound that applies only in the small data setting. In
1584 contrast, **ProbAbilistic Gradient Estimator (PAGE)** (Li et al., 2021) stands out for its simplicity, ease
1585 of implementation, and ability to achieve optimal convergence in non-convex optimization. **PAGE**
1586 alternates between a full gradient update with probability q_t and a low-cost gradient adjustment with
1587 probability $1 - q_t$. **Bernoulli-LoRA-PAGE** is a new method based on **PAGE** within our **Bernoulli-LoRA**
1588 framework.
15891590 **Bernoulli-LoRA-MVR.** VR methods outperform **SGD** in reaching first-order critical points but
1591 often require finely tuned learning rates and large batch sizes to be effective. To overcome these
1592 challenges, **Momentum Variance Reduction (MVR)** (Cutkosky & Orabona, 2019) was introduced for
1593 server-only stochastic non-convex optimization. **MVR** uses a modified momentum technique to reduce
1594 variance without relying on large batch sizes. Several works employ this powerful approach (Tyurin &
1595 Richtárik, 2023; Karagulyan et al., 2024). We propose **Bernoulli-LoRA-MVR**, where the base estimator
1596 G^t is updated using the MVR rule: a combination of the current stochastic gradient and a momentum
1597 term that incorporates the difference between past estimators and gradients.
15981599 **G EXTENSIONS FOR FEDERATED LEARNING**
16001601 **Sun et al. (2024)** identified instability in **LoRA**, arising from the mismatch between local clients simul-
1602 taneously optimizing two low-rank matrices and the central server aggregating them independently.
1603 Factors such as data heterogeneity, multi-step local updates, and the amplification of additive noise
1604 applied to gradients for ensuring differential privacy (DP) significantly impact the process. Addition-
1605 ally, the final performance is highly sensitive to hyperparameter choices. Their proposed solution
1606 centers on keeping the randomly initialized non-zero matrices fixed while exclusively fine-tuning
1607 the zero-initialized ones. Based on this asymmetric approach, **Malinovsky et al. (2024)** proposed a
1608 distributed method **Fed-RAC-LoRA**.
16091610 We develop the theory further by incorporating compression, VR and EF techniques into FL methods
1611 for **LoRA** within the novel **Bernoulli-LoRA** framework.
16121613 The effectiveness of a distributed training method is primarily measured by its communication
1614 complexity, defined as the product of the required communication rounds and the communication
1615 volume per round. Following common practice, we assume client-to-server communication is the
1616 main bottleneck and exclude server-to-client communication from our analysis.
16171618 **Fed-Bernoulli-LoRA-QGD.** A key challenge for distributed methods lies in the high communica-
1619 tion cost of gradient updates. Lossy compression techniques, such as **QSGD** (Alistarh et al., 2017),
1620 address this by enabling clients to send quantized gradients. We design **Fed-Bernoulli-LoRA-QGD**
1621 based on **QSGD**. The clients send compressed versions of their gradients. The base estimator G^t is
1622 formed by averaging the compressed local gradients received from all clients.
1623

1620 **Fed-Bernoulli-LoRA-MARINA.** MARINA (Gorbunov et al., 2021) is a communication-efficient
 1621 method for non-convex distributed learning on heterogeneous datasets that uses a novel gradient
 1622 difference compression strategy. Its biased gradient estimator underpins its strong theoretical and
 1623 practical performance, with proven communication complexity bounds surpassing all prior first-order
 1624 methods. We propose Fed-Bernoulli-LoRA-MARINA, where each client’s local estimator G_l^t is updated
 1625 either with a full local gradient (with probability q) or by adding a compressed gradient difference to
 1626 its previous estimator. The server’s base estimator G^t is the average of these local estimators.

1627 **Fed-Bernoulli-LoRA-EF21.** Error Feedback (EF) (Seide et al., 2014; Stich et al., 2018; Alistarh
 1628 et al., 2018; Richtárik et al., 2021) is a widely adopted technique for stabilizing training with
 1629 contractive compressors. We propose Fed-Bernoulli-LoRA-EF21, based on the modern EF21. Here,
 1630 each client updates its local estimator G_l^t by adding a compressed version of the difference between
 1631 the current local gradient and the previous local estimator. The server’s base estimator G^t is again
 1632 the average of the clients’ estimators.

1633
 1634
 1635
 1636
 1637
 1638
 1639
 1640
 1641
 1642
 1643
 1644
 1645
 1646
 1647
 1648
 1649
 1650
 1651
 1652
 1653
 1654
 1655
 1656
 1657
 1658
 1659
 1660
 1661
 1662
 1663
 1664
 1665
 1666
 1667
 1668
 1669
 1670
 1671
 1672
 1673

1674 **H PROOFS FOR CORE ALGORITHMIC VARIANTS**
16751676
1677 **H.1 ANALYSIS OF BERNoulli-LoRA-GD**
16781679
1680 **Algorithm 2** Bernoulli-LoRA-GD
1681

```

1: Parameters: pre-trained model  $W^0 \in \mathbb{R}^{m \times n}$ , rank  $r \ll \min\{m, n\}$ , scaling factor  $\alpha > 0$ ,
2: stepsize  $\gamma_t$  chain length  $T$ , sketch distribution  $\mathcal{D}_S^B$  or  $\mathcal{D}_S^A$ , Bernoulli probability  $p$ 
3: for  $t = 0, 1, \dots, T - 1$  do
4:   Sample  $c^t \sim \text{Be}(p)$  Bernoulli random variable
5:   Sample  $B_S^t \sim \mathcal{D}_S^B$  Left sketch
6:    $\hat{A}^t = -\eta \left( (B_S^t)^\top B_S^t \right)^\dagger (B_S^t)^\top \nabla f(W^t)$ 
7:    $W^{t+1} = W^t + \frac{\alpha}{r} B_S^t \hat{A}^t$ 
8:   else
9:     Sample  $A_S^t \sim \mathcal{D}_S^A$  Right sketch
10:     $\hat{B}^t = -\eta \nabla f(W^t) (A_S^t)^\top \left( A_S^t (A_S^t)^\top \right)^\dagger$ 
11:     $W^{t+1} = W^t + \frac{\alpha}{r} \hat{B}^t A_S^t$ 
12:   end if
13: end for

```

1698
1699
1700 The following lemma establishes that the **Bernoulli-LoRA** update can be reformulated as a standard
1701 projected gradient descent step, providing a crucial foundation for our subsequent convergence
1702 analysis.

1703 **Lemma 10.** Consider the updates \hat{A}^t and \hat{B}^t from Algorithm 2 computed as solutions to the following
1704 optimization problems:

$$\begin{aligned} \hat{A}^t &:= \arg \min_A \left\{ f(W^t) + \frac{\alpha}{r} \langle \nabla f(W^t), B_S^t A \rangle_F + \frac{\alpha^2}{2\gamma r^2} \|B_S^t A\|_F^2 \right\}, \\ \hat{B}^t &:= \arg \min_B \left\{ f(W^t) + \frac{\alpha}{r} \langle \nabla f(W^t), B A_S^t \rangle_F + \frac{\alpha^2}{2\gamma r^2} \|B A_S^t\|_F^2 \right\}. \end{aligned} \quad (25)$$

1710 Then the Left and Right sketch updates can be expressed as a gradient descent step:

$$W^{t+1} = W^t - \gamma G^t, \quad (26)$$

1711 where G^t is defined by

$$G^t = \begin{cases} H_B^t \nabla f(W^t), & \text{with probability } p \\ \nabla f(W^t) H_A^t, & \text{with probability } 1 - p \end{cases} \quad (27)$$

1712 with projection matrices H_A^t and H_B^t given by:

$$H_A^t := (A_S^t)^\top \left(A_S^t (A_S^t)^\top \right)^\dagger A_S^t \quad \text{and} \quad H_B^t := B_S^t \left((B_S^t)^\top B_S^t \right)^\dagger (B_S^t)^\top, \quad (28)$$

1713 where \dagger denotes the Moore-Penrose pseudoinverse.

1714
1715
1716
1717
1718
1719
1720
1721
1722
1723 *Proof.* Following Algorithm 2, at each iteration we randomly select either the Left sketch (with
1724 probability p) or the Right sketch (with probability $1 - p$). We analyze both cases separately and then
1725 combine them into a unified update rule.

1726 **Left Sketch Analysis.** When the Left sketch is selected, the update takes the form:

$$W^{t+1} = W^t + \frac{\alpha}{r} B_S^t \hat{A}^t. \quad (29)$$

1728 Minimizing the right-hand side with respect to \hat{A}^t yields:
 1729

$$\begin{aligned} \frac{\alpha}{r} (B_S^t)^\top \nabla f(W^t) + \frac{\alpha^2}{\gamma r^2} (B_S^t)^\top B_S^t \hat{A}^t &= 0; \\ (B_S^t)^\top B_S^t \hat{A}^t &= -\frac{\gamma r}{\alpha} (B_S^t)^\top \nabla f(W^t); \\ \hat{A}^t &= -\frac{\gamma r}{\alpha} ((B_S^t)^\top B_S^t)^\dagger (B_S^t)^\top \nabla f(W^t). \end{aligned} \quad (30)$$

1730 This leads to the Left sketch update:
 1731

$$\begin{aligned} W^{t+1} &= W^t + \frac{\alpha}{r} B_S^t \hat{A}^t \\ &= W^t - \gamma B_S^t ((B_S^t)^\top B_S^t)^\dagger (B_S^t)^\top \nabla f(W^t) \\ &= W^t - \gamma H_B^t \nabla f(W^t), \end{aligned} \quad (31)$$

1732 where $H_B^t := B_S^t ((B_S^t)^\top B_S^t)^\dagger (B_S^t)^\top$ is a projection matrix.
 1733

1734 **Right Sketch Analysis.** For the Right sketch, we follow a similar approach. The update rule is:
 1735

$$W^{t+1} = W^t + \frac{\alpha}{r} \hat{B}^t A_S^t. \quad (32)$$

1736 First, observe that:
 1737

$$\|\hat{B}^t A_S^t\|_F^2 = \langle \hat{B}^t A_S^t, \hat{B}^t A_S^t \rangle_F = \left\langle A_S^t, (\hat{B}^t)^\top \hat{B}^t A_S^t \right\rangle_F. \quad (33)$$

1738 For the linear term from (25):
 1739

$$\frac{\alpha}{r} \langle \nabla f(W^t), \hat{B}^t A_S^t \rangle_F = \frac{\alpha}{r} \text{Tr} ((\nabla f(W^t))^\top \hat{B}^t A_S^t), \quad (34)$$

1740 with gradient $\nabla f(W^t) (A_S^t)^\top$ with respect to \hat{B}^t . Using the matrix calculus identity $\nabla_X \|X\|_F^2 = 2X$,
 1741 the gradient of the quadratic term is:
 1742

$$\frac{\alpha^2}{\gamma r^2} \hat{B}^t A_S^t (A_S^t)^\top. \quad (35)$$

1743 Setting the total gradient to zero and solving for \hat{B}^t :
 1744

$$\hat{B}^t = -\frac{\gamma r}{\alpha} \nabla f(W^t) (A_S^t)^\top (A_S^t (A_S^t)^\top)^\dagger, \quad (36)$$

1745 which yields the Right sketch update:
 1746

$$\begin{aligned} W^{t+1} &= W^t + \frac{\alpha}{r} \hat{B}^t A_S^t \\ &= W^t - \gamma \nabla f(W^t) (A_S^t)^\top (A_S^t (A_S^t)^\top)^\dagger A_S^t \\ &= W^t - \gamma \nabla f(W^t) H_A^t, \end{aligned} \quad (37)$$

1747 where $H_A^t := (A_S^t)^\top (A_S^t (A_S^t)^\top)^\dagger A_S^t$ is a projection matrix.
 1748

1749 **Combined Update Rule.** Combining equations (31) and (37), we obtain the unified update:
 1750

$$W^{t+1} = W^t - \gamma G^t, \quad (38)$$

1751 where G^t takes the form given in the lemma statement, completing the proof. \square
 1752

1753 With these assumptions in place, we can now state our main convergence result for RAC-LoRA with
 1754 Gradient Descent updates.
 1755

1756 H.1.1 CONVERGENCE FOR SMOOTH NON-CONVEX FUNCTIONS

1757 **Theorem 1.** *Let Assumptions 1, 3, and 2 hold, and let the stepsize satisfy $0 < \gamma \leq \frac{1}{L}$. Then the
 1758 iterates of Bernoulli-LoRA-GD (Algorithm 2), with matrices \hat{A}^t and \hat{B}^t computed according to Lemma
 1759 10, satisfy*

$$\mathbb{E} \left[\left\| \nabla f(\widetilde{W}^T) \right\|_F^2 \right] \leq \frac{2(f(W^0) - f^*)}{\gamma \lambda_{\min}^p T}, \quad (39)$$

1782 where $\lambda_{\min}^p := p\lambda_{\min}^{H_B} + (1-p)\lambda_{\min}^{H_A}$ and \widetilde{W}^T is drawn uniformly at random from the iterate sequence
 1783 $\{W^0, W^1, \dots, W^{T-1}\}$.
 1784

1785
 1786
 1787
 1788
 1789
 1790
 1791
 1792
 1793
 1794
 1795 *Proof.* From Lemma 10, we know that Bernoulli-LoRA updates can be expressed as

$$W^{t+1} = W^t - \gamma G^t, \quad (40)$$

1796 where G^t takes the form
 1797

$$G^t = \begin{cases} H_B^t \nabla f(W^t), & \text{with probability } p \\ \nabla f(W^t) H_A^t, & \text{with probability } 1-p \end{cases} \quad (41)$$

1798 with projection matrices H_A^t and H_B^t as defined in the lemma.
 1799

1800 To analyze the convergence, we first compute the conditional expectation and second moment of G^t :
 1801

$$\begin{aligned} \mathbb{E}[G^t | W^t, H^t] &= p H_B^t \nabla f(W^t) + (1-p) \nabla f(W^t) H_A^t, \\ \mathbb{E}[\|G^t\|_F^2 | W^t, H^t] &= p \|H_B^t \nabla f(W^t)\|_F^2 + (1-p) \|\nabla f(W^t) H_A^t\|_F^2, \end{aligned} \quad (42)$$

1802 where we defined $H^t := \{H_A^t, H_B^t\}$.
 1803

1804 We begin by establishing several key auxiliary bounds. For the Left sketch term:
 1805

$$\begin{aligned} & -\gamma p \langle \nabla f(W^t), H_B^t \nabla f(W^t) \rangle_F + \frac{L\gamma^2}{2} p \|H_B^t \nabla f(W^t)\|_F^2 \\ &= -\gamma p \langle \nabla f(W^t), H_B^t \nabla f(W^t) \rangle_F + \frac{L\gamma^2}{2} p \langle H_B^t \nabla f(W^t), H_B^t \nabla f(W^t) \rangle_F \\ &= -\gamma p \langle \nabla f(W^t), H_B^t \nabla f(W^t) \rangle_F + \frac{L\gamma^2}{2} p \langle \nabla f(W^t), (H_B^t)^\top H_B^t \nabla f(W^t) \rangle_F \\ &= p \left(-\gamma \langle \nabla f(W^t), H_B^t \nabla f(W^t) \rangle_F + \frac{L\gamma^2}{2} \langle \nabla f(W^t), H_B^t \nabla f(W^t) \rangle_F \right) \\ &\stackrel{\gamma \leq 1/L}{\leq} -\frac{\gamma}{2} p \langle \nabla f(W^t), H_B^t \nabla f(W^t) \rangle_F. \end{aligned} \quad (43)$$

1806 For any projection matrix H_A^t , we have:
 1807

$$\begin{aligned} \langle \nabla f(W^t) H_A^t, \nabla f(W^t) H_A^t \rangle_F &= \text{Tr} \left((H_A^t)^\top (\nabla f(W^t))^\top \nabla f(W^t) H_A^t \right) \\ &= \text{Tr} \left((\nabla f(W^t))^\top \nabla f(W^t) H_A^t (H_A^t)^\top \right) \\ &= \text{Tr} \left((\nabla f(W^t))^\top \nabla f(W^t) H_A^t \right) \\ &= \langle \nabla f(W^t), \nabla f(W^t) H_A^t \rangle_F. \end{aligned} \quad (44)$$

1808 Therefore:
 1809

$$\begin{aligned} & -\gamma(1-p) \langle \nabla f(W^t), \nabla f(W^t) H_A^t \rangle_F + \frac{L\gamma^2}{2} (1-p) \|\nabla f(W^t) H_A^t\|_F^2 \\ &= -\gamma(1-p) \langle \nabla f(W^t), \nabla f(W^t) H_A^t \rangle_F + \frac{L\gamma^2}{2} (1-p) \langle \nabla f(W^t) H_A^t, \nabla f(W^t) H_A^t \rangle_F \\ &= -\gamma(1-p) \langle \nabla f(W^t), \nabla f(W^t) H_A^t \rangle_F + \frac{L\gamma^2}{2} (1-p) \langle \nabla f(W^t), \nabla f(W^t) H_A^t \rangle_F \\ &\stackrel{\gamma \leq 1/L}{\leq} -\frac{\gamma}{2} (1-p) \langle \nabla f(W^t), \nabla f(W^t) H_A^t \rangle_F. \end{aligned} \quad (45)$$

1836 Using the Lipschitz gradient condition and the above bounds:
1837
$$\begin{aligned} \mathbb{E}[f(W^{t+1}) | W^t, H^t] &\leq f(W^t) + \mathbb{E}[\langle \nabla f(W^t), W^{t+1} - W^t \rangle_F | W^t, H^t] \\ 1838 &+ \frac{L}{2} \mathbb{E}[\|W^{t+1} - W^t\|_F^2 | W^t, H^t] \\ 1839 &= f(W^t) - \gamma \langle \nabla f(W^t), \mathbb{E}[G^t | W^t, H^t] \rangle_F + \frac{L\gamma^2}{2} \mathbb{E}[\|G^t\|_F^2 | W^t, H^t] \\ 1840 &= f(W^t) - \gamma p \langle \nabla f(W^t), H_B^t \nabla f(W^t) \rangle_F - \gamma(1-p) \langle \nabla f(W^t), \nabla f(W^t) H_A^t \rangle_F \\ 1841 &+ \frac{L\gamma^2}{2} p \|H_B^t \nabla f(W^t)\|_F^2 + \frac{L\gamma^2}{2} (1-p) \|\nabla f(W^t) H_A^t\|_F^2 \\ 1842 &\stackrel{(43),(45)}{\leq} f(W^t) - \frac{\gamma}{2} (p \langle \nabla f(W^t), H_B^t \nabla f(W^t) \rangle_F + (1-p) \langle \nabla f(W^t), \nabla f(W^t) H_A^t \rangle_F). \\ 1843 & \end{aligned} \tag{46}$$

1844 For the first term:
1845

$$\begin{aligned} 1846 - \langle \nabla f(W^t), \mathbb{E}[H_B^t] \nabla f(W^t) \rangle_F &= -\text{Tr}((\nabla f(W^t))^\top \mathbb{E}[H_B^t] \nabla f(W^t)) \\ 1847 &\leq -\lambda_{\min}(\mathbb{E}[H_B^t]) \text{Tr}((\nabla f(W^t))^\top \nabla f(W^t)) \\ 1848 &= -\lambda_{\min}^{H_B} \|\nabla f(W^t)\|_F^2. \end{aligned} \tag{47}$$

1849 Similarly, for the second term:
1850

$$\begin{aligned} 1851 - \langle \nabla f(W^t), \nabla f(W^t) \mathbb{E}[H_A^t] \rangle_F &= -\text{Tr}((\nabla f(W^t))^\top \nabla f(W^t) \mathbb{E}[H_A^t]) \\ 1852 &= -\text{Tr}(\mathbb{E}[H_A^t] (\nabla f(W^t))^\top \nabla f(W^t)) \\ 1853 &\leq -\lambda_{\min}^{H_A} \|\nabla f(W^t)\|_F^2. \end{aligned} \tag{48}$$

1854 Therefore:
1855

$$\begin{aligned} 1856 \mathbb{E}[f(W^{t+1}) | W^t] &= \mathbb{E}[\mathbb{E}[f(W^{t+1}) | W^t, H^t] | W^t] \\ 1857 &\leq f(W^t) - \frac{\gamma}{2} (p \langle \nabla f(W^t), \mathbb{E}[H_B^t] \nabla f(W^t) \rangle_F + (1-p) \langle \nabla f(W^t), \nabla f(W^t) \mathbb{E}[H_A^t] \rangle_F) \\ 1858 &\leq f(W^t) - \frac{\gamma}{2} (p \lambda_{\min}^{H_B} + (1-p) \lambda_{\min}^{H_A}) \|\nabla f(W^t)\|_F^2 \\ 1859 &= f(W^t) - \frac{\gamma}{2} \lambda_{\min}^p \|\nabla f(W^t)\|_F^2, \end{aligned} \tag{49}$$

1860 where $\lambda_{\min}^p := p \lambda_{\min}^{H_B} + (1-p) \lambda_{\min}^{H_A}$. Further,
1861

$$\mathbb{E}[\mathbb{E}[f(W^{t+1}) | W^t, H^t] | W^t] - f^* \leq f(W^t) - f^* - \frac{\gamma}{2} \lambda_{\min}^p \|\nabla f(W^t)\|_F^2. \tag{50}$$

1862 Taking the sum over $t = 0, \dots, T-1$ and using the tower property of expectation:
1863

$$\mathbb{E}[f(W^T) - f^*] \leq f(W^0) - f^* - \frac{\gamma}{2} \lambda_{\min}^p \sum_{t=0}^{T-1} \mathbb{E}[\|\nabla f(W^t)\|_F^2]. \tag{51}$$

1864 By rearranging terms, we get:
1865

$$\frac{\gamma}{2} \lambda_{\min}^p \sum_{t=0}^{T-1} \mathbb{E}[\|\nabla f(W^t)\|_F^2] \leq f(W^0) - f^*. \tag{52}$$

1866 Finally, dividing both sides by $\frac{\gamma T}{2} \lambda_{\min}^p$ yields:
1867

$$\mathbb{E}[\|\nabla f(\widetilde{W}^T)\|_F^2] \leq \frac{2(f(W^0) - f^*)}{\gamma \lambda_{\min}^p T}, \tag{53}$$

1868 where \widetilde{W}^T is chosen uniformly at random from $\{W^0, W^1, \dots, W^{T-1}\}$, completing the proof.
1869

□

1890 H.1.2 CONVERGENCE UNDER POLYAK-ŁOJASIEWICZ CONDITION
1891

1892 **Theorem 9.** Let Assumptions 1, 2, 3, and 6 hold, and let the stepsize satisfy $0 < \gamma \leq \frac{1}{L}$. Then
1893 the iterates of Bernoulli-LoRA-GD (Algorithm 2), with matrices \hat{A}^t and \hat{B}^t computed according to
1894 Lemma 10, satisfy

1895
$$\mathbb{E} [f(W^T) - f^*] \leq (1 - \gamma\mu\lambda_{\min}^p)^T (f(W^0) - f^*),$$

1896 where $\lambda_{\min}^p := p\lambda_{\min}^{H_B} + (1-p)\lambda_{\min}^{H_A}$.
1897

1898 *Proof.* We begin our analysis from a key inequality derived in the proof of Theorem 1:
1899

$$\mathbb{E} [f(W^{t+1}) | W^t] \leq f(W^t) - \frac{\gamma}{2} \lambda_{\min}^p \|\nabla f(W^t)\|_F^2. \quad (54)$$

1900 By invoking the Polyak-Łojasiewicz condition (Assumption 6), which states that $\frac{1}{2} \|\nabla f(W)\|_F^2 \geq$
1901 $\mu (f(W) - f^*)$, we can further bound the right-hand side of the inequality (54):
1902

$$\mathbb{E} [f(W^{t+1}) | W^t] \leq f(W^t) - \gamma\lambda_{\min}^p (\mu (f(W^t) - f^*)).$$

1903 Subtracting the optimal function value f^* from both sides, we get a recursive relationship for the
1904 expected suboptimality gap:
1905

$$\begin{aligned} \mathbb{E} [f(W^{t+1}) - f^* | W^t] &\leq (f(W^t) - f^*) - \gamma\mu\lambda_{\min}^p (f(W^t) - f^*) \\ &= (1 - \gamma\mu\lambda_{\min}^p) (f(W^t) - f^*). \end{aligned}$$

1906 By taking the full expectation over all randomness up to iteration t and applying the tower property,
1907 we obtain:
1908

$$\mathbb{E} [f(W^{t+1}) - f^*] \leq (1 - \gamma\mu\lambda_{\min}^p) \mathbb{E} [f(W^t) - f^*].$$

1909 Unrolling this recursion from $t = T - 1$ down to $t = 0$ yields the final linear convergence result:
1910

$$\mathbb{E} [f(W^T) - f^*] \leq (1 - \gamma\mu\lambda_{\min}^p)^T (f(W^0) - f^*).$$

1911 This completes the proof. \square
1912

1913 H.1.3 CONVERGENCE FOR NON-SMOOTH CONVEX FUNCTIONS
19141915 **Algorithm 3** Bernoulli-LoRA-GD (Non-smooth setting)
1916

1917 1: **Parameters:** pre-trained model $W^0 \in \mathbb{R}^{m \times n}$, rank $r \ll \min\{m,n\}$, scaling factor $\alpha > 0$,
1918 stepsize γ_t chain length T , sketch distribution \mathcal{D}_S^B or \mathcal{D}_S^A , Bernoulli probability p
1919 2: **for** $t = 0, 1, \dots, T - 1$ **do**

1920 3: Sample $c^t \sim \text{Be}(p)$ Bernoulli random variable
1921 4: **if** $c^t = 1$ **then**
1922 5: Sample $B_S^t \sim \mathcal{D}_S^B$ Left sketch
1923 6: $\hat{A}^t = \arg \min_A \left\{ f(W^t) + \frac{\alpha}{r} \langle \partial f(W^t), B_S^t A \rangle_F + \frac{\alpha^2}{2\gamma_t r^2} \|B_S^t A\|_F^2 \right\}$
1924 7: $W^{t+1} = W^t + \frac{\alpha}{r} B_S^t \hat{A}^t$
1925 8: **else**
1926 9: Sample $A_S^t \sim \mathcal{D}_S^A$ Right sketch
1927 10: $\hat{B}^t = \arg \min_B \left\{ f(W^t) + \frac{\alpha}{r} \langle \partial f(W^t), B A_S^t \rangle_F + \frac{\alpha^2}{2\gamma_t r^2} \|B A_S^t\|_F^2 \right\}$
1928 11: $W^{t+1} = W^t + \frac{\alpha}{r} \hat{B}^t A_S^t$
1929 12: **end if**
1930 13: **end for**

1931 Our analysis relies on the following standard assumptions that are widely used in non-smooth
1932 optimization theory:
1933

1934 **Assumption 7.** The function f has at least one minimizer, denoted by W^* .
1935

1936 **Assumption 8.** The function f is convex.
1937

1938 **Assumption 9** (Lipschitz continuity). The function f is L_0 -Lipschitz continuous. That is, there exists
1939 $L_0 > 0$ such that
1940

$$|f(W) - f(V)| \leq L_0 \|W - V\|_F, \quad \forall W, V \in \mathbb{R}^{m \times n}. \quad (55)$$

1941 The combination of convexity and Lipschitz continuity represents a standard framework in non-
1942 smooth optimization (Vorontsova et al., 2021; Nesterov, 2013; Bubeck, 2015; Beck, 2017; Duchi,
1943

1944 2018; Lan, 2020; Drusvyatskiy, 2020). Notably, the L_0 -Lipschitz continuity implies uniformly
 1945 bounded subgradients (Beck, 2017), a property that plays a crucial role in our analysis:

$$1946 \quad \|\partial f(W)\|_F \leq L_0, \quad \forall W \in \mathbb{R}^{m \times n}. \quad (56)$$

1947 This boundedness of subgradients ensures the stability of our optimization process and enables us to
 1948 establish rigorous convergence guarantees.

1949 The following lemma establishes that the Bernoulli-LoRA update in the non-smooth case can also be
 1950 reformulated as a subgradient descent step, which plays a central role in our convergence analysis for
 1951 non-smooth objectives.

1952 **Lemma 11.** Consider the updates \hat{A}^t and \hat{B}^t from Algorithm 3 computed as solutions to the following
 1953 optimization problems:

$$1955 \quad \hat{A}^t := \arg \min_A \left\{ f(W^t) + \frac{\alpha}{r} \langle \partial f(W^t), B_S^t A \rangle_F + \frac{\alpha^2}{2\gamma_t r^2} \|B_S^t A\|_F^2 \right\},$$

$$1958 \quad \hat{B}^t := \arg \min_B \left\{ f(W^t) + \frac{\alpha}{r} \langle \partial f(W^t), B A_S^t \rangle_F + \frac{\alpha^2}{2\gamma_t r^2} \|B A_S^t\|_F^2 \right\}. \quad (57)$$

1959 Then the Left and Right sketch updates can be expressed as a subgradient descent step:

$$1960 \quad W^{t+1} = W^t - \gamma_t G^t, \quad (58)$$

1961 where G^t is defined by

$$1963 \quad G^t = \begin{cases} H_B^t \partial f(W^t), & \text{with probability } p \\ \partial f(W^t) H_A^t, & \text{with probability } 1 - p \end{cases} \quad (59)$$

1964 with projection matrices H_A^t and H_B^t given by:

$$1966 \quad H_A^t := (A_S^t)^\top \left(A_S^t (A_S^t)^\top \right)^\dagger A_S^t \quad \text{and} \quad H_B^t := B_S^t \left((B_S^t)^\top B_S^t \right)^\dagger (B_S^t)^\top, \quad (60)$$

1967 where \dagger denotes the Moore-Penrose pseudoinverse.

1968
 1969
 1970 *Proof.* The proof follows a similar structure to that of Lemma 10, with subgradients replacing
 1971 gradients throughout the analysis. We examine both sketch types separately before combining them
 1972 into a unified update rule.

1973 **Left Sketch Analysis.** When the Left sketch is selected, the update takes the form:

$$1975 \quad W^{t+1} = W^t + \frac{\alpha}{r} B_S^t \hat{A}^t. \quad (61)$$

1977 The matrix \hat{A}^t is defined as the solution to the optimization problem:

$$1978 \quad \hat{A}^t := \arg \min_A \left\{ f(W^t) + \frac{\alpha}{r} \langle \partial f(W^t), B_S^t A \rangle_F + \frac{\alpha^2}{2\gamma_t r^2} \|B_S^t A\|_F^2 \right\}. \quad (62)$$

1979 By computing the gradient of the objective with respect to A and setting it to zero, we obtain:

$$1982 \quad \frac{\alpha}{r} (B_S^t)^\top \partial f(W^t) + \frac{\alpha^2}{\gamma_t r^2} (B_S^t)^\top B_S^t \hat{A}^t = 0;$$

$$1984 \quad \hat{A}^t = -\frac{\gamma_t r}{\alpha} \left((B_S^t)^\top B_S^t \right)^\dagger (B_S^t)^\top \partial f(W^t). \quad (63)$$

1986 Substituting this expression back into the update equation yields the Left sketch update:

$$1987 \quad W^{t+1} = W^t + \frac{\alpha}{r} B_S^t \hat{A}^t$$

$$1989 \quad = W^t - \gamma_t B_S^t \left((B_S^t)^\top B_S^t \right)^\dagger (B_S^t)^\top \partial f(W^t)$$

$$1990 \quad = W^t - \gamma_t H_B^t \partial f(W^t). \quad (64)$$

1992 **Right Sketch Analysis.** For the Right sketch, we follow an analogous approach. The update rule
 1993 takes the form:

$$1994 \quad W^{t+1} = W^t + \frac{\alpha}{r} \hat{B}^t A_S^t. \quad (65)$$

1996 Applying similar optimization steps but now with respect to matrix B , we obtain:

$$1997 \quad \hat{B}^t = -\frac{\gamma_t r}{\alpha} \partial f(W^t) (A_S^t)^\top \left(A_S^t (A_S^t)^\top \right)^\dagger, \quad (66)$$

2052 For projection matrices, we have the following properties:
 2053

$$\begin{aligned}
 \|\partial f(W^t)H_A^t\|_F^2 &= \langle \partial f(W^t)H_A^t, \partial f(W^t)H_A^t \rangle_F \\
 &= \text{Tr} \left((H_A^t)^\top (\partial f(W^t))^\top \partial f(W^t)H_A^t \right) \\
 &= \text{Tr} \left((\nabla f(W^t))^\top \nabla f(W^t)H_A^t (H_A^t)^\top \right) \\
 &= \text{Tr} \left((\partial f(W^t))^\top \partial f(W^t)H_A^t \right) \\
 &= \langle \partial f(W^t), \partial f(W^t)H_A^t \rangle_F,
 \end{aligned} \tag{81}$$

2061 and similarly, one can show that

$$\|H_B^t \partial f(W^t)\|_F^2 = \langle \partial f(W^t), H_B^t \partial f(W^t) \rangle_F. \tag{82}$$

2064 This allows us to express the second moment term as:

$$\begin{aligned}
 \gamma_t^2 \mathbb{E} \left[\|G^t\|_F^2 \mid W^t, H^t \right] &\stackrel{(77)}{=} \gamma_t^2 p \|H_B^t \partial f(W^t)\|_F^2 + \gamma_t^2 (1-p) \|\partial f(W^t)H_A^t\|_F^2 \\
 &\stackrel{(81),(82)}{=} \gamma_t^2 p \langle \partial f(W^t), H_B^t \partial f(W^t) \rangle_F + \gamma_t^2 (1-p) \langle \partial f(W^t), \partial f(W^t)H_A^t \rangle_F.
 \end{aligned} \tag{83}$$

2069 Combining these bounds, we can analyze the distance to the optimal solution:

$$\begin{aligned}
 \mathbb{E} \left[\|W^{t+1} - W^*\|_F^2 \mid W^t, H^t \right] &= \mathbb{E} \left[\|W^t - \gamma_t G^t - W^*\|_F^2 \mid W^t, H^t \right] \\
 &= \|W^t - W^*\|_F^2 - 2\gamma_t \mathbb{E} \left[\langle G^t, W^t - W^* \rangle_F \mid W^t, H^t \right] \\
 &\quad + \gamma_t^2 \mathbb{E} \left[\|G^t\|_F^2 \mid W^t, H^t \right] \\
 &\stackrel{(80),(83)}{=} \|W^t - W^*\|_F^2 - 2\gamma_t p \langle H_B^t \partial f(W^t), W^t - W^* \rangle_F \\
 &\quad - 2\gamma_t (1-p) \langle \partial f(W^t)H_A^t, W^t - W^* \rangle_F + \gamma_t^2 p \langle \partial f(W^t), H_B^t \partial f(W^t) \rangle_F \\
 &\quad + \gamma_t^2 (1-p) \langle \partial f(W^t), \partial f(W^t)H_A^t \rangle_F.
 \end{aligned} \tag{84}$$

2080 For the expected projection matrices (see Assumption 10), we have:

$$\begin{aligned}
 \langle \partial f(W^t), \mathbb{E} [H_B^t] \partial f(W^t) \rangle_F &= \text{Tr} \left((\partial f(W^t))^\top \mathbb{E} [H_B^t] \partial f(W^t) \right) \\
 &= \alpha \text{Tr} \left((\partial f(W^t))^\top \partial f(W^t) \right) \\
 &= \alpha \|\partial f(W^t)\|_F^2,
 \end{aligned} \tag{85}$$

2086 and similarly,

$$\langle \partial f(W^t), \partial f(W^t) \mathbb{E} [H_A^t] \rangle_F = \alpha \|\partial f(W^t)\|_F^2. \tag{86}$$

2089 Taking expectation of both sides of (84) again, we get

$$\mathbb{E} \left[\|W^{t+1} - W^*\|_F^2 \mid W^t \right] = \mathbb{E} \left[\mathbb{E} \left[\|W^{t+1} - W^*\|_F^2 \mid W^t, H^t \right] \mid W^t \right] \tag{87}$$

$$\begin{aligned}
 &= \|W^t - W^*\|_F^2 - 2\gamma_t p \langle \mathbb{E} [H_B^t] \partial f(W^t), W^t - W^* \rangle_F \\
 &\quad - 2\gamma_t (1-p) \langle \partial f(W^t) \mathbb{E} [H_A^t], W^t - W^* \rangle_F
 \end{aligned} \tag{88}$$

$$\begin{aligned}
 &\quad + \gamma_t^2 p \langle \partial f(W^t), \mathbb{E} [H_B^t] \partial f(W^t) \rangle_F + \gamma_t^2 (1-p) \langle \partial f(W^t), \partial f(W^t) \mathbb{E} [H_A^t] \rangle_F \\
 &\stackrel{(85),(86)}{=} \|W^t - W^*\|_F^2 - 2\gamma_t p \alpha \langle \partial f(W^t), W^t - W^* \rangle_F
 \end{aligned} \tag{89}$$

$$\begin{aligned}
 &\quad - 2\gamma_t (1-p) \alpha \langle \partial f(W^t), W^t - W^* \rangle_F + \gamma_t^2 \alpha \|\partial f(W^t)\|_F^2 \\
 &= \|W^t - W^*\|_F^2 - 2\gamma_t \alpha \langle \partial f(W^t), W^t - W^* \rangle_F + \gamma_t^2 \alpha \|\partial f(W^t)\|_F^2 \\
 &\stackrel{(79)}{=} \|W^t - W^*\|_F^2 - 2\gamma_t \alpha (f(W^t) - f(W^*)) + \gamma_t^2 \alpha \|\partial f(W^t)\|_F^2.
 \end{aligned} \tag{90}$$

2101 By Assumption 9, subgradients are uniformly bounded (see (Beck, 2017)):

$$\|\partial f(W)\|_F \leq L_0 \quad \forall W \in \mathbb{R}^{m \times n}. \tag{91}$$

2104 Now we analyze both stepsize strategies separately.

2105

2106 **1. (Constant stepsize).** Let us first consider using a fixed stepsize $\gamma_t := \gamma > 0$. Taking expectation
 2107 of both sides of (87) again, applying tower property (11) and using the bound (91), we obtain:
 2108

$$\mathbb{E} \left[\|W^{t+1} - W^*\|_F^2 \right] \leq \mathbb{E} \left[\|W^t - W^*\|_F^2 \right] - 2\gamma\alpha \mathbb{E} [f(W^t) - f(W^*)] + \gamma^2\alpha L_0^2. \quad (92)$$

2110 Rearranging terms in (92):
 2111

$$2\gamma\alpha \mathbb{E} [f(W^t) - f(W^*)] \leq \mathbb{E} \left[\|W^t - W^*\|_F^2 \right] - \mathbb{E} \left[\|W^{t+1} - W^*\|_F^2 \right] + \gamma^2\alpha L_0^2. \quad (93)$$

2113 Summing inequality (93) for $t = 0, \dots, T-1$:
 2114

$$\begin{aligned} 2\gamma\alpha \sum_{t=0}^{T-1} \mathbb{E} [f(W^t) - f(W^*)] &\leq \sum_{t=0}^{T-1} \left(\mathbb{E} \left[\|W^t - W^*\|_F^2 \right] - \mathbb{E} \left[\|W^{t+1} - W^*\|_F^2 \right] \right) \\ &\quad + T\gamma^2\alpha L_0^2 \\ &= \mathbb{E} \left[\|W^0 - W^*\|_F^2 \right] - \mathbb{E} \left[\|W^T - W^*\|_F^2 \right] + T\gamma^2\alpha L_0^2 \\ &\leq \|W^0 - W^*\|_F^2 + T\gamma^2\alpha L_0^2, \end{aligned} \quad (94)$$

2122 where the last inequality follows from the non-negativity of $\|W^T - W^*\|_F^2$.
 2123

2124 For the averaged iterate $\bar{W}^T := \frac{1}{T} \sum_{t=0}^{T-1} W^t$, by convexity of f we have:
 2125

$$\begin{aligned} \mathbb{E} \left[f(\bar{W}^T) - f(W^*) \right] &\leq \frac{1}{T} \sum_{t=0}^{T-1} \mathbb{E} [f(W^t) - f(W^*)] \\ &\stackrel{(94)}{\leq} \frac{\|W^0 - W^*\|_F^2}{2\gamma\alpha T} + \frac{\gamma L_0^2}{2} \\ &= \frac{(R^0)^2}{2\gamma\alpha T} + \frac{\gamma L_0^2}{2}, \end{aligned} \quad (95)$$

2132 where we denoted $(R^0)^2 := \|W^0 - W^*\|_F^2$.
 2133

2134 To optimize this bound, we minimize it with respect to γ . The optimal stepsize γ_* solves:
 2135

$$\begin{aligned} \gamma_* &= \arg \min_{\gamma > 0} \left(\frac{(R^0)^2}{2\gamma\alpha T} + \frac{\gamma L_0^2}{2} \right) \\ &= \sqrt{\frac{(R^0)^2}{T\alpha L_0^2}}. \end{aligned} \quad (96)$$

2140 Substituting γ_* back into (95), we obtain the optimal convergence rate:
 2141

$$\mathbb{E} \left[f(\bar{W}^T) - f(W^*) \right] \leq \frac{R^0 L_0}{\sqrt{\alpha T}}. \quad (97)$$

2144 **2. (Polyak stepsize).** For this strategy, we choose the stepsize adaptively based on the current
 2145 function value:
 2146

$$\begin{aligned} \gamma_t &= \arg \min_{\gamma > 0} \left\{ \|W^t - W^*\|_F^2 - 2\gamma\alpha (f(W^t) - f(W^*)) + \gamma^2\alpha \|\partial f(W^t)\|_F^2 \right\} \\ &= \frac{(f(W^t) - f(W^*))}{\|\partial f(W^t)\|_F^2}. \end{aligned} \quad (98)$$

2150 Substituting this stepsize into inequality (87):
 2151

$$\begin{aligned} \mathbb{E} \left[\|W^{t+1} - W^*\|_F^2 \mid W^t \right] &= \mathbb{E} \left[\mathbb{E} \left[\|W^{t+1} - W^*\|_F^2 \mid W^t, H^t \right] \mid W^t \right] \\ &\leq \|W^t - W^*\|_F^2 - 2\gamma_t\alpha (f(W^t) - f(W^*)) + \gamma_t^2\alpha \|\partial f(W^t)\|_F^2 \\ &\stackrel{(98)}{=} \|W^t - W^*\|_F^2 - \frac{\alpha (f(W^t) - f(W^*))^2}{\|\partial f(W^t)\|_F^2} \\ &\stackrel{(91)}{\leq} \|W^t - W^*\|_F^2 - \frac{\alpha (f(W^t) - f(W^*))^2}{L_0^2}. \end{aligned} \quad (99)$$

2160 Taking expectation of both sides of (99) again and applying the tower property
 2161

$$2162 \mathbb{E} \left[\|W^{t+1} - W^*\|_{\text{F}}^2 \right] \leq \mathbb{E} \left[\|W^t - W^*\|_{\text{F}}^2 \right] - \frac{\alpha \mathbb{E} \left[(f(W^t) - f(W^*))^2 \right]}{L_0^2} \quad (100)$$

2164 Since f is convex, by Jensen's inequality (14) and the Cauchy-Bunyakovsky-Schwarz inequality (12)
 2165 with $X := f(W^t) - f(W^*)$ and $\bar{Y} := 1$, we have

$$\begin{aligned} 2166 \mathbb{E} \left[f_i(\bar{W}^T) - f(W^*) \right] &\stackrel{(14)}{\leq} \mathbb{E} \left[\frac{1}{T} \sum_{t=0}^{T-1} f(W^t) - f(W^*) \right] \\ 2167 &\leq \frac{1}{T} \sum_{t=0}^{T-1} \mathbb{E} [f(W^t) - f(W^*)] \\ 2168 &\stackrel{(12)}{\leq} \frac{1}{T} \sum_{t=0}^{T-1} \sqrt{\mathbb{E} \left[(f(W^t) - f(W^*))^2 \right]} \\ 2169 &\leq \sqrt{\frac{1}{T} \sum_{t=0}^{T-1} \mathbb{E} \left[(f(W^t) - f(W^*))^2 \right]} \\ 2170 &\stackrel{(100)}{\leq} \frac{R^0 L_0}{\sqrt{\alpha T}}, \end{aligned} \quad (101)$$

2171 which matches the optimal rate achieved by the constant stepsize strategy with optimal tuning. \square
 2172

2173
 2174
 2175
 2176
 2177
 2178
 2179
 2180
 2181
 2182
 2183
 2184
 2185
 2186
 2187
 2188
 2189
 2190
 2191
 2192
 2193
 2194
 2195
 2196
 2197
 2198
 2199
 2200
 2201
 2202
 2203
 2204
 2205
 2206
 2207
 2208
 2209
 2210
 2211
 2212
 2213

2214 H.2 ANALYSIS OF BERNOUlli-LoRA-SGD

2215

2216

2217

2218 **Algorithm 4** Bernoulli-LoRA-SGD

```

2219 1: Parameters: pre-trained model  $W^0 \in \mathbb{R}^{m \times n}$ , rank  $r \ll \min\{m, n\}$ , scaling factor  $\alpha > 0$ , chain
2220 length  $T$ , sketch distribution  $\mathcal{D}_S^B$  or  $\mathcal{D}_S^A$ , Bernoulli probability  $p$ 
2221 2: for  $t = 0, 1, \dots, T - 1$  do
2222 3:   Sample  $c^t \sim \text{Be}(p)$  Bernoulli random variable
2223 4:   if  $c^t = 1$  then
2224 5:     Sample  $B_S^t \sim \mathcal{D}_S^B$  Left sketch
2225 6:      $\hat{A}^t = -\eta \left( (B_S^t)^\top B_S^t \right)^\dagger (B_S^t)^\top g(W^t)$ 
2226 7:      $W^{t+1} = W^t + \frac{\alpha}{r} B_S^t \hat{A}^t$ 
2227 8:   else
2228 9:     Sample  $A_S^t \sim \mathcal{D}_S^A$  Right sketch
2229 10:     $\hat{B}^t = -\eta g(W^t) (A_S^t)^\top \left( A_S^t (A_S^t)^\top \right)^\dagger$ 
2230 11:     $W^{t+1} = W^t + \frac{\alpha}{r} \hat{B}^t A_S^t$ 
2231 12:  end if
2232 13: end for

```

2235

2236

2237

Earlier findings were derived utilizing full gradient computations. Nonetheless, this method proves impractical in deep learning applications, where obtaining full gradients is rarely feasible. Our focus moves to a framework that employs **Stochastic Gradient Descent (SGD)** while incorporating a more flexible and generalized data sampling strategy, enabling greater adaptability in the selection and utilization of data throughout the training process. General sampling techniques for strongly convex functions have been thoroughly examined in (Gower et al., 2019). For broader convex optimization problems, Khaled et al. (2023) provide a comprehensive study of how **SGD** performs under different sampling strategies. In non-convex scenarios, the works of Khaled & Richtárik (2023) and (Demidovich et al., 2023b) investigate the effects of generalized sampling methods on **SGD**’s convergence and efficiency, offering valuable insights into its adaptability for diverse machine learning applications. In this section we focus on **Bernoulli-LoRA-SGD**, a method, designed in the scope of **Bernoulli-LoRA** framework, based on the classical **SGD** algorithm.

2249

2250

For convergence analysis, we notice the gradient step in Algorithm 4 is equivalent to the following update

$$2251 \quad W^{t+1} = W^t - \gamma \hat{G}^t, \quad \text{where} \quad \hat{G}^t = \begin{cases} H_B^t G^t, & \text{with probability } p \\ G^t H_A^t, & \text{with probability } 1 - p \end{cases}, \quad (102)$$

2252

where $G^t = g(W^t)$ is an unbiased stochastic gradient, which satisfies Assumption 4.

2253

2254

2255

2256

H.2.1 CONVERGENCE FOR SMOOTH NON-CONVEX FUNCTIONS

2257

2258

Theorem 11. *Let Assumptions 2, 3, and 4 hold, and stepsize satisfy*

$$2259 \quad 0 < \gamma \leq \min \left\{ \frac{1}{\sqrt{LA_1 \lambda_{\max}^p T}}, \frac{1}{LB_1} \left(\frac{\lambda_{\max}^p}{\lambda_{\min}^p} \right)^{-1} \right\}.$$

2260

Then iterates generated by Bernoulli-LoRA-SGD (Algorithm 4) satisfy

2261

2262

2263

2264

2265

2266

2267

$$\mathbb{E} \left[\left\| \nabla f(\tilde{W}^T) \right\|_F^2 \right] \leq \frac{6(f(W^0) - f^*)}{\gamma \lambda_{\min}^p T} + \gamma LC_1 \frac{\lambda_{\max}^p}{\lambda_{\min}^p},$$

where $\lambda_{\min}^p := p\lambda_{\min}^{H_B} + (1-p)\lambda_{\min}^{H_A}$, $\lambda_{\max}^p := p\lambda_{\max}^{H_B} + (1-p)\lambda_{\max}^{H_A}$, and \tilde{W}^T is chosen at random from $\{W^0, W^1, \dots, W^{T-1}\}$ with probabilities $\{\frac{w_t}{\mathcal{W}_{T-1}}\}_{t=0}^{T-1}$, where $w_t = \frac{w_{t-1}}{(1+\gamma^2 LA_1 \lambda_{\max}^p)}$,

$$\mathcal{W}_{T-1} = \sum_{t=0}^{T-1} w_t, \text{ and } w^{-1} > 0.$$

2268 *Proof.* We start with smoothness of function f :

$$\begin{aligned} 2269 \quad f(W^{t+1}) &\leq f(W^t) + \langle \nabla f(W^t), W^{t+1} - W^t \rangle + \frac{L}{2} \|W^{t+1} - W^t\|_F^2 \\ 2270 &\stackrel{(102)}{=} f(W^t) - \gamma \langle \nabla f(W^t), \hat{G}^t \rangle + \frac{\gamma^2 L}{2} \|\hat{G}^t\|_F^2. \end{aligned} \quad (103)$$

2271 Taking a conditional expectation by W^t , we bound the second and the third terms from inequality
 2272 (103):

$$\begin{aligned} 2273 \quad \mathbb{E} [\langle \nabla f(W^t), \hat{G}^t \rangle | W^t] &= \langle \nabla f(W^t), \mathbb{E} [\hat{G}^t | W^t] \rangle \\ 2274 &\stackrel{(102)}{=} p \langle \nabla f(W^t), \mathbb{E} [H_B^t G^t | W^t] \rangle + (1-p) \langle \nabla f(W^t), \mathbb{E} [G^t H_A^t | W^t] \rangle \\ 2275 &\stackrel{(*)}{=} p \langle \nabla f(W^t), \mathbb{E} [H_B^t | W^t] \mathbb{E} [G^t | W^t] \rangle + (1-p) \langle \nabla f(W^t), \mathbb{E} [G^t | W^t] \mathbb{E} [H_A^t | W^t] \rangle \\ 2276 &= p \langle \nabla f(W^t), \mathbb{E} [H_B^t | W^t] \nabla f(W^t) \rangle + (1-p) \langle \nabla f(W^t), \nabla f(W^t) \mathbb{E} [H_A^t | W^t] \rangle \\ 2277 &\geq \underbrace{(p \lambda_{\min}(\mathbb{E} [H_B^t]) + (1-p) \lambda_{\min}(\mathbb{E} [H_A^t])) \|\nabla f(W^t)\|_F^2}_{:= \lambda_{\min}^p} \\ 2278 &= \lambda_{\min}^p \|\nabla f(W^t)\|_F^2, \end{aligned} \quad (104)$$

2279 where in $(*)$ we used that H_B^t , H_A^t and G^t are independent. Now we bound the third term:

$$\begin{aligned} 2280 \quad \mathbb{E} [\|\hat{G}^t\|_F^2 | W^t] &\stackrel{(102)}{=} p \mathbb{E} [\|H_B^t G^t\|_F^2 | W^t] + (1-p) \mathbb{E} [\|G^t H_A^t\|_F^2 | W^t] \\ 2281 &= p \mathbb{E} [\langle H_B^t G^t, H_B^t G^t \rangle | W^t] + (1-p) \mathbb{E} [\langle G^t H_A^t, G^t H_A^t \rangle | W^t] \\ 2282 &\stackrel{(**)}{=} p \mathbb{E} [\langle G^t, H_B^t G^t \rangle | W^t] + (1-p) \mathbb{E} [\langle G^t, G^t H_A^t \rangle | W^t], \end{aligned}$$

2283 where in $(**)$ we used property of projection matrices H_B^t , H_A^t . By the independence of H_B^t , H_A^t , G^t ,
 2284 we obtain

$$\begin{aligned} 2285 \quad \mathbb{E} [\|\hat{G}^t\|_F^2 | W^t] &= p \mathbb{E} [\langle G^t, \mathbb{E} [H_B^t | W^t] G^t \rangle | W^t] + (1-p) \mathbb{E} [\langle G^t, G^t \mathbb{E} [H_A^t | W^t] \rangle | W^t] \\ 2286 &\leq p \lambda_{\max}(\mathbb{E} [H_B^t | W^t]) \mathbb{E} [\|G^t\|_F^2 | W^t] + (1-p) \lambda_{\max}(\mathbb{E} [H_A^t | W^t]) \mathbb{E} [\|G^t\|_F^2 | W^t] \\ 2287 &= \underbrace{(p \lambda_{\max}(\mathbb{E} [H_B^t | W^t]) + (1-p) \lambda_{\max}(\mathbb{E} [H_A^t | W^t]))}_{:= \lambda_{\max}^p} \mathbb{E} [\|G^t\|_F^2 | W^t] \\ 2288 &= \lambda_{\max}^p \mathbb{E} [\|G^t\|_F^2 | W^t]. \end{aligned} \quad (105)$$

2289 Plugging (104) and (105) into (103), we obtain

$$\begin{aligned} 2290 \quad \mathbb{E} [f(W^{t+1}) | W^t] &\leq f(W^t) - \gamma \mathbb{E} [\langle \nabla f(W^t), \hat{G}^t \rangle | W^t] + \frac{\gamma^2 L}{2} \mathbb{E} [\|\hat{G}^t\|_F^2 | W^t] \\ 2291 &\leq f(W^t) - \gamma \lambda_{\min}^p \|\nabla f(W^t)\|_F^2 + \frac{\gamma^2 \lambda_{\max}^p L}{2} \mathbb{E} [\|G^t\|_F^2 | W^t]. \end{aligned}$$

2292 By Assumption 4,

$$\begin{aligned} 2293 \quad \mathbb{E} [f(W^{t+1}) - f^* | W^t] &\leq f(W^t) - \gamma \mathbb{E} [\langle \nabla f(W^t), \hat{G}^t \rangle | W^t] + \frac{\gamma^2 L}{2} \mathbb{E} [\|\hat{G}^t\|_F^2 | W^t] \\ 2294 &\leq f(W^t) - f^* - \gamma \lambda_{\min}^p \|\nabla f(W^t)\|_F^2 \\ 2295 &\quad + \frac{\gamma^2 \lambda_{\max}^p L}{2} (2A_1(f(W^t) - f^*) + B_1 \|\nabla f(W^t)\|_F^2 + C_1) \\ 2296 &\leq (1 + \gamma^2 \lambda_{\max}^p L A_1) (f(W^t) - f^*) - \gamma \lambda_{\min}^p \left(1 - \frac{\gamma L B_1 \lambda_{\max}^p}{2 \lambda_{\min}^p}\right) \|\nabla f(W^t)\|_F^2 \\ 2297 &\quad + \frac{\gamma^2 \lambda_{\max}^p L C_1}{2}. \end{aligned}$$

2322 Taking mathematical expectation and selecting a stepsize as $0 < \gamma \leq \frac{1}{LB_1} \left(\frac{\lambda_{\max}^p}{\lambda_{\min}^p} \right)^{-1}$, we get
 2323

$$\begin{aligned} \mathbb{E}[f(W^{t+1}) - f^*] &\leq (1 + \gamma^2 \lambda_{\max}^p L A_1) \mathbb{E}[f(W^t) - f^*] \\ &\quad - \frac{\gamma \lambda_{\min}^p}{2} \mathbb{E}[\|\nabla f(W^t)\|_{\text{F}}^2] + \frac{\gamma^2 \lambda_{\max}^p L C_1}{2}. \end{aligned} \quad (106)$$

2327 Defining $\delta^t := \mathbb{E}[f(W^t) - f^*]$, $r^t := \mathbb{E}[\|\nabla f(W^t)\|_{\text{F}}^2]$ for every $t \geq 0$, we have
 2328

$$\delta^{t+1} \leq (1 + \gamma^2 \lambda_{\max}^p L A_1) \delta^t - \frac{\gamma \lambda_{\min}^p}{2} r^t + \frac{\gamma^2 \lambda_{\max}^p L C_1}{2}.$$

2329 Fixing $w^{-1} > 0$ and defining $w_t = \frac{w_{t-1}}{1 + \gamma^2 L A_1 \lambda_{\max}^p}$ for all $t \geq 0$, we have
 2330

$$\begin{aligned} \frac{1}{2} \lambda_{\min}^p w_t r^t &\leq \frac{w_t}{\gamma} (1 + \gamma^2 \lambda_{\max}^p L A_1) \delta^t - \frac{w_t}{\gamma} \delta^{t+1} + \frac{1}{2} \gamma L C_1 \lambda_{\max}^p w_t \\ &= \frac{w_{t-1} \delta^t}{\gamma} - \frac{w_t \delta^{t+1}}{\gamma} + \frac{1}{2} \gamma L C_1 \lambda_{\max}^p w_t. \end{aligned}$$

2331 Summing over t from 0 to $T-1$, we have
 2332

$$\sum_{t=0}^{T-1} w_t r^t \leq \frac{2w_{-1} \delta^0}{\gamma \lambda_{\min}^p} - \frac{2w_{T-1} \delta^T}{\gamma \lambda_{\min}^p} + \gamma L C_1 \frac{\lambda_{\max}^p}{\lambda_{\min}^p} \sum_{t=0}^{T-1} w_t.$$

2333 Defining $\mathcal{W}_{T-1} = \sum_{t=0}^{T-1} w_t$, we acquire
 2334

$$\sum_{t=0}^{T-1} \frac{w_t}{\mathcal{W}_{T-1}} r^t \leq \frac{2w_{-1} \delta^0}{\gamma \lambda_{\min}^p \mathcal{W}_{T-1}} + \gamma L C_1 \frac{\lambda_{\max}^p}{\lambda_{\min}^p}.$$

2335 Using the next chain of inequalities
 2336

$$W_{T-1} = \sum_{t=0}^{T-1} w_t \geq T \min_{0 \leq t \leq T-1} w_t = T w_{T-1} = \frac{T w_{-1}}{(1 + \gamma^2 \lambda_{\max}^p L A_1)^T},$$

2337 we have
 2338

$$\sum_{t=0}^{T-1} \frac{w_t}{\mathcal{W}_{T-1}} r^t \leq \frac{2(1 + \gamma^2 \lambda_{\max}^p L A_1)^T}{\gamma T \lambda_{\min}^p} (f(W^0) - f^*) + \gamma L C_1 \frac{\lambda_{\max}^p}{\lambda_{\min}^p}.$$

2339 Selecting $0 < \gamma \leq \frac{1}{\sqrt{L A_1 \lambda_{\max}^p T}}$, and using $(1 + \gamma^2 \lambda_{\max}^p L A_1)^T \leq \exp(\gamma^2 \lambda_{\max}^p L A_1 T) \leq \exp(1) \leq 3$, we obtain
 2340

$$\sum_{t=0}^{T-1} \frac{w_t}{\mathcal{W}_{T-1}} r^t \leq \frac{6\delta^0}{\gamma T \lambda_{\min}^p} + \gamma L C_1 \frac{\lambda_{\max}^p}{\lambda_{\min}^p}.$$

2341 \square

2342 Next we show convergence of Bernoulli-LoRA-SGD under additional Assumption 6.
 2343

2344 H.2.2 CONVERGENCE UNDER POLYAK-ŁOJASIEWICZ CONDITION

2345 **Theorem 12.** *Let Assumptions 2, 3, 4, and 6 hold, and stepsize satisfy*

2346 $0 < \gamma \leq \min \left\{ \frac{\mu \lambda_{\min}^p}{2 L A_1 \lambda_{\max}^p}, \frac{2}{\mu \lambda_{\min}^p}, \frac{1}{LB_1} \left(\frac{\lambda_{\max}^p}{\lambda_{\min}^p} \right)^{-1} \right\}$. Then iterates generated by Bernoulli-LoRA-SGD
 2347 (Algorithm 4) satisfy

$$\mathbb{E}[f(W^T) - f^*] \leq \left(1 - \frac{1}{2} \gamma \mu \lambda_{\min}^p \right)^T (f(W^0) - f^*) + \frac{\gamma L C_1}{\mu} \cdot \frac{\lambda_{\max}^p}{\lambda_{\min}^p},$$

2348 where $\lambda_{\min}^p := p \lambda_{\min}^{H_B} + (1-p) \lambda_{\min}^{H_A}$, $\lambda_{\max}^p := p \lambda_{\max}^{H_B} + (1-p) \lambda_{\max}^{H_A}$.
 2349

2350 *Proof.* We start our proof with inequality 106. Using PL-inequality (see Assumption 6), we have
 2351

$$\begin{aligned} \mathbb{E}[f(W^{t+1}) - f^*] &\leq (1 + \gamma^2 \lambda_{\max}^p L A_1) \mathbb{E}[f(W^t) - f^*] - \frac{\gamma \lambda_{\min}^p}{2} \mathbb{E}[\|\nabla f(W^t)\|_{\text{F}}^2] + \frac{\gamma^2 \lambda_{\max}^p L C_1}{2} \\ &\leq (1 - \gamma \mu \lambda_{\min}^p + \gamma^2 \lambda_{\max}^p L A_1) \mathbb{E}[f(W^t) - f^*] + \frac{\gamma^2 \lambda_{\max}^p L C_1}{2}. \end{aligned}$$

2376 Taking the stepsize as $0 < \gamma \leq \min \left\{ \frac{\mu \lambda_{\min}^p}{2LA_1 \lambda_{\max}^p}, \frac{2}{\mu \lambda_{\min}^p} \right\}$, we obtain
 2377

$$\begin{aligned}
 \mathbb{E} [f(W^{t+1}) - f^*] &\leq \left(1 - \frac{1}{2}\gamma\mu\lambda_{\min}^p\right) \mathbb{E} [f(W^t) - f^*] + \frac{\gamma^2 \lambda_{\max}^p LC_1}{2} \\
 &\leq \left(1 - \frac{1}{2}\gamma\mu\lambda_{\min}^p\right)^{t+1} \mathbb{E} [f(W^0) - f^*] + \frac{\gamma^2 \lambda_{\max}^p LC_1}{2} \sum_{\tau=0}^t \left(1 - \frac{1}{2}\gamma\mu\lambda_{\min}^p\right)^{t-\tau} \\
 &\leq \left(1 - \frac{1}{2}\gamma\mu\lambda_{\min}^p\right)^{t+1} \mathbb{E} [f(W^0) - f^*] + \frac{\gamma^2 \lambda_{\max}^p LC_1}{2} \sum_{\tau=0}^{\infty} \left(1 - \frac{1}{2}\gamma\mu\lambda_{\min}^p\right)^{\tau} \\
 &= \left(1 - \frac{1}{2}\gamma\mu\lambda_{\min}^p\right)^{t+1} \mathbb{E} [f(W^0) - f^*] + \frac{\gamma^2 \lambda_{\max}^p LC_1}{\gamma\mu\lambda_{\min}^p},
 \end{aligned}$$

2388 where in the last equation we use the formula of the sum of geometric progression. \square

2389
 2390
 2391
 2392
 2393
 2394
 2395
 2396
 2397
 2398
 2399
 2400
 2401
 2402
 2403
 2404
 2405
 2406
 2407
 2408
 2409
 2410
 2411
 2412
 2413
 2414
 2415
 2416
 2417
 2418
 2419
 2420
 2421
 2422
 2423
 2424
 2425
 2426
 2427
 2428
 2429

2430 H.3 ANALYSIS OF BERNOUlli-LoRA-MVR
2431
2432
24332434 **Algorithm 5** Bernoulli-LoRA-MVR

```

2435 1: Parameters: pre-trained model  $W^0 \in \mathbb{R}^{m \times n}$ ,  $G^0 \in \mathbb{R}^{m \times n}$  rank  $r \ll \min\{m, n\}$ , scaling
2436  factor  $\alpha > 0$ , chain length  $T$ , sketch distribution  $\mathcal{D}_S^B$  or  $\mathcal{D}_S^A$ , Bernoulli probability  $p$ , momentum
2437  parameter  $b \in [0, 1]$ 
2438 2: for  $t = 0, 1, \dots, T - 1$  do
2439 3:   Sample  $c^t \sim \text{Be}(p)$  Bernoulli random variable
2440 4:   if  $c^t = 1$  then
2441 5:     Sample  $B_S^t \sim \mathcal{D}_S^B$  Left sketch
2442 6:      $\hat{A}^t = -\eta \left( (B_S^t)^\top B_S^t \right)^\dagger (B_S^t)^\top G^t$ 
2443 7:      $W^{t+1} = W^t + \frac{\alpha}{r} B_S^t \hat{A}^t$ 
2444 8:   else
2445 9:     Sample  $A_S^t \sim \mathcal{D}_S^A$  Right sketch
2446 10:     $\hat{B}^t = -\eta G^t (A_S^t)^\top \left( A_S^t (A_S^t)^\top \right)^\dagger$ 
2447 11:     $W^{t+1} = W^t + \frac{\alpha}{r} \hat{B}^t A_S^t$ 
2448 12:   end if
2449 13:   Sample  $\xi^{t+1} \sim \mathcal{D}$ 
2450 14:    $G^{t+1} = \nabla f_{\xi^{t+1}}(W^{t+1}) + (1 - b) (G^t - \nabla f_{\xi^{t+1}}(W^t))$ 
2451 15: end for

```

2453
2454
2455
2456 Recently, there has been a significant surge of interest in variance-reduced methods for addressing
2457 finite-sum problems (J Reddi et al., 2015; Shang et al., 2018; Malinovsky et al., 2022; Richtárik
2458 et al., 2024). It has gained prominence as a formidable alternative to stochastic gradient descent
2459 (SGD) in tackling non-convex optimization problems. Notably, it has been pivotal in introducing the
2460 first algorithms capable of surpassing SGD's convergence rate for locating first-order critical points.
2461 Despite these advancements, variance reduction methods often come with challenges, including
2462 the necessity for meticulously tuned learning rates and the reliance on overly large batch sizes to
2463 realize their benefits. To address some of these limitations, Momentum Variance Reduction (MVR)
2464 was proposed specifically for server-only stochastic non-convex optimization (Cutkosky & Orabona,
2465 2019). This approach leverages a modified form of momentum to achieve variance reduction while
2466 eliminating the dependence on large batch sizes. A proof on MVR technique with better dependence
2467 on momentum parameter was obtained by Tyurin & Richtárik (2023). In the context of Federated
2468 Learning, Karagulyan et al. (2024) proposed the SPAM method. On the server side, MVR is utilized
2469 to enhance optimization efficiency, while the client side incorporates the Stochastic Proximal Point
2470 Method updates. This section is devoted to **Bernoulli-LoRA-MVR**, a method, designed in the scope of
2471 **Bernoulli-LoRA** framework, based on the MVR technique.

2472 To show convergence guarantees for **Bernoulli-LoRA-MVR**, the iterates of the method can be rewritten
2473 in following way

$$W^{t+1} = W^t - \gamma \hat{G}^t, \quad \text{where} \quad \hat{G}^t = \begin{cases} H_B^t G^t, & \text{with probability } p \\ G^t H_A^t, & \text{with probability } 1 - p \end{cases} \quad (107)$$

$$G^{t+1} = \nabla f_{\xi^{t+1}}(W^{t+1}) + (1 - b) (G^t - \nabla f_{\xi^{t+1}}(W^t)). \quad (108)$$

2474 First of all, we reprove descent lemma from the paper of Li et al. (2021) for generic gradient step
2475 (107).

2476 **Lemma 12.** *Let Assumptions 1, 3 hold. Then, iterates defined as (107) satisfy*

$$\begin{aligned} \mathbb{E} [f(W^{t+1}) - f^* \mid W^t] &\leq f(W^t) - f^* - \frac{\gamma \lambda_{\min}^p}{2} \|\nabla f(W^t)\|_{\text{F}}^2 \\ &\quad + \frac{\gamma \lambda_{\max}^p}{2} \|G^t - \nabla f(W^t)\|_{\text{F}}^2 - \left(\frac{1}{2\gamma} - \frac{L}{2} \right) \mathbb{E} [\|W^{t+1} - W^t\|_{\text{F}}^2 \mid W^t]. \end{aligned}$$

2484 *Proof.* By Assumption 3, we have

$$\begin{aligned}
 2486 \quad f(W^{t+1}) &\leq f(W^t) + \langle \nabla f(W^t), W^{t+1} - W^t \rangle_F + \frac{L}{2} \|W^{t+1} - W^t\|_F^2 \\
 2487 \\
 2488 &= f(W^t) - \gamma \langle \nabla f(W^t), \hat{G}^t \rangle_F + \frac{L}{2} \|W^{t+1} - W^t\|_F^2. \tag{109}
 \end{aligned}$$

2489 To continue our proof, we need to bound the second term from (109). Taking conditional expectation
2490 by H^t, W^t , we obtain

$$\begin{aligned}
 2491 \quad \mathbb{E} [\langle \nabla f(W^t), \hat{G}^t \rangle_F | H^t, W^t] &\stackrel{(107)}{=} p \langle \nabla f(W^t), H_B^t G^t \rangle_F + (1-p) \langle \nabla f(W^t), G^t H_A^t \rangle_F \\
 2492 \\
 2493 &= p \langle H_B^t \nabla f(W^t), H_B^t G^t \rangle_F + (1-p) \langle \nabla f(W^t) H_A^t, G^t H_A^t \rangle_F \\
 2494 \\
 2495 &= \frac{p}{2} \left(\|H_B^t \nabla f(W^t)\|_F^2 + \|H_B^t G^t\|_F^2 - \|H_B^t G^t - H_B^t \nabla f(W^t)\|_F^2 \right) \\
 2496 \\
 2497 &\quad + \frac{1-p}{2} \left(\|\nabla f(W^t) H_A^t\|_F^2 + \|G^t H_A^t\|_F^2 - \|G^t H_A^t - \nabla f(W^t) H_A^t\|_F^2 \right) \\
 2498 \\
 2499 &\geq \frac{1}{2} \left(p \|H_B^t \nabla f(W^t)\|_F^2 + (1-p) \|\nabla f(W^t) H_A^t\|_F^2 \right) + \frac{1}{2} \mathbb{E} [\|\hat{G}^t\|_F^2 | H^t, W^t] \\
 2500 \\
 2501 &\quad - \frac{1}{2} \left(p \|H_B^t G^t - H_B^t \nabla f(W^t)\|_F^2 + (1-p) \|G^t H_A^t - \nabla f(W^t) H_A^t\|_F^2 \right).
 \end{aligned}$$

2502 Taking conditional expectation by W^t , we have

$$\begin{aligned}
 2503 \quad \mathbb{E} [\langle \nabla f(W^t), \hat{G}^t \rangle_F | W^t] &\geq \frac{1}{2} \left(p \mathbb{E} [\|H_B^t \nabla f(W^t)\|_F^2 | W^t] + (1-p) \mathbb{E} [\|\nabla f(W^t) H_A^t\|_F^2 | W^t] \right) + \frac{1}{2} \mathbb{E} [\|\hat{G}^t\|_F^2 | W^t] \\
 2504 \\
 2505 &\quad - \frac{1}{2} \left(p \mathbb{E} [\|H_B^t G^t - H_B^t \nabla f(W^t)\|_F^2 | W^t] + (1-p) \mathbb{E} [\|G^t H_A^t - \nabla f(W^t) H_A^t\|_F^2 | W^t] \right) \\
 2506 \\
 2507 &\stackrel{(*)}{\geq} \frac{1}{2} \underbrace{\left(p \lambda_{\min}(\mathbb{E}[H_B^t]) + (1-p) \lambda_{\min}(\mathbb{E}[H_A^t]) \right)}_{:= \lambda_{\min}^p} \|\nabla f(W^t)\|_F^2 + \frac{1}{2} \mathbb{E} [\|\hat{G}^t\|_F^2 | W^t] \\
 2508 \\
 2509 &\quad - \frac{1}{2} \underbrace{\left(p \lambda_{\max}(\mathbb{E}[H_B^t]) + (1-p) \lambda_{\max}(\mathbb{E}[H_A^t]) \right)}_{:= \lambda_{\max}^p} \|G^t - \nabla f(W^t)\|_F^2 \\
 2510 \\
 2511 &\stackrel{(107)}{=} \frac{\lambda_{\min}^p}{2} \|\nabla f(W^t)\|_F^2 + \frac{1}{2\gamma^2} \mathbb{E} [\|W^{t+1} - W^t\|_F^2 | W^t] - \frac{\lambda_{\max}^p}{2} \|G^t - \nabla f(W^t)\|_F^2, \tag{110}
 2512 \\
 2513 \\
 2514
 \end{aligned}$$

2515 where in $(*)$ we used the following inequalities for any matrix $V \in \mathbb{R}^{m \times n}$

$$\begin{aligned}
 2516 \quad \mathbb{E} [\|H_B^t V\|_F^2] &= \mathbb{E} [\langle H_B^t V, H_B^t V \rangle_F] = \langle \mathbb{E}[H_B^t] V, V \rangle_F \geq \lambda_{\min}(\mathbb{E}[H_B^t]) \|V\|_F^2, \\
 2517 \\
 2518 \quad \mathbb{E} [\|H_B^t V\|_F^2] &\leq \lambda_{\max}(\mathbb{E}[H_B^t]) \|V\|_F^2, \\
 2519 \\
 2520 \quad \mathbb{E} [\|V H_A^t\|_F^2] &= \mathbb{E} [\langle V H_A^t, V H_A^t \rangle_F] = \langle V \mathbb{E}[H_A^t], V \rangle_F \geq \lambda_{\min}(\mathbb{E}[H_A^t]) \|V\|_F^2, \\
 2521 \\
 2522 \quad \mathbb{E} [\|V H_A^t\|_F^2] &\leq \lambda_{\max}(\mathbb{E}[H_A^t]) \|V\|_F^2.
 \end{aligned}$$

2523 Plugging in (110) into (109), we get

$$\begin{aligned}
 2524 \quad \mathbb{E} [f(W^{t+1}) | W^t] &\leq f(W^t) - \frac{\gamma \lambda_{\min}^p}{2} \|\nabla f(W^t)\|_F^2 - \frac{1}{2\gamma} \mathbb{E} [\|W^{t+1} - W^t\|_F^2 | W^t] \\
 2525 \\
 2526 &\quad + \frac{\gamma \lambda_{\max}^p}{2} \|G^t - \nabla f(W^t)\|_F^2 + \frac{L}{2} \mathbb{E} [\|W^{t+1} - W^t\|_F^2 | W^t].
 \end{aligned}$$

2528 \square

2529 **Lemma 13.** Let Assumptions 3, 5 hold. Then, iterates generated by Bernoulli-LoRA-MVR (Algorithm 5) satisfy

$$\mathbb{E} [\|G^{t+1} - \nabla f(W^{t+1})\|_F^2] \leq (1-b)^2 \mathbb{E} [\|G^t - \nabla f(W^t)\|_F^2] + 2(1-b)^2 L^2 \mathbb{E} [\|W^{t+1} - W^t\|_F^2] + 2b^2 \sigma^2 \tag{111}$$

2538 *Proof.* Taking conditional expectation by $\mathcal{F}^{t+1} = \{W^{t+1}, G^t\}$, we obtain
2539
$$\mathbb{E} \left[\|G^{t+1} - \nabla f(W^{t+1})\|_{\text{F}}^2 | \mathcal{F}^{t+1} \right] \stackrel{(108)}{=} \mathbb{E} \left[\|\nabla f_{\xi^{t+1}}(W^{t+1}) - \nabla f(W^{t+1}) + (1-b)(G^t - \nabla f_{\xi^{t+1}}(W^t))\|_{\text{F}}^2 | \mathcal{F}^{t+1} \right]$$

2540
$$\stackrel{(13)}{=} (1-b)^2 \|G^t - \nabla f(W^t)\|_{\text{F}}^2$$

2541
$$+ \mathbb{E} \left[\|\nabla f_{\xi^{t+1}}(W^{t+1}) - \nabla f(W^{t+1}) + (1-b)(\nabla f(W^t) - \nabla f_{\xi^{t+1}}(W^t))\|_{\text{F}}^2 | \mathcal{F}^{t+1} \right]$$

2542
$$\leq (1-b)^2 \|G^t - \nabla f(W^t)\|_{\text{F}}^2 + 2b^2 \mathbb{E} \left[\|\nabla f_{\xi^{t+1}}(W^{t+1}) - \nabla f(W^{t+1})\|_{\text{F}}^2 | \mathcal{F}^{t+1} \right]$$

2543
$$+ 2(1-b)^2 \mathbb{E} \left[\|\nabla f_{\xi^{t+1}}(W^{t+1}) - \nabla f_{\xi^{t+1}}(W^t) - \nabla f(W^{t+1}) + \nabla f(W^t)\|_{\text{F}}^2 | \mathcal{F}^{t+1} \right]$$

2544
$$\leq (1-b)^2 \|G^t - \nabla f(W^t)\|_{\text{F}}^2 + 2b^2 \mathbb{E} \left[\|\nabla f_{\xi^{t+1}}(W^{t+1}) - \nabla f(W^{t+1})\|_{\text{F}}^2 | \mathcal{F}^{t+1} \right]$$

2545
$$+ 2(1-b)^2 \mathbb{E} \left[\|\nabla f_{\xi^{t+1}}(W^{t+1}) - \nabla f_{\xi^{t+1}}(W^t)\|_{\text{F}}^2 | \mathcal{F}^{t+1} \right]$$

2546
$$\leq (1-b)^2 \|G^t - \nabla f(W^t)\|_{\text{F}}^2 + 2(1-b)^2 L^2 \|W^{t+1} - W^t\|_{\text{F}}^2 + 2b^2 \sigma^2,$$

2547 where in the last inequality we used smoothness of f_ξ and bounded variance assumption. Taking
2548 math expectation, we conclude the proof. \square

2549
2550
25512552 H.3.1 CONVERGENCE FOR SMOOTH NON-CONVEX FUNCTIONS
25532554 **Theorem 13.** *Let Assumptions 1, 2, 3, and 5 hold, and let the stepsize satisfy $0 < \gamma \leq$
2555 $\frac{1}{L \left(1 + \sqrt{\frac{2\lambda_{\max}^p(1-b)^2}{b}} \right)}$. Then the iterates of Bernoulli-LoRA-MVR (Algorithm 5) satisfy*

2556
$$\mathbb{E} \left[\|\nabla f(\widetilde{W}^T)\|_{\text{F}}^2 \right] \leq \frac{2(f(W^0) - f^*)}{\lambda_{\min}^p \gamma T} + \frac{\|G^0 - \nabla f(W^0)\|_{\text{F}}^2}{b(2-b)T} \cdot \frac{\lambda_{\max}^p}{\lambda_{\min}^p} + \frac{2b\sigma^2}{2-b} \cdot \frac{\lambda_{\max}^p}{\lambda_{\min}^p}, \quad (112)$$

2557 where $\lambda_{\min}^p := p\lambda_{\min}^{H_B} + (1-p)\lambda_{\min}^{H_A}$, $\lambda_{\max}^p := p\lambda_{\max}^{H_B} + (1-p)\lambda_{\max}^{H_A}$, \widetilde{W}^T is drawn uniformly at
2558 random from the iterate sequence $\{W^0, W^1, \dots, W^{T-1}\}$.
25592560
2561
2562
2563
25642565 *Proof.* Denote Lyapunov function Φ_t as follows

2566
$$\Phi_t = f(W^t) - f^* + \frac{\gamma \lambda_{\max}^p}{2b(2-b)} \|G^t - \nabla f(W^t)\|_{\text{F}}^2. \quad (113)$$

2567 By Lemma 12 and Lemma 13, we have
2568

2569
$$\begin{aligned} \mathbb{E} [\Phi_{t+1}] &\leq \mathbb{E} [f(W^t)] - f^* - \frac{\gamma \lambda_{\min}^p}{2} \mathbb{E} \left[\|\nabla f(W^t)\|_{\text{F}}^2 \right] - \left(\frac{1}{2\gamma} - \frac{L}{2} \right) \mathbb{E} \left[\|W^{t+1} - W^t\|_{\text{F}}^2 \right] \\ &\quad + \frac{\gamma \lambda_{\max}^p}{2} \mathbb{E} \left[\|G^t - \nabla f(W^t)\|_{\text{F}}^2 \right] + \frac{\gamma(1-b)^2 \lambda_{\max}^p}{2b(2-b)} \mathbb{E} \left[\|G^t - \nabla f(W^t)\|_{\text{F}}^2 \right] \\ &\quad + \frac{\gamma(1-b)^2 L^2 \lambda_{\max}^p}{2b(2-b)} \mathbb{E} \left[\|W^{t+1} - W^t\|_{\text{F}}^2 \right] + \frac{\gamma \lambda_{\max}^p b \sigma^2}{2-b} \\ &\leq \mathbb{E} [\Phi_t] - \frac{\gamma \lambda_{\min}^p}{2} \mathbb{E} \left[\|\nabla f(W^t)\|_{\text{F}}^2 \right] + \frac{\gamma \lambda_{\max}^p b \sigma^2}{2-b} \\ &\quad - \left(\frac{1}{2\gamma} - \frac{L}{2} - \frac{\gamma(1-b)^2 L^2 \lambda_{\max}^p}{2b(2-b)} \right) \mathbb{E} \left[\|W^{t+1} - W^t\|_{\text{F}}^2 \right]. \end{aligned}$$

2570
2571
2572
2573
2574
2575
2576
2577
2578
2579
2580
2581
2582
2583
2584
2585
2586
2587
2588
2589
2590
25912582 Selecting $0 < \gamma \leq \frac{1}{L \left(1 + \sqrt{\frac{(1-b)^2}{b(2-b)} \lambda_{\max}^p} \right)}$, we obtain

2583
$$\mathbb{E} [\Phi_{t+1}] \leq \mathbb{E} [\Phi_t] - \frac{\gamma \lambda_{\min}^p}{2} \mathbb{E} \left[\|\nabla f(W^t)\|_{\text{F}}^2 \right] + \frac{\gamma \lambda_{\max}^p b \sigma^2}{2-b}.$$

2584 Summing over t from 0 to $T-1$, we get
2585

2586
$$\frac{\gamma \lambda_{\min}^p}{2} \sum_{t=0}^{T-1} \mathbb{E} \left[\|\nabla f(W^t)\|_{\text{F}}^2 \right] \leq \mathbb{E} [\Phi_0] - \mathbb{E} [\Phi_T] + \frac{\gamma \lambda_{\max}^p b \sigma^2}{2-b} T.$$

2587 Finally, dividing both sides by $\frac{\gamma \lambda_{\min}^p}{2}$ yields
2588

2589
$$\mathbb{E} \left[\|\nabla f(\widetilde{W}^T)\|_{\text{F}}^2 \right] \leq \frac{2\Phi_0}{\lambda_{\min}^p \gamma T} + \frac{2b\sigma^2}{2-b} \cdot \frac{\lambda_{\max}^p}{\lambda_{\min}^p},$$

2592 where \widetilde{W}^T is drawn uniformly at random from the iterate sequence $\{W^0, W^1, \dots, W^{T-1}\}$. \square
 2593

2594 Next we show convergence guarantee for **Bernoulli-LoRA-MVR**, supposing additionally Assumption 6
 2595 holds.
 2596

2597 H.3.2 CONVERGENCE UNDER POLYAK-ŁOJASIEWICZ CONDITION
 2598

2599 **Theorem 14.** *Let Assumptions 1, 2, 3, 5, and 6 hold, and let the stepsize satisfy*

$$2600 \quad 0 < \gamma \leq \min \left\{ \frac{1}{L \left(1 + \sqrt{\frac{2(1-b)^2}{b(2-b)} \lambda_{\max}^p} \right)}, \frac{b}{2\mu\lambda_{\min}^p} \right\}.$$

2603 Then the iterates of **Bernoulli-LoRA-MVR** (Algorithm 5) satisfy

$$2604 \quad \mathbb{E} [f(W^T) - f^*] \leq (1 - \gamma\mu\lambda_{\min}^p)^T \Phi_0 + \frac{b\sigma^2}{(2-b)\mu} \cdot \frac{\lambda_{\max}^p}{\lambda_{\min}^p}, \quad (114)$$

2605 where $\lambda_{\min}^p := p\lambda_{\min}^{H_B} + (1-p)\lambda_{\min}^{H_A}$, $\lambda_{\max}^p := p\lambda_{\max}^{H_B} + (1-p)\lambda_{\max}^{H_A}$, and $\Phi_0 = f(W^0) - f^* +$
 2606 $\frac{\gamma\lambda_{\max}^p}{b(2-b)} \|G^0 - \nabla f(W^0)\|_{\text{F}}^2$.
 2607

2609 *Proof.* Denote Lyapunov function Φ_t as follows

$$2610 \quad \Phi_t = f(W^t) - f^* + \frac{\gamma\lambda_{\max}^p}{b(2-b)} \|G^t - \nabla f(W^t)\|_{\text{F}}^2. \quad (115)$$

2613 By Lemma 12 and Lemma 13, we have

$$2614 \quad \mathbb{E} [\Phi_{t+1}] \leq \mathbb{E} [f(W^t)] - f^* - \frac{\gamma\lambda_{\min}^p}{2} \mathbb{E} [\|\nabla f(W^t)\|_{\text{F}}^2] - \left(\frac{1}{2\gamma} - \frac{L}{2} \right) \mathbb{E} [\|W^{t+1} - W^t\|_{\text{F}}^2] \\ 2615 \quad + \frac{\gamma\lambda_{\max}^p}{2} \mathbb{E} [\|G^t - \nabla f(W^t)\|_{\text{F}}^2] + \frac{\gamma(1-b)^2\lambda_{\max}^p}{b(2-b)} \mathbb{E} [\|G^t - \nabla f(W^t)\|_{\text{F}}^2] \\ 2616 \quad + \frac{\gamma(1-b)^2L^2\lambda_{\max}^p}{b(2-b)} \mathbb{E} [\|W^{t+1} - W^t\|_{\text{F}}^2] + \frac{\gamma\lambda_{\max}^p b\sigma^2}{2-b} \\ 2617 \quad \leq \max \left\{ 1 - \gamma\mu\lambda_{\min}^p, 1 - \frac{b}{2} \right\} \mathbb{E} [\Phi_t] + \frac{\gamma\lambda_{\max}^p b\sigma^2}{2-b} \\ 2618 \quad - \left(\frac{1}{2\gamma} - \frac{L}{2} - \frac{\gamma(1-b)^2L^2\lambda_{\max}^p}{b(2-b)} \right) \mathbb{E} [\|W^{t+1} - W^t\|_{\text{F}}^2],$$

2625 where in the last inequality we used Assumption 6. Selecting positive stepsize γ satisfying the upper
 2626 bound assumed in the theorem statement, we obtain

$$2627 \quad \mathbb{E} [\Phi_{t+1}] \leq (1 - \gamma\mu\lambda_{\min}^p) \mathbb{E} [\Phi_t] + \frac{\gamma\lambda_{\max}^p b\sigma^2}{2-b} \\ 2628 \quad \leq (1 - \gamma\mu\lambda_{\min}^p)^{t+1} \mathbb{E} [\Phi_0] + \frac{\gamma\lambda_{\max}^p b\sigma^2}{2-b} \sum_{\tau=0}^t (1 - \gamma\mu\lambda_{\min}^p)^{t-\tau} \\ 2629 \quad \leq (1 - \gamma\mu\lambda_{\min}^p)^{t+1} \mathbb{E} [\Phi_0] + \frac{\gamma\lambda_{\max}^p b\sigma^2}{2-b} \sum_{\tau=0}^{\infty} (1 - \gamma\mu\lambda_{\min}^p)^{\tau} \\ 2630 \quad = (1 - \gamma\mu\lambda_{\min}^p)^{t+1} \mathbb{E} [\Phi_0] + \frac{\gamma\lambda_{\max}^p b\sigma^2}{(2-b)\gamma\mu\lambda_{\min}^p},$$

2637 where, in the last equation, we used the formula for the sum of a geometric progression.
 2638 \square
 2639

2640
 2641
 2642
 2643
 2644
 2645

2646 H 4 ANALYSIS OF BERNOULLI-LORA-PAGE

H 4 ANALYSIS OF BERNoulli-JORDA-PAGE

Algorithm 6 Bernoulli-LoRA-PAGE

```

1: Parameters: pre-trained model  $W^0 \in \mathbb{R}^{m \times n}$ , a vector  $G^0 \in \mathbb{R}^{m \times n}$ , rank  $r \ll \min\{m, n\}$ ,  

   scaling factor  $\alpha > 0$ , chain length  $T$ , sketch distribution  $\mathcal{D}_S^B$  or  $\mathcal{D}_S^A$ , Bernoulli probability  $p$ ,  

   probability  $q$ 
2: for  $t = 0, 1, \dots, T - 1$  do
3:   Sample  $c^t \sim \text{Be}(p)$  Bernoulli random variable
4:   if  $c^t = 1$  then
5:     Sample  $B_S^t \sim \mathcal{D}_S^B$  Left sketch
6:      $\hat{A}^t = -\eta \left( (B_S^t)^\top B_S^t \right)^\dagger (B_S^t)^\top G^t$ 
7:      $W^{t+1} = W^t + \frac{\alpha}{r} B_S^t \hat{A}^t$ 
8:   else
9:     Sample  $A_S^t \sim \mathcal{D}_S^A$  Right sketch
10:     $\hat{B}^t = -\eta g(W^t) (A_S^t)^\top \left( A_S^t (A_S^t)^\top \right)^\dagger A_S^t$ 
11:     $W^{t+1} = W^t + \frac{\alpha}{r} \hat{B}^t A_S^t$ 
12:   end if
13:   Sample  $i_{t+1}$  uniformly at random from  $[n]$ 
14:    $G^{t+1} = \begin{cases} \nabla f(W^{t+1}), & \text{with probability } q \\ G^t + (\nabla f_{i_{t+1}}(W^{t+1}) - \nabla f_{i_{t+1}}(W^t)), & \text{with probability } 1 - q \end{cases}$ 
15: end for

```

There exist several optimal methods for solving a general non-convex optimization problem, e.g. **SPIDER** (Fang et al., 2018) and **SARAH** (Pham et al., 2020). However, the known lower bound used to establish their optimality works only in the small data regime. **ProbAbilistic Gradient Estimator (PAGE)** (Li et al., 2021) is a very simple and easy to implement algorithm, known for achieving optimal convergence results in non-convex optimization. **PAGE** uses the full gradient update with probability q_t , or reuses the previous gradient with a small adjustment (at a low computational cost) with probability $1 - q_t$. A general version of **PAGE** on Riemannian manifolds is considered in (Demidovich et al., 2024a). In this section we present **Bernoulli-LoRA-PAGE**, a new method within **Bernoulli-LoRA** framework, based on **PAGE** algorithm.

Notice, that the iterates of [Bernoulli-LoRA-PAGE](#) (Algorithm 6) can be rewritten in the following simple way

$$W^{t+1} = W^t - \gamma \hat{G}^t, \quad \text{where} \quad \hat{G}^t = \begin{cases} H_B^t G^t, & \text{with probability } p \\ G^t H_A^t, & \text{with probability } 1-p \end{cases} \quad (116)$$

$$G^{t+1} = \begin{cases} \nabla f(W^{t+1}), & \text{with probability } q \\ G^t + (\nabla f_{i_{t+1}}(W^{t+1}) - \nabla f_{i_{t+1}}(W^t)), & \text{with probability } 1-q \end{cases} \quad (117)$$

Lemma 14. *Let Assumption 3 hold. Then, iterates generated by Bernoulli-LoRA-PAGE*

$$\mathbb{E} \left[\|G^{t+1} - \nabla f(W^{t+1})\|_{\text{F}}^2 \right] \leq (1-q)\mathbb{E} \left[\|G^t - \nabla f(W^t)\|_{\text{F}}^2 \right] + (1-q)L^2\mathbb{E} \left[\|W^{t+1} - W^t\|_{\text{F}}^2 \right]. \quad (118)$$

2700 *Proof.* Taking the full mathematical expectation, we obtain
 2701
$$\mathbb{E} \left[\|G^{t+1} - \nabla f(W^{t+1})\|_F^2 \right] \stackrel{(117)}{=} (1-q)\mathbb{E} \left[\|G^t - \nabla f(W^{t+1}) + (\nabla f_{i_{t+1}}(W^{t+1}) - \nabla f_{i_{t+1}}(W^t))\|_F^2 \right]$$

 2702
$$\stackrel{(13)}{=} (1-q)\mathbb{E} \left[\|G^t - \nabla f(W^t)\|_F^2 \right]$$

 2703
$$+ (1-q)\mathbb{E} \left[\|(\nabla f_{i_{t+1}}(W^{t+1}) - \nabla f_{i_{t+1}}(W^t)) - (\nabla f(W^{t+1}) - \nabla f(W^t))\|_F^2 \right]$$

 2704
$$\leq (1-q)\mathbb{E} \left[\|G^t - \nabla f(W^t)\|_F^2 \right]$$

 2705
$$+ (1-q)\mathbb{E} \left[\|\nabla f_{i_{t+1}}(W^{t+1}) - \nabla f_{i_{t+1}}(W^t)\|_F^2 \right]$$

 2706
$$\leq (1-q)\mathbb{E} \left[\|G^t - \nabla f(W^t)\|_F^2 \right] + (1-q)L^2\mathbb{E} \left[\|W^{t+1} - W^t\|_F^2 \right],$$

 2707 where in the last inequality we used smoothness of each f_i . \square

2713
 2714
 2715
 2716 **H.4.1 CONVERGENCE FOR SMOOTH NON-CONVEX FUNCTIONS**
 2717

2718 **Theorem 15.** *Let Assumptions 1, 2, and 3 hold, and let the stepsize satisfy*

$$0 < \gamma \leq \frac{1}{L \left(1 + \sqrt{\frac{1-q}{q} \lambda_{\max}^p} \right)}.$$

2719 *Then the iterates of PAGE-Bernoulli-LoRA (Algorithm 6) satisfy*

$$\mathbb{E} \left[\|\nabla f(\widetilde{W}^T)\|_F^2 \right] \leq \frac{2(f(W^0) - f^*)}{\lambda_{\min}^p \gamma T} + q \frac{\|G^0 - \nabla f(W^0)\|_F^2}{T} \cdot \frac{\lambda_{\max}^p}{\lambda_{\min}^p}, \quad (119)$$

2720 *where $\lambda_{\min}^p := p\lambda_{\min}^{H_B} + (1-p)\lambda_{\min}^{H_A}$, $\lambda_{\max}^p := p\lambda_{\max}^{H_B} + (1-p)\lambda_{\max}^{H_A}$, \widetilde{W}^T is drawn uniformly at*
 2721 *random from the iterate sequence $\{W^0, W^1, \dots, W^{T-1}\}$.*

2722
 2723
 2724
 2725
 2726
 2727
 2728
 2729 *Proof.* Denote Lyapunov function Φ_t as follows

$$\Phi_t = f(W^t) - f^* + \frac{\gamma \lambda_{\max}^p}{2q} \|G^t - \nabla f(W^t)\|_F^2. \quad (120)$$

2730 By Lemma 12 and Lemma 14, we have

$$\begin{aligned} \mathbb{E} [\Phi_{t+1}] &\leq \mathbb{E} [f(W^t)] - f^* - \frac{\gamma \lambda_{\min}^p}{2} \mathbb{E} \left[\|\nabla f(W^t)\|_F^2 \right] \\ &\quad - \left(\frac{1}{2\gamma} - \frac{L}{2} \right) \mathbb{E} \left[\|W^{t+1} - W^t\|_F^2 \right] + \frac{\gamma \lambda_{\max}^p}{2} \mathbb{E} \left[\|G^t - \nabla f(W^t)\|_F^2 \right] \\ &\quad + \frac{\gamma \lambda_{\max}^p (1-q)}{2q} \mathbb{E} \left[\|G^t - \nabla f(W^t)\|_F^2 \right] + \frac{\gamma \lambda_{\max}^p (1-q)L^2}{2q} \mathbb{E} \left[\|W^{t+1} - W^t\|_F^2 \right] \\ &\leq \mathbb{E} [\Phi_t] - \frac{\gamma \lambda_{\min}^p}{2} \mathbb{E} \left[\|\nabla f(W^t)\|_F^2 \right] - \left(\frac{1}{2\gamma} - \frac{L}{2} - \frac{\gamma(1-q)L^2 \lambda_{\max}^p}{2q} \right) \mathbb{E} \left[\|W^{t+1} - W^t\|_F^2 \right]. \end{aligned}$$

2731 Selecting $0 < \gamma \leq \frac{1}{L(1 + \sqrt{\frac{1-q}{q} \lambda_{\max}^p})}$, we obtain

$$\mathbb{E} [\Phi_{t+1}] \leq \mathbb{E} [\Phi_t] - \frac{\gamma \lambda_{\min}^p}{2} \mathbb{E} \left[\|\nabla f(W^t)\|_F^2 \right].$$

2732 Summing over t from 0 to $T-1$, we get

$$\frac{\gamma \lambda_{\min}^p}{2} \sum_{t=0}^{T-1} \mathbb{E} \left[\|\nabla f(W^t)\|_F^2 \right] \leq \mathbb{E} [\Phi_0] - \mathbb{E} [\Phi_T].$$

2733 Finally, dividing both sides by $\frac{\gamma \lambda_{\min}^p}{2}$ yields

$$\mathbb{E} \left[\|\nabla f(\widetilde{W}^T)\|_F^2 \right] \leq \frac{2\Phi_0}{\gamma \lambda_{\min}^p T}.$$

2734 where \widetilde{W}^T is drawn uniformly at random from the iterate sequence $\{W^0, W^1, \dots, W^{T-1}\}$. \square

2754 H.4.2 CONVERGENCE UNDER POLYAK-ŁOJASIEWICZ CONDITION
27552756 **Theorem 16.** *Let Assumptions 1, 2, 3, and 6 hold, and let the stepsize satisfy*

2757
$$0 < \gamma \leq \min \left\{ \frac{1}{L \left(1 + 2\sqrt{\frac{1-q}{q} \lambda_{\max}^p} \right)}, \frac{q}{2\mu\lambda_{\min}^p} \right\}.$$

2758

2759 *Then the iterates of Bernoulli-LoRA-PAGE (Algorithm 6) satisfy*

2760
$$\mathbb{E} [f(W^T) - f^*] \leq (1 - \gamma\mu\lambda_{\min}^p)^T \Phi_0, \quad (121)$$

2761

2762 *where $\lambda_{\min}^p := p\lambda_{\min}^{H_B} + (1-p)\lambda_{\min}^{H_A}$, and $\Phi_0 = f(W^0) - f^* + \frac{\gamma\lambda_{\max}^p}{q} \|G^0 - \nabla f(W^0)\|_F^2$.*
27632764 *Proof.* Denote Lyapunov function Φ_t as follows

2765
$$\Phi_t = f(W^t) - f^* + \frac{\gamma\lambda_{\max}^p}{q} \|G^t - \nabla f(W^t)\|_F^2. \quad (122)$$

2766

2767 By Lemma 12 and Lemma 14, we have

2768
$$\begin{aligned} \mathbb{E} [\Phi_{t+1}] &\leq \mathbb{E} [f(W^t)] - f^* - \frac{\gamma\lambda_{\min}^p}{2} \mathbb{E} [\|\nabla f(W^t)\|_F^2] - \left(\frac{1}{2\gamma} - \frac{L}{2} \right) \mathbb{E} [\|W^{t+1} - W^t\|_F^2] \\ &\quad + \frac{\gamma\lambda_{\max}^p}{2} \mathbb{E} [\|G^t - \nabla f(W^t)\|_F^2] + \frac{\gamma(1-q)\lambda_{\max}^p}{q} \mathbb{E} [\|G^t - \nabla f(W^t)\|_F^2] \\ &\quad + \frac{\gamma(1-q)L^2\lambda_{\max}^p}{q} \mathbb{E} [\|W^{t+1} - W^t\|_F^2] \\ &\leq (1 - \gamma\mu\lambda_{\min}^p) \mathbb{E} [f(W^t) - f^*] + \left(1 - \frac{q}{2} \right) \frac{\gamma\lambda_{\max}^p}{q} \mathbb{E} [\|G^t - \nabla f(W^t)\|_F^2] \\ &\quad - \left(\frac{1}{2\gamma} - \frac{L}{2} - \frac{\gamma(1-q)L^2\lambda_{\max}^p}{q} \right) \mathbb{E} [\|W^{t+1} - W^t\|_F^2], \end{aligned}$$

2768

2769 where in the last inequality we used Assumption 6. Selecting $0 < \gamma \leq$
2770 $\min \left\{ \frac{1}{L \left(1 + 2\sqrt{\frac{1-q}{q} \lambda_{\max}^p} \right)}, \frac{q}{2\mu\lambda_{\min}^p} \right\}$, we obtain

2771
$$\mathbb{E} [\Phi_{t+1}] \leq (1 - \gamma\mu\lambda_{\min}^p) \mathbb{E} [\Phi_t].$$

2772 Unrolling the recursion, we obtain

2773
$$\mathbb{E} [\Phi_T] \leq (1 - \gamma\mu\lambda_{\min}^p)^T \Phi_0.$$

2774 \square 2775
2776
2777
2778
2779
2780
2781
2782
2783
2784
2785
2786
2787
2788
2789
2790
2791
2792
2793
2794
2795
2796
2797
2798
2799
2800
2801
2802
2803
2804
2805
2806
2807

 2808 **I PROOFS FOR FEDERATED LEARNING EXTENSIONS**
 2809

 2810 In recent years, distributed optimization problems and algorithms have become a focal point in the
 2811 Machine Learning (ML) community. This surge in interest is driven by the need to train modern deep
 2812 neural networks, which often involve billions of parameters and massive datasets (Brown et al., 2020;
 2813 Kolesnikov et al., 2020). To achieve practical training times (Li, 2020), parallelizing computations,
 2814 such as stochastic gradient evaluations, has emerged as a natural solution, leading to the widespread
 2815 adoption of distributed training algorithms (Goyal et al., 2017; You et al., 2019; Le Scao et al., 2023).
 2816 Additionally, distributed methods are crucial when data is inherently distributed across multiple
 2817 devices or clients, often accompanied by privacy constraints—a common scenario in Federated
 2818 Learning (FL) (Konečný et al., 2016; McMahan et al., 2016; Kairouz et al., 2019; Demidovich et al.,
 2819 2024b; Sadiev et al., 2024; Yi et al., 2024).
 2820

 2821 We develop several FL methods within the Bernoulli-LoRA framework and provide a convergence
 2822 analysis for them.
 2823

 2824 **I.1 ANALYSIS OF FED-BERNOULLI-LORA-QGD**
 2825

 2826 **Algorithm 7** Fed-Bernoulli-LoRA-QGD

 2827 1: **Parameters:** pre-trained model $W^0 \in \mathbb{R}^{m \times n}$, rank $r \ll \min\{m, n\}$, scaling factor $\alpha > 0$, chain
 2828 length T , sketch distribution \mathcal{D}_S^B or \mathcal{D}_S^A , Bernoulli probabilities p and q
 2829 2: **for** $t = 0, 1, \dots, T - 1$ **do**
 2830 3: **for** any client $l \in [M]$ in parallel **do**
 2831 4: Compute gradient $\nabla f_l(W^{t+1})$ and send compressed version $G_l^t = \mathcal{Q}_l^t(\nabla f_l(W^{t+1}))$ to the
 2832 server
 2833 5: **end for**
 2834 6: $G^t = \frac{1}{M} \sum_{l=1}^M G_l^t$
 2835 7: Sample $c^t \sim \text{Be}(p)$ Bernoulli random variable
 2836 8: **if** $c^t = 1$ **then**
 2837 9: Sample $B_S^t \sim \mathcal{D}_S^B$ Left sketch
 2838 10: $\hat{A}^t = -\eta \left((B_S^t)^\top B_S^t \right)^\dagger (B_S^t)^\top G^t$
 2839 11: $W^{t+1} = W^t + \frac{\alpha}{r} B_S^t \hat{A}^t$
 2840 12: **else**
 2841 13: Sample $A_S^t \sim \mathcal{D}_S^A$ Right sketch
 2842 14: $\hat{B}^t = -\eta G^t (A_S^t)^\top \left(A_S^t (A_S^t)^\top \right)^\dagger$
 2843 15: $W^{t+1} = W^t + \frac{\alpha}{r} \hat{B}^t A_S^t$
 2844 16: **end if**
 2845 17: Broadcast W^{t+1} to each client $l \in [M]$
 2846 18: **end for**
 2847

 2848 Parallel implementations of SGD have become a prominent area of study due to their impressive
 2849 scalability. However, one of the primary challenges in parallelizing SGD lies in the substantial
 2850 communication overhead required to exchange gradient updates across nodes. To address this,
 2851 numerous lossy compression techniques have been developed, enabling nodes to transmit quantized
 2852 gradients instead of full gradients. While these methods often work well in practice, they are not
 2853 universally reliable and may fail to ensure convergence.
 2854

 2855 To overcome these limitations, Quantized SGD (QSGD) by Alistarh et al. (2017) introduces a family
 2856 of compression techniques that provide both theoretical convergence guarantees and strong empirical
 2857 performance. QSGD offers a flexible mechanism for balancing communication bandwidth and
 2858 convergence speed. By adjusting the number of bits transmitted per iteration, nodes can reduce
 2859 bandwidth usage, albeit at the potential cost of increased variance in the gradient estimates. Different
 2860 variants of QSGD were considered by Horváth et al. (2022); Wen et al. (2017); Panferov et al. (2024).
 2861

2862 We consider the following distributed optimization problem:
 2863

$$2864 \min_{W \in \mathbb{R}^{m \times n}} \frac{1}{M} \sum_{l=1}^M f_l(W),$$

2866 where M represents the number of clients. In Federated Learning, a primary bottleneck is the
 2867 communication overhead between clients and the central server. A common approach to mitigate this
 2868 issue is communication compression.
 2869

2870 **Definition 2.** A randomized operator $\mathcal{Q} : \mathbb{R}^{m \times n} \rightarrow \mathbb{R}^{m \times n}$ is called an unbiased compression
 2871 operator (or compressor) if there exists a constant $\omega > 0$ such that, for any matrix $W \in \mathbb{R}^{m \times n}$, the
 2872 following conditions hold:

$$2873 \mathbb{E}[\mathcal{Q}(W)] = W, \quad \text{and} \quad \mathbb{E} \left[\|\mathcal{Q}(W) - W\|_{\text{F}}^2 \right] \leq \omega \|W\|_{\text{F}}^2. \quad (123)$$

2875 To analyze the optimization process, we introduce the following assumption regarding function
 2876 dissimilarity:
 2877

2879 **Assumption 11.** Let $f^* := \inf_W f(W)$ and $f_l^* := \inf_W f_l$ for each $l \in [M]$. In the non-convex
 2880 case, the difference at the optimum is defined as:

$$2882 \Delta^* := f^* - \frac{1}{M} \sum_{l=1}^M f_l^* \geq 0. \quad (124)$$

2885 This assumption quantifies the discrepancy between the global optimal function value and the average
 2886 of the local optimal function values between the clients.
 2887

2889 To start convergence analysis, we rewrite the updates for W^t and G^t generated by [Fed-Bernoulli-LoRA-QGD](#) (Algorithm 7) as follows
 2890

$$2891 G^t = \frac{1}{M} \sum_{l=1}^M \mathcal{Q}_l^t (\nabla f_l(W^t)); \quad (125)$$

$$2894 W^{t+1} = W^t - \gamma \hat{G}^t, \quad \text{where} \quad \hat{G}^t = \begin{cases} H_B^t G^t, & \text{with probability } p \\ G^t H_A^t, & \text{with probability } 1 - p \end{cases}. \quad (126)$$

2896 To establish the convergence guarantee for [Fed-Bernoulli-LoRA-QGD](#) (Algorithm 7), we first demonstrate
 2897 that the gradient estimator G^t satisfies Assumption 4. Once this is verified, the convergence
 2898 rate follows directly using the same reasoning as in the proof of Theorem 2.
 2899

2900 **Lemma 15.** Let Assumptions 2, 3, and 11 hold. Then, G^t defined in Algorithm 7 (see (125)) satisfies
 2901 Assumption 4 with the following constants:

$$2903 A_1 = \frac{L\omega}{M}, \quad B_1 = 1, \quad C_1 = 2 \frac{L\omega\Delta^*}{M}.$$

2913 *Proof.* First, we show G^t is an unbiased estimator of $\nabla f(W^t)$:

$$2914 \mathbb{E} [G^t | W^t] = \frac{1}{M} \sum_{l=1}^M \mathbb{E} [\mathcal{Q}_l^t (\nabla f_l(W^t)) | W^t] \stackrel{(123)}{=} \frac{1}{M} \sum_{l=1}^M \nabla f_l(W^t) = \nabla f(W^t).$$

Now we establish that G^t satisfies Assumption 4. Taking the conditional expectation with respect to W^t , we have

$$\begin{aligned}
\mathbb{E} \left[\|G^t\|_{\text{F}}^2 | W^t \right] &= \mathbb{E} \left[\left\| \frac{1}{M} \sum_{l=1}^M \mathcal{Q}_l^t (\nabla f_l(W^t)) - \nabla f(W^t) + \nabla f(W^t) \right\|_{\text{F}}^2 | W^t \right] \\
&\stackrel{(13)}{=} \mathbb{E} \left[\left\| \frac{1}{M} \sum_{l=1}^M \mathcal{Q}_l^t (\nabla f_l(W^t)) - \nabla f(W^t) \right\|_{\text{F}}^2 | W^t \right] + \|\nabla f(W^t)\|_{\text{F}}^2 \\
&= \frac{1}{M^2} \sum_{l=1}^M \mathbb{E} \left[\|\mathcal{Q}_l^t (\nabla f_l(W^t)) - \nabla f_l(W^t)\|_{\text{F}}^2 | W^t \right] + \|\nabla f(W^t)\|_{\text{F}}^2 \\
&\stackrel{(123)}{\leq} \frac{\omega}{M^2} \sum_{l=1}^M \|\nabla f_l(W^t)\|_{\text{F}}^2 + \|\nabla f(W^t)\|_{\text{F}}^2 \\
&\stackrel{(*)}{\leq} \frac{2L\omega}{M^2} \sum_{l=1}^M (f_l(W^t) - f_l^*) + \|\nabla f(W^t)\|_{\text{F}}^2 \\
&= 2\frac{L\omega}{M} (f(W^t) - f^*) + \|\nabla f(W^t)\|_{\text{F}}^2 + 2\frac{L\omega}{M} \underbrace{\left(f^* - \frac{1}{M} \sum_{l=1}^M f_l^* \right)}_{:= \Delta^*},
\end{aligned}$$

where in $(*)$ we used smoothness of each f_l . Thus, we have shown that G^t satisfies Assumption 4 with following constants

$$A_1 = \frac{L\omega}{M}, \quad B_1 = 1, \quad C_1 = 2\frac{L\omega\Delta^*}{M}.$$

□

I.1.1 CONVERGENCE FOR SMOOTH NON-CONVEX FUNCTIONS

Theorem 17. *Let Assumptions 1 2, and 3 hold, and stepsize satisfy*

$$0 < \gamma \leq \min \left\{ \frac{1}{L\sqrt{\frac{\omega}{M}\lambda_{\max}^p T}}, \frac{1}{L} \left(\frac{\lambda_{\max}^p}{\lambda_{\min}^p} \right)^{-1} \right\}.$$

Then iterates generated by Fed-Bernoulli-LoRA-QGD (Algorithm 7) satisfy

$$\mathbb{E} \left[\|\nabla f(\widetilde{W}^T)\|_{\text{F}}^2 \right] \leq \frac{6(f(W^0) - f^*)}{\gamma\lambda_{\min}^p T} + \frac{2\gamma L\omega\Delta^*}{M} \frac{\lambda_{\max}^p}{\lambda_{\min}^p},$$

where $\lambda_{\min}^p := p\lambda_{\min}^{H_B} + (1-p)\lambda_{\min}^{H_A}$, $\lambda_{\max}^p := p\lambda_{\max}^{H_B} + (1-p)\lambda_{\max}^{H_A}$, and \widetilde{W}^T is chosen at random from $\{W^0, W^1, \dots, W^{T-1}\}$ with probabilities $\{\frac{w_t}{\mathcal{W}_{T-1}}\}_{t=0}^{T-1}$, where $w_t = \frac{w_{t-1}}{(1+\gamma^2 L^2 \lambda_{\max}^p \omega / M)}$, $\mathcal{W}_{T-1} = \sum_{t=0}^{T-1} w_t$, and $w^{-1} > 0$.

Proof. By Lemma 15, and Theorem 2, we directly obtain the statement of the theorem. □

I.1.2 CONVERGENCE UNDER POLYAK-ŁOJASIEWICZ CONDITION

Theorem 18. *Let Assumptions 1, 2, 3, and 6 hold, and stepsize satisfy*

$$0 < \gamma \leq \min \left\{ \frac{\mu}{2L^2\omega/M} \left(\frac{\lambda_{\max}^p}{\lambda_{\min}^p} \right)^{-1}, \frac{2}{\mu\lambda_{\min}^p}, \frac{1}{L} \left(\frac{\lambda_{\max}^p}{\lambda_{\min}^p} \right)^{-1} \right\}.$$

Then iterates generated by Fed-Bernoulli-LoRA-QGD (Algorithm 7) satisfy

$$\mathbb{E} [f(W^T) - f^*] \leq \left(1 - \frac{1}{2} \gamma \mu \lambda_{\min}^p \right)^T (f(W^0) - f^*) + \frac{2\gamma L^2}{\mu} \cdot \frac{\omega}{M} \cdot \frac{\lambda_{\max}^p}{\lambda_{\min}^p},$$

where $\lambda_{\min}^p := p\lambda_{\min}^{H_B} + (1-p)\lambda_{\min}^{H_A}$, $\lambda_{\max}^p := p\lambda_{\max}^{H_B} + (1-p)\lambda_{\max}^{H_A}$.

Proof. By Lemma 15, and Theorem 12, we directly obtain the statement of the theorem. □

2970 I.2 ANALYSIS OF FED-BERNOULLI-LORA-MARINA
2971
2972
29732974 **Algorithm 8** Fed-Bernoulli-LoRA-MARINA

```

2975 1: Parameters: pre-trained model  $W^0 \in \mathbb{R}^{m \times n}$ ,  $\{G_l^0\}_{l \in [M]} \in \mathbb{R}^{m \times n}$  rank  $r \ll \min\{m, n\}$ ,
2976   scaling factor  $\alpha > 0$ , chain length  $T$ , sketch distribution  $\mathcal{D}_S^B$  or  $\mathcal{D}_S^A$ , Bernoulli probabilities  $p$ 
2977   and  $q$ 
2978 2: for  $t = 0, 1, \dots, T - 1$  do
2979   3:   Sample  $c^t \sim \text{Be}(p)$  Bernoulli random variable
2980   4:   if  $c^t = 1$  then
2981     5:     Sample  $B_S^t \sim \mathcal{D}_S^B$  Left sketch
2982     6:      $\hat{A}^t = -\eta \left( (B_S^t)^\top B_S^t \right)^\dagger (B_S^t)^\top G^t$ 
2983     7:      $W^{t+1} = W^t + \frac{\alpha}{r} B_S^t \hat{A}^t$ 
2984   8:   else
2985     9:     Sample  $A_S^t \sim \mathcal{D}_S^A$  Right sketch
2986     10:     $\hat{B}^t = -\eta G^t (A_S^t)^\top \left( A_S^t (A_S^t)^\top \right)^\dagger$ 
2987     11:     $W^{t+1} = W^t + \frac{\alpha}{r} \hat{B}^t A_S^t$ 
2988   12:   end if
2989   13:   Broadcast  $W^{t+1}$  to each client  $l \in [M]$ 
2990   14:   Sample  $s^t \sim \text{Be}(q)$ 
2991   15:   for any client  $l \in [M]$  in parallel do
2992     16:     Compute gradient  $\nabla f_l(W^{t+1})$ 
2993     17:      $G_l^{t+1} = \begin{cases} \nabla f_l(W^{t+1}), & \text{with probability } q \\ G_l^t + \mathcal{Q}_l^t (\nabla f_l(W^{t+1}) - \nabla f_l(W^t)), & \text{with probability } 1 - q \end{cases}$ 
2994     18:     Send  $G_l^{t+1}$  to the server
2995   19:   end for
2996   20:    $G^{t+1} = \frac{1}{M} \sum_{l=1}^M G_l^{t+1}$ 
2997 21: end for
3001
3002
3003
```

3004 **MARINA** (Gorbunov et al., 2021) is an advanced method that significantly enhances communication
3005 efficiency in non-convex distributed learning across heterogeneous datasets. Its core innovation lies
3006 in a communication reduction mechanism that compresses the differences between gradients. The
3007 communication complexity bounds for **MARINA** are known to be better than those of all previous
3008 first-order methods. Non-smooth convex analysis of **MARINA** with different stepsize strategies can
3009 be found in (Sokolov & Richtárik, 2024). This section is devoted to **Fed-Bernoulli-LoRA-MARINA**
3010 (Algorithm 8), a method within the **Bernoulli-LoRA** framework, based on **MARINA** algorithm.

3011 In order to start convergence analysis, we rewrite the updates W^t, G^t generated by **Fed-Bernoulli-LoRA-MARINA** (Algorithm 8):

$$3012 W^{t+1} = W^t - \gamma \hat{G}^t, \quad \text{where} \quad \hat{G}^t = \begin{cases} H_B^t G^t, & \text{with probability } p \\ G^t H_A^t, & \text{with probability } 1 - p \end{cases} \quad (127)$$

$$3013 G_l^{t+1} = \begin{cases} \nabla f_l(W^{t+1}), & \text{with probability } q \\ G_l^t + \mathcal{Q}_l^t (\nabla f_l(W^{t+1}) - \nabla f_l(W^t)), & \text{with probability } 1 - q \end{cases} \quad (128)$$

$$3014 G^{t+1} = \frac{1}{M} \sum_{l=1}^M G_l^{t+1}. \quad (129)$$

3021 **Lemma 16.** *Let Assumption 3 hold. Then iterates generated by **Fed-Bernoulli-LoRA-MARINA** satisfy*

$$3022 \mathbb{E} \left[\|G^{t+1} - \nabla f(W^{t+1})\|_F^2 \right] \leq (1 - q) \mathbb{E} \left[\|G^t - \nabla f(W^t)\|_F^2 \right] + (1 - q) \frac{\omega L^2}{M} \mathbb{E} \left[\|W^{t+1} - W^t\|_F^2 \right]. \quad (130)$$

3024 *Proof.* Taking the conditional expectation with respect to W^{t+1} and defining $D_l^{t+1} := \nabla f_l(W^{t+1}) -$
 3025 $\nabla f_l(W^t)$, $D^{t+1} = \frac{1}{M} \sum_{l=1}^M D_l^{t+1}$, we obtain
 3026

$$\begin{aligned}
 \mathbb{E} \left[\|G^{t+1} - \nabla f(W^{t+1})\|_{\text{F}}^2 | W^{t+1} \right] &= (1-q) \mathbb{E} \left[\left\| G^t - \nabla f(W^t) + \frac{1}{M} \sum_{l=1}^M \mathcal{Q}_l^t (\nabla f_l(W^{t+1}) - \nabla f_l(W^t)) \right\|_{\text{F}}^2 | W^{t+1} \right] \\
 &\stackrel{(13)}{=} (1-q) \|G^t - \nabla f(W^t)\|_{\text{F}}^2 + (1-q) \mathbb{E} \left[\left\| \frac{1}{M} \sum_{l=1}^M \mathcal{Q}_l^t (D_l^{t+1}) - D^{t+1} \right\|_{\text{F}}^2 | W^{t+1} \right] \\
 &= (1-q) \|G^t - \nabla f(W^t)\|_{\text{F}}^2 + \frac{1-q}{M^2} \sum_{m=1}^M \mathbb{E} \left[\|\mathcal{Q}_l^t (D_l^{t+1}) - D_l^{t+1}\|_{\text{F}}^2 | W^{t+1} \right] \\
 &\stackrel{(123)}{\leq} (1-q) \|G^t - \nabla f(W^t)\|_{\text{F}}^2 + \frac{(1-q)\omega}{M^2} \sum_{l=1}^M \|\nabla f_l(W^{t+1}) - \nabla f_l(W^t)\|_{\text{F}}^2 \\
 &\leq (1-q) \|G^t - \nabla f(W^t)\|_{\text{F}}^2 + \frac{(1-q)\omega L^2}{M} \|W^{t+1} - W^t\|_{\text{F}}^2,
 \end{aligned}$$

3039 where in the last inequality we used that the gradient of each f_l is Lipschitz continuous. \square
 3040

3042 I.2.1 CONVERGENCE FOR SMOOTH NON-CONVEX FUNCTIONS

3044 **Theorem 19.** *Let Assumptions 1, 2, 3, and hold, and let the stepsize satisfy*

$$0 < \gamma \leq \frac{1}{L \left(1 + \sqrt{\lambda_{\max}^p \frac{1-q}{q} \cdot \frac{\omega}{M}} \right)}.$$

3047 *Then the iterates of Fed-Bernoulli-LoRA-MARINA (Algorithm 8) satisfy*

$$\mathbb{E} \left[\|\nabla f(\widetilde{W}^T)\|_{\text{F}}^2 \right] \leq \frac{2(f(W^0) - f^*)}{\gamma \lambda_{\min}^p T} + \frac{\|G^0 - \nabla f(W^0)\|_{\text{F}}^2}{qT} \cdot \frac{\lambda_{\max}^p}{\lambda_{\min}^p}, \quad (131)$$

3051 where $\lambda_{\min}^p := p\lambda_{\min}^{H_B} + (1-p)\lambda_{\min}^{H_A}$, $\lambda_{\max}^p := p\lambda_{\max}^{H_B} + (1-p)\lambda_{\max}^{H_A}$, and \widetilde{W}^T is drawn uniformly
 3052 at random from the iterate sequence $\{W^0, W^1, \dots, W^{T-1}\}$.
 3053

3054 *Proof.* Denote Lyapunov function Φ_t as follows

$$\Phi_t = f(W^t) - f^* + \frac{\gamma \lambda_{\max}^p}{2q} \|G^t - \nabla f(W^t)\|_{\text{F}}^2. \quad (132)$$

3055 By Lemma 12 and Lemma 16, we have

$$\begin{aligned}
 \mathbb{E} [\Phi_{t+1}] &\leq \mathbb{E} [f(W^t)] - f^* - \frac{\gamma \lambda_{\min}^p}{2} \mathbb{E} [\|\nabla f(W^t)\|_{\text{F}}^2] - \left(\frac{1}{2\gamma} - \frac{L}{2} \right) \mathbb{E} [\|W^{t+1} - W^t\|_{\text{F}}^2] \\
 &\quad + \frac{\gamma \lambda_{\max}^p}{2} \mathbb{E} [\|G^t - \nabla f(W^t)\|_{\text{F}}^2] + \frac{\gamma(1-q)\lambda_{\max}^p}{2q} \mathbb{E} [\|G^t - \nabla f(W^t)\|_{\text{F}}^2] \\
 &\quad + \frac{\gamma(1-q)L^2\omega\lambda_{\max}^p}{2qM} \mathbb{E} [\|W^{t+1} - W^t\|_{\text{F}}^2] \\
 &\leq \mathbb{E} [\Phi_t] - \frac{\gamma \lambda_{\min}^p}{2} \mathbb{E} [\|\nabla f(W^t)\|_{\text{F}}^2] - \left(\frac{1}{2\gamma} - \frac{L}{2} - \frac{\gamma(1-q)L^2\omega\lambda_{\max}^p}{2qM} \right) \mathbb{E} [\|W^{t+1} - W^t\|_{\text{F}}^2].
 \end{aligned}$$

3067 Selecting $0 < \gamma \leq \frac{1}{L(1 + \sqrt{\lambda_{\max}^p \frac{1-q}{q} \cdot \frac{\omega}{M}})}$, we obtain
 3068

$$\mathbb{E} [\Phi_{t+1}] \leq \mathbb{E} [\Phi_t] - \frac{\gamma \lambda_{\min}^p}{2} \mathbb{E} [\|\nabla f(W^t)\|_{\text{F}}^2].$$

3071 Summing over, we get

$$\frac{\gamma \lambda_{\min}^p}{2} \sum_{t=0}^{T-1} \mathbb{E} [\|\nabla f(W^t)\|_{\text{F}}^2] \leq \mathbb{E} [\Phi_0] - \mathbb{E} [\Phi_T].$$

3074 Finally, we derive

$$\mathbb{E} \left[\|\nabla f(\widetilde{W}^T)\|_{\text{F}}^2 \right] \leq \frac{2\Phi_0}{\lambda_{\min}^p \gamma T}.$$

3075 where \widetilde{W}^T is drawn uniformly at random from the iterate sequence $\{W^0, W^1, \dots, W^{T-1}\}$. \square
 3076
 3077

3078 I.2.2 CONVERGENCE UNDER POLYAK-ŁOJASIEWICZ CONDITION
30793080 **Theorem 20.** *Let Assumptions 1, 2, 3, and 6 hold, and let the stepsize satisfy*

3081
$$0 < \gamma \leq \min \left\{ \frac{1}{L \left(1 + \sqrt{2\lambda_{\max}^p \frac{1-q}{q} \cdot \frac{\omega}{M}} \right)}, \frac{q}{2\mu\lambda_{\min}^p} \right\}.$$

3082

3083 *Then the iterates of Fed-Bernoulli-LoRA-MARINA (Algorithm 8) satisfy*

3084
$$\mathbb{E} [f(W^T) - f^*] \leq (1 - \gamma\mu\lambda_{\min}^p)^T \Phi_0, \quad (133)$$

3085

3086 *where $\lambda_{\min}^p := p\lambda_{\min}^{H_B} + (1-p)\lambda_{\min}^{H_A}$, $\lambda_{\max}^p := p\lambda_{\max}^{H_B} + (1-p)\lambda_{\max}^{H_A}$, and $\Phi_0 = f(W^0) - f^* +$
3087 $\frac{\gamma\lambda_{\max}^p}{q} \|G^0 - \nabla f(W^0)\|_F^2$.*
30883089 *Proof.* Denote Lyapunov function Φ_t as follows
3090

3091
$$\Phi_t = f(W^t) - f^* + \frac{\gamma\lambda_{\max}^p}{q} \|G^t - \nabla f(W^t)\|_F^2. \quad (134)$$

3092

3093 By Lemma 12 and Lemma 14, we have
3094

3095
$$\begin{aligned} \mathbb{E} [\Phi_{t+1}] &\leq \mathbb{E} [f(W^t)] - f^* - \frac{\gamma\lambda_{\min}^p}{2} \mathbb{E} [\|\nabla f(W^t)\|_F^2] - \left(\frac{1}{2\gamma} - \frac{L}{2} \right) \mathbb{E} [\|W^{t+1} - W^t\|_F^2] \\ &\quad + \frac{\gamma\lambda_{\max}^p}{2} \mathbb{E} [\|G^t - \nabla f(W^t)\|_F^2] + \frac{\gamma(1-q)\lambda_{\max}^p}{q} \mathbb{E} [\|G^t - \nabla f(W^t)\|_F^2] \\ &\quad + \frac{\gamma(1-q)L^2\lambda_{\max}^p}{q} \cdot \frac{\omega}{M} \mathbb{E} [\|W^{t+1} - W^t\|_F^2] \\ &\leq (1 - \gamma\mu\lambda_{\min}^p) \mathbb{E} [f(W^t) - f^*] + \left(1 - \frac{q}{2} \right) \frac{\gamma\lambda_{\max}^p}{q} \mathbb{E} [\|G^t - \nabla f(W^t)\|_F^2] \\ &\quad - \left(\frac{1}{2\gamma} - \frac{L}{2} - \frac{\gamma(1-q)L^2\lambda_{\max}^p}{q} \cdot \frac{\omega}{M} \right) \mathbb{E} [\|W^{t+1} - W^t\|_F^2], \end{aligned}$$

3100

3101 where in the last inequality we used Assumption 6. Selecting $0 < \gamma \leq$
3102 $\min \left\{ \frac{1}{L \left(1 + \sqrt{\frac{2(1-q)\omega}{qM} \lambda_{\max}^p} \right)}, \frac{q}{2\mu\lambda_{\min}^p} \right\}$, we obtain
3103

3104
$$\mathbb{E} [\Phi_{t+1}] \leq (1 - \gamma\mu\lambda_{\min}^p) \mathbb{E} [\Phi_t].$$

3105

3106 Taking recursion, we have
3107

3108
$$\mathbb{E} [\Phi_T] \leq (1 - \gamma\mu\lambda_{\min}^p)^T \Phi_0.$$

3109

□

3110
3111
3112
3113
3114
3115
3116
3117
3118
3119
3120
3121
3122
3123
3124
3125
3126
3127
3128
3129
3130
3131

I.3 ANALYSIS OF FED-BERNOULLI-LoRA-EF21

Algorithm 9 Fed-Bernoulli-LoRA-EF21

```

1: Parameters: pre-trained model  $W^0 \in \mathbb{R}^{m \times n}$ ,  $\{G_l^0\}_{l \in [M]} \in \mathbb{R}^{m \times n}$  rank  $r \ll \min\{m, n\}$ ,  

   scaling factor  $\alpha > 0$ , chain length  $T$ , sketch distribution  $\mathcal{D}_S^B$  or  $\mathcal{D}_S^A$ , Bernoulli probability  $p$ 
2: for  $t = 0, 1, \dots, T - 1$  do
3:   Sample  $c^t \sim \text{Be}(p)$  Bernoulli random variable
4:   if  $c^t = 1$  then
5:     Sample  $B_S^t \sim \mathcal{D}_S^B$  Left sketch
6:      $\hat{A}^t = -\eta \left( (B_S^t)^\top B_S^t \right)^\dagger (B_S^t)^\top G^t$ 
7:      $W^{t+1} = W^t + \frac{\alpha}{r} B_S^t \hat{A}^t$ 
8:   else
9:     Sample  $A_S^t \sim \mathcal{D}_S^A$  Right sketch
10:     $\hat{B}^t = -\eta G^t (A_S^t)^\top \left( A_S^t (A_S^t)^\top \right)^\dagger$ 
11:     $W^{t+1} = W^t + \frac{\alpha}{r} \hat{B}^t A_S^t$ 
12:   end if
13:   Broadcast  $W^{t+1}$  to each client  $l \in [M]$ 
14:   for any client  $l \in [M]$  in parallel do
15:     Compute gradient  $\nabla f_l(W^{t+1})$ 
16:      $G_l^{t+1} = G_l^t + C_l^t (\nabla f_l(W^{t+1}) - G_l^t)$ 
17:     Send  $G_l^{t+1}$  to the server
18:   end for
19:    $G^{t+1} = \frac{1}{M} \sum_{l=1}^M G_l^{t+1}$ 
20: end for

```

Error Feedback (EF) (Seide et al., 2014; Stich et al., 2018; Alistarh et al., 2018; Richtárik et al., 2021; Fatkullin et al., 2021; Richtárik et al., 2022; Khirirat et al., 2024), often referred to as error compensation, is an exceptionally influential mechanism for stabilizing convergence in distributed training of supervised machine learning models, particularly when contractive communication compression techniques are employed. We design `Fed-Bernoulli-LoRA-EF21` within the `Bernoulli-LoRA` framework, based on `EF-21` method. Our theoretical analysis, built on standard assumptions, applies to distributed training in heterogeneous data settings and achieves the best known convergence rates.

Compared to [Fed-Bernoulli-LoRA-MARINA](#), in this section we work with the wider class of compression operators called contractive.

Definition 3. A randomized operator $\mathcal{C} : \mathbb{R}^{m \times n} \rightarrow \mathbb{R}^{m \times n}$ is called a contractive compression operator (compressor) if it satisfies the following condition: there exists a constant $0 < \beta \leq 1$ such that

$$\mathbb{E} \left[\|\mathcal{C}(W) - W\|_{\text{F}}^2 \right] \leq (1 - \beta) \|W\|_{\text{F}}^2, \quad \forall W \in \mathbb{R}^{m \times n}. \quad (135)$$

The iterates of Fed-Bernoulli-LoBA-FF21 can be rewritten as follows

$$W^{t+1} = W^t - \gamma \hat{G}^t, \quad \text{where} \quad \hat{G}^t = \begin{cases} H_B^t G^t, & \text{with probability } p \\ C^t H^t, & \text{with probability } 1-p \end{cases} \quad (136)$$

$$G_i^{t+1} \equiv G_i^t + \mathcal{C}_i^t (\nabla f_l(W^{t+1}) - G_i^t), \quad \forall l \in [M] \quad (137)$$

$$G^{t+1} = \frac{1}{M} \sum_{l=1}^M G_l^{t+1}. \quad (138)$$

Lemma 17. *Let Assumption 3 hold. Then for the iterates generated by Fed-Bernoulli-LoRA-EF21 (Algorithm 9) satisfy*

$$\mathbb{E} \left[\|G_l^{t+1} - \nabla f_l(W^{t+1})\|_{\text{F}}^2 \right] \leq \sqrt{1-\beta} \mathbb{E} \left[\|G_l^t - \nabla f_l(W^t)\|_{\text{F}}^2 \right] + \frac{(1-\beta)L^2}{1-\sqrt{1-\beta}} \mathbb{E} \left[\|W^{t+1} - W^t\|_{\text{F}}^2 \right]$$

3186 *Proof.* For each $l \in [M]$ we have
3187
$$\mathbb{E} \left[\|G_l^{t+1} - \nabla f_l(W^{t+1})\|_F^2 \right] \stackrel{(137),(138)}{=} \mathbb{E} \left[\mathbb{E} \left[\left\| \mathcal{C}_l^t (\nabla f_l(W^{t+1}) - G_l^t) - (\nabla f_l(W^{t+1}) - G_l^t) \right\|_F^2 | G_l^{t+1}, W^{t+1} \right] \right]$$

3188
$$\stackrel{(135)}{\leq} (1 - \beta) \mathbb{E} \left[\|G_l^t - \nabla f_l(W^{t+1})\|_F^2 \right]$$

3189
$$\leq (1 - \beta) (1 + \theta) \mathbb{E} \left[\|G_l^t - \nabla f_l(W^t)\|_F^2 \right]$$

3190
$$+ (1 - \beta) \left(1 + \frac{1}{\theta} \right) \mathbb{E} \left[\|\nabla f_l(W^{t+1}) - \nabla f_l(W^t)\|_F^2 \right],$$

3191

3192 where in the last inequality we used $\|U + V\|_F^2 \leq (1 + \theta) \|U\|_F^2 + (1 + \frac{1}{\theta}) \|V\|_F^2$ for any constant
3193 $\theta > 0$, and matrices $U, V \in \mathbb{R}^{m \times n}$. Taking $\theta = \frac{1}{\sqrt{1-\beta}} - 1$, we acquire
3194
$$\mathbb{E} \left[\|G_l^{t+1} - \nabla f_l(W^{t+1})\|_F^2 \right] \leq \sqrt{1 - \beta} \mathbb{E} \left[\|G_l^t - \nabla f_l(W^t)\|_F^2 \right] + \frac{1 - \beta}{1 - \sqrt{1 - \beta}} \mathbb{E} \left[\|\nabla f_l(W^{t+1}) - \nabla f_l(W^t)\|_F^2 \right]$$

3195
$$\leq \sqrt{1 - \beta} \mathbb{E} \left[\|G_l^t - \nabla f_l(W^t)\|_F^2 \right] + \frac{(1 - \beta)L^2}{1 - \sqrt{1 - \beta}} \mathbb{E} \left[\|W^{t+1} - W^t\|_F^2 \right],$$

3196

3197 where in the last inequality we used that the gradient of each f_l is Lipschitz continuous. Summing
3198 over l from 1 to M , we finish the proof. \square
3199

3200 I.3.1 CONVERGENCE FOR SMOOTH NON-CONVEX FUNCTIONS

3201 **Theorem 21.** *Let Assumptions 1, 2, and 3 hold, and let the stepsize satisfy*

$$0 < \gamma \leq \frac{1}{L \left(1 + \frac{\sqrt{\lambda_{\max}^p(1-\beta)}}{1-\sqrt{1-\beta}} \right)}.$$

3202 *Then the iterates of Fed-Bernoulli-LoRA-EF21 (Algorithm 9) satisfy*

$$\mathbb{E} \left[\left\| \nabla f(\widetilde{W}^T) \right\|_F^2 \right] \leq \frac{2(f(W^0) - f^*)}{\gamma \lambda_{\min}^p T} + \frac{\mathcal{G}^0}{(1 - \sqrt{1 - \beta})T} \cdot \frac{\lambda_{\max}^p}{\lambda_{\min}^p}, \quad (139)$$

3203 where $\lambda_{\min}^p := p\lambda_{\min}^{H_B} + (1-p)\lambda_{\min}^{H_A}$, and $\lambda_{\max}^p := p\lambda_{\max}^{H_B} + (1-p)\lambda_{\max}^{H_A}$, \widetilde{W}^T is drawn uniformly at
3204 random from the iterate sequence $\{W^0, W^1, \dots, W^{T-1}\}$, and $\mathcal{G}^0 := \frac{1}{M} \sum_{l=1}^M \|G_l^0 - \nabla f_l(W^0)\|_F^2$.
3205

3206 *Proof.* Denote Lyapunov function Φ_t as follows

$$\Phi_t = f(W^t) - f^* + \frac{\gamma \lambda_{\max}^p}{2(1 - \sqrt{1 - \beta})} \cdot \frac{1}{M} \sum_{l=1}^M \|G_l^t - \nabla f_l(W^t)\|_F^2. \quad (140)$$

3207 By Lemma 12 and Lemma 17, we have

$$\begin{aligned} \mathbb{E} [\Phi_{t+1}] &\leq \mathbb{E} [f(W^t)] - f^* - \frac{\gamma \lambda_{\min}^p}{2} \mathbb{E} \left[\left\| \nabla f(W^t) \right\|_F^2 \right] - \left(\frac{1}{2\gamma} - \frac{L}{2} \right) \mathbb{E} \left[\|W^{t+1} - W^t\|_F^2 \right] \\ &\quad + \frac{\gamma \lambda_{\max}^p}{2} \mathbb{E} \left[\|G^t - \nabla f(W^t)\|_F^2 \right] + \frac{\gamma \lambda_{\max}^p \sqrt{1 - \beta}}{2(1 - \sqrt{1 - \beta})} \cdot \frac{1}{M} \sum_{l=1}^M \mathbb{E} \left[\|G_l^t - \nabla f_l(W^t)\|_F^2 \right] \\ &\quad + \frac{\gamma \lambda_{\max}^p L^2 (1 - \beta)}{2(1 - \sqrt{1 - \beta})^2} \mathbb{E} \left[\|W^{t+1} - W^t\|_F^2 \right] \\ &\leq \mathbb{E} [\Phi_t] - \frac{\gamma \lambda_{\min}^p}{2} \mathbb{E} \left[\left\| \nabla f(W^t) \right\|_F^2 \right] - \left(\frac{1}{2\gamma} - \frac{L}{2} - \frac{\gamma \lambda_{\max}^p L^2 (1 - \beta)}{2(1 - \sqrt{1 - \beta})^2} \right) \mathbb{E} \left[\|W^{t+1} - W^t\|_F^2 \right]. \end{aligned}$$

3208 Selecting $0 < \gamma \leq \frac{1}{L \left(1 + \frac{\sqrt{\lambda_{\max}^p(1-\beta)}}{1-\sqrt{1-\beta}} \right)}$, we obtain

$$\mathbb{E} [\Phi_{t+1}] \leq \mathbb{E} [\Phi_t] - \frac{\gamma \lambda_{\min}^p}{2} \mathbb{E} \left[\left\| \nabla f(W^t) \right\|_F^2 \right].$$

3209 Summing over t from 0 to $T - 1$, we get

$$\frac{\gamma \lambda_{\min}^p}{2} \sum_{t=0}^{T-1} \mathbb{E} \left[\left\| \nabla f(W^t) \right\|_F^2 \right] \leq \mathbb{E} [\Phi_0] - \mathbb{E} [\Phi_T].$$

3240 Finally, dividing both sides by $\frac{\gamma\lambda_{\min}^p}{2}$ yields
 3241
 3242
 3243

$$\mathbb{E} \left[\left\| \nabla f(\widetilde{W}^T) \right\|_{\text{F}}^2 \right] \leq \frac{2\Phi_0}{\gamma\lambda_{\min}^p T}.$$

3244 where \widetilde{W}^T is drawn uniformly at random from the iterate sequence $\{W^0, W^1, \dots, W^{T-1}\}$. \square
 3245
 3246

I.3.2 CONVERGENCE UNDER POLYAK-ŁOJASIEWICZ CONDITION

3247 **Theorem 22.** *Let Assumptions 1, 2, 3, and 6 hold, and let the stepsize satisfy*

$$0 < \gamma \leq \min \left\{ \frac{1}{L \left(1 + \frac{\sqrt{2\lambda_{\max}^p(1-\beta)}}{1-\sqrt{1-\beta}} \right)}, \frac{1+\sqrt{1-\beta}}{2\mu\lambda_{\min}^p} \right\}$$

3248 . Then the iterates of Fed-Bernoulli-LoRA-EF21 (Algorithm 9) satisfy
 3249

$$\mathbb{E} [f(W^T) - f^*] \leq (1 - \gamma\mu\lambda_{\min}^p)^T \Phi_0, \quad (141)$$

3250 where $\lambda_{\min}^p := p\lambda_{\min}^{H_B} + (1-p)\lambda_{\min}^{H_A}$, $\lambda_{\max}^p := p\lambda_{\max}^{H_B} + (1-p)\lambda_{\max}^{H_A}$, and $\Phi_0 = f(W^0) - f^* +$
 3251 $\frac{\gamma\lambda_{\max}^p}{1-\sqrt{1-\beta}} \frac{1}{M} \sum_{l=1}^M \|G_l^0 - \nabla f_l(W^0)\|_{\text{F}}^2$.
 3252

3253 *Proof.* Denote Lyapunov function Φ_t as follows
 3254

$$\Phi_t = f(W^t) - f^* + \frac{\gamma\lambda_{\max}^p}{1-\sqrt{1-\beta}} \cdot \frac{1}{M} \sum_{l=1}^M \|G_l^t - \nabla f_l(W^t)\|_{\text{F}}^2. \quad (142)$$

3255 By Lemma 12 and Lemma 17, we have
 3256

$$\begin{aligned} \mathbb{E} [\Phi_{t+1}] &\leq \mathbb{E} [f(W^t)] - f^* - \frac{\gamma\lambda_{\min}^p}{2} \mathbb{E} [\|\nabla f(W^t)\|_{\text{F}}^2] - \left(\frac{1}{2\gamma} - \frac{L}{2} \right) \mathbb{E} [\|W^{t+1} - W^t\|_{\text{F}}^2] \\ &\quad + \frac{\gamma\lambda_{\max}^p}{2} \cdot \mathbb{E} [\|G^t - \nabla f(W^t)\|_{\text{F}}^2] + \frac{\gamma\lambda_{\max}^p\sqrt{1-\beta}}{1-\sqrt{1-\beta}} \cdot \frac{1}{M} \sum_{l=1}^M \mathbb{E} [\|G_l^t - \nabla f_l(W^t)\|_{\text{F}}^2] \\ &\quad + \frac{\gamma\lambda_{\max}^p(1-\beta)L^2}{(1-\sqrt{1-\beta})^2} \mathbb{E} [\|W^{t+1} - W^t\|_{\text{F}}^2] \\ &\leq (1 - \gamma\mu\lambda_{\min}^p) \mathbb{E} [f(W^t) - f^*] + \frac{\gamma\lambda_{\max}^p(1+\sqrt{1-\beta})}{2(1-\sqrt{1-\beta})} \cdot \frac{1}{M} \sum_{l=1}^M \mathbb{E} [\|G_l^t - \nabla f_l(W^t)\|_{\text{F}}^2] \\ &\quad - \left(\frac{1}{2\gamma} - \frac{L}{2} - \frac{\gamma\lambda_{\max}^p(1-\beta)L^2}{(1-\sqrt{1-\beta})^2} \right) \mathbb{E} [\|W^{t+1} - W^t\|_{\text{F}}^2], \end{aligned}$$

3257 where in the last inequality we used Assumption 6. Selecting $0 < \gamma \leq$
 3258

3259 $\min \left\{ \frac{1}{L \left(1 + \frac{\sqrt{2\lambda_{\max}^p(1-\beta)}}{1-\sqrt{1-\beta}} \right)}, \frac{1+\sqrt{1-\beta}}{2\mu\lambda_{\min}^p} \right\}$, we obtain
 3260

$$\mathbb{E} [\Phi_{t+1}] \leq (1 - \gamma\mu\lambda_{\min}^p) \mathbb{E} [\Phi_t].$$

3261 Taking the recursion, we have
 3262

$$\mathbb{E} [\Phi_T] \leq (1 - \gamma\mu\lambda_{\min}^p)^T \Phi_0.$$

\square

3263
 3264
 3265
 3266
 3267
 3268
 3269
 3270
 3271
 3272
 3273
 3274
 3275
 3276
 3277
 3278
 3279
 3280
 3281
 3282
 3283
 3284
 3285
 3286
 3287
 3288
 3289
 3290
 3291
 3292
 3293

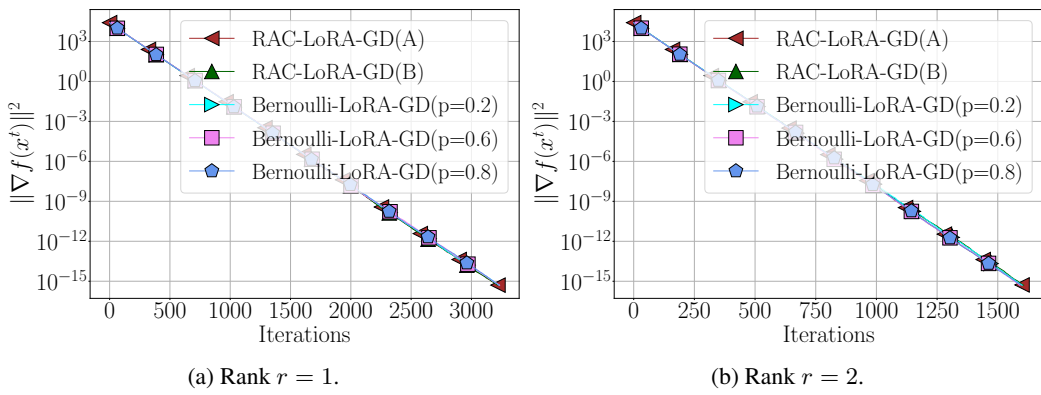
3294 complete it was that from new reps
 3295

3296 J EXPERIMENTS: MISSING DETAILS

3297 In this section, we provide additional details regarding the experimental setting from Section 7.

3300 J.1 LINEAR REGRESSION WITH NON-CONVEX REGULARIZATION

3302 **Full gradient setting.** We begin by evaluating these methods in a standard optimization setting where
 3303 full gradients are computed at each iteration. In this regime, we compare **Bernoulli-LoRA-GD** and
 3304 **RAC-LoRA-GD**.



3317 Figure 2: Comparison of **RAC-LoRA-GD** and **Bernoulli-LoRA-GD** on linear regression fine-tuning.
 3318 Curves with $p = 0.01, 0.2, \dots$ indicate **Bernoulli-LoRA-GD** sampling parameters. **RAC-LoRA-GD(A)**
 3319 trains B after resampling A , while **RAC-LoRA-GD(B)** does the reverse. All methods use $\gamma = c/\hat{L}$ with
 3320 $c \in \{1, 2\}$ tuned individually.

3323
 3324 Figure 2 shows that, across all tested probabilities, **Bernoulli-LoRA-GD** and both variants of **RAC-LoRA-GD**
 3325 exhibit similar convergence on the linear regression task. This numerical stability suggests
 3326 that the ratio of updates between A and B has little effect on the performance for this problem. We
 3327 also observe that higher ranks r produce faster convergence, which aligns with the theoretical r/n
 3328 factor in our analysis.

3329
 3330 **Hardware and Software.** All algorithms were implemented in Python 3.10 and executed on three
 3331 different CPU cluster node types:

- 3333 1. AMD EPYC 7702 64-Core,
- 3334 2. Intel(R) Xeon(R) Gold 6148 CPU @ 2.40GHz,
- 3335 3. Intel(R) Xeon(R) Gold 6248 CPU @ 2.50GHz.

3337 **Implementation Details.** For each method, we set the stepsize to $\gamma = c/\hat{L}$, where c is a constant
 3338 multiplier tuned individually for every algorithm. Convergence was monitored by computing the
 3339 squared norm of the full gradient at each iteration. The algorithms terminated when either a maximum
 3340 iteration limit was reached or the criterion $\|\nabla f(x^t)\|_2^2 \leq 5 \times 10^{-16}$ was satisfied. To ensure
 3341 reliability, each method was run 20 times using different random seeds, and all figures show the
 3342 median performance over these trials.

3343
 3344 **Datasets.** The synthetic pre-training dataset (\tilde{D}, \tilde{b}) was generated using

```
3345           sklearn.datasets.make_regression
```

3346 with moderate noise and a controlled rank structure:

```

3348 1 wt_D, wt_b = make_regression(n_samples=90000, n_features=4096,
3349 2 n_informative=4096, noise=20.0,
3350 3 bias=0.0, tail_strength=0.8,
3351 4 effective_rank=64, random_state=42)
3352

```

3353 followed by standard scaling. The fine-tuning dataset (\hat{D}, \hat{b}) was produced similarly:

```

3354 1 h_D, h_b = make_regression(n_samples=10000, n_features=4096,
3355 2 n_informative=4096//2, noise=50.0,
3356 3 bias=10.0, tail_strength=0.9,
3357 4 effective_rank=32, random_state=84)
3358

```

3359 and subsequently adjusted with a biased scaling (mean 1, standard deviation 2).

3360

3361 LLM USE ACKNOWLEDGMENT

3362

3363 In this paper, we used large language models (LLMs) to assist with grammar and wording during
 3364 the preparation of the manuscript. We did not use LLMs to derive convergence theorems, generate
 3365 empirical plots, or search for citations. This usage is in accordance with two primary LLM-related
 3366 policies.

3367

3368

3369

3370

3371

3372

3373

3374

3375

3376

3377

3378

3379

3380

3381

3382

3383

3384

3385

3386

3387

3388

3389

3390

3391

3392

3393

3394

3395

3396

3397

3398

3399

3400

3401